Role of the nuclear receptor LRH-1 in T cell development and function

Dissertation zur Erlangung des

akademischen Grades eines Doktors der

Naturwissenschaften

vorgelegt von

Seitz, Carina

an der

Mathematisch-Naturwissenschaftliche Sektion

Fachbereich Biologie

Konstanz, 2017

Tag der mündlichen Prüfung: 20.02.2018

1. Referent/Referentin: Prof. Dr. Thomas Brunner

2. Referent/Referentin: Prof. Dr. Daniel Legler

Acknowledgements

Reflecting my time as a PhD student, I have to admit: it was a long way – and without you, Thomi, I would have never made it!

In 2012, I started with a molecular biology and chemical background and minimal knowledge about the immune system. Thank you, Thomi, for taking me by the hand and introducing me into this fascinating world of immunology. You gave me the opportunity to start something completely new, you encouraged me, motivated when it was necessary and you proofed a good portion of patience.

Just when I became a little bit more confident with all the immunological tools and the handling of mice, little Nora stepped into my life and I had to pause all experiments. I really appreciate your understanding and the support in helping me to juggle work and life.

Back in the lab, I resumed my studies and was faced with a lot of new (and old) challenges. I remember in particular the difficulties I had in sorting cells and the subsequent quantification of LRH-1 expression, which accompanied me from the beginning until the very end of my work. However, although my experiments were now again interrupted, with the birth of Jakob, you still encouraged me to finish my work and overcome these troubles. It was not always easy (for both of us), but I am happy to have known you always by my side and your confidence in me and my work. You are the best "Doktorvater" I can imagine! Thank you, Thomi!

During the last part of my way, I was further supported by Anna-Lena Geiselhöringer who performed the transfer colitis and protection experiments during her master thesis and thereby contributed a big part to this work. Great help was also offered by the best Vertiefungskurs-students I can imagine - Josefine Negrassus and Daniela Eichbichler - which I appreciate a lot as well as the valuable work of Theresa Schnalzger.

Further support came from Marcus Groettrup and Daniel Legler – thank you for the discussions and suggestions on my project especially during the Hornberg meetings

and for taking over the “Zweitgutachten”. Michael Basler and Marcus Groettrup also provided me the cell harvester/β-counter and shared the Rag1$^{-/-}$ animals with me. Thank you!

Ein ganz besonderer Dank geht an Cindy! Du bist nicht nur eine herausragende Wissenschaftlerin sondern auch eine ganz besondere Freundin geworden in dieser Zeit. Danke für Deine Unterstützung – und Hut ab vor dem, was Du täglich leistest!

Niemals hätte ich die Mausarbeiten ohne die Unterstützung von Heidi und Anna geschafft! Vielen Dank für eure Hilfe, euer Vertrauen und die offenen Gespräche!

My thanks go to Thomas and Anette who welcomed me very warmly in the group and who left their marks in my life. Thank you for the encouraging words, the great atmosphere in the lab and your never ending support. I learned a lot from you and will never forget (at least some of your) jokes, Thomas! Thanks also for proof-reading my thesis!

Special thanks go to San and his burning scientific interest, the endless discussions and his good mood as well as Juan, without whom I could not have coped with the virus work at all. I would also like to expand my thanks to the rest of the working group!

Financial and ideological support was further provided by the RTG 1331 and a big thank you goes to Josepha Ittner who helped me with managing all the bureaucracy that incurred with the birth of my children.

Schließlich möchte ich auch meinen Eltern, Schwiegereltern, Kommilitonen und nicht zuletzt meiner kleinen Familie danken – Danke für eure Unterstützung, euer Verständnis und all die aufbauenden Worte! Danke auch an das Team von „Knirps & Co.“ – dafür, dass ihr uns so zuverlässig durch diese Zeit begleitet habt!

Thank you - Danke!

Table of contents

Abstract

The nuclear transcription factor liver receptor homolog-1 (LRH-1) has been extensively studied in tissues of endodermal origin. However, its expression and function in hematopoietic cells, especially T lymphocytes, is currently unknown.

This study describes the expression of LRH-1 in immature and mature murine T cells as well as human PBMCs and its mitogen-induced upregulation. It furthermore characterizes the effect of conditional LRH-1 deletion on T cell development and describes a severe loss of mature T lymphocytes in secondary lymphatic organs. While LRH-1 deficiency did not cause any defects regarding T cell activation or sensitivity to apoptosis inducing agents, activation-induced proliferation was significantly reduced *in vitro* and *in vivo*. Furthermore, effector functions were severely impaired in $CD4^+$ T cells as characterized by defective B cell help and the failure to induce or protect experimental colitis. Viral infection lead to virus-specific activation and expansion of $CD8^+$ T lymphocytes, however, cytotoxic T cells were not able to control virus expansion.

This study describes for the first time a critical role of LRH-1 in the maturation of T cells, the regulation of homeostatic expansion, T cell proliferation and effector functions. Sucessful transient inhibition further proposes LRH-1 as a target in the treatment of T cell-mediated pathologies.

Zusammenfassung

LRH-1 (Liver receptor homolog-1) ist ein nukleärer Transkriptionsfaktor der hauptsächlich in endodermalem Gewebe exprimiert wird. Dort ist er maßgeblich an der Regulation von Genen beteiligt, die während der Embryonalentwicklung, im Stoffwechsel sowie bei der Zellproliferation eine wichtige Rolle spielen. Die derzeitigen Kenntnisse über die Expression und eine mögliche Funktion von LRH-1 in hämatopoietischen Zellen wie T-Lymphozyten sind sehr gering.

In der vorliegenden Arbeit wird die Expression von LRH-1 sowohl in unreifen und reifen murinen T-Zellen beschrieben als auch in den mononukleären Zellen des menschlichen Bluts. Weitherhin konnte eine Aufregulierung der Genexpression nach T-Zell-Aktivierung beobachtet werden. Die Zucht einer konditionalen Mauslinie erlaubte es, Auswirkungen von LRH-1 auf die T-Zell-Entwicklung zu untersuchen, die sich in einem charakteristischen Verlust reifer T-Lymphozyten manifestierten.

Es konnte gezeigt werden, dass ein Fehlen funktionalen LRH-1 Proteins weder die Aktivierbarkeit von Lymphozyten einschränkt, noch gravierende Auswirkungen auf die Sensitivität von T-Zellen gegenüber apoptotischen Stimuli hat. Die Proliferationsfähigkeit LRH-1 defizienter Lymphozyten war dagegen sowohl *in vitro* als auch *in vivo* stark beinträchtigt und $CD4^+$ T-Zellen zeigten eingeschränkte Effektorfunktionen. Dies äußerste sich in der mangelhaften Antikörperproduktion durch B-Zellen und der Unfähigkeit von T-Helferzellen, experimentelle Colitis zu induzieren bzw. Mäuse davor zu protektieren. Die Effektorfunktion zytotoxischer $CD8^+$ T-Zellen war ebenfalls beeinträchtigt. Trotz unauffälliger Aktivierung und virus-spezifischer Expansion war es LRH-1 defizienten $CD8^+$ T-Lymphozyten nicht möglich LCM-Viren zu eliminieren.

Diese Arbeit beschreibt zum ersten Mal eine kritische Rolle für LRH-1 in der T-Zell-Reifung, Regulation der homeostatischen Expansion, T-Zell Proliferation sowie $CD4^+$ und $CD8^+$ Effektorfunktionen. Die erfolgreiche Anwendung LRH-1 spezifischer Inhibitoren und die Expression in humanen Zellen legen LRH-1 als potenzielles Ziel für die pharmakologische Behandlung T-Zell verursachter Pathologien nahe.

1 Introduction

For unicellular organisms such as bacteria and yeast, life is pretty simple: every cell is equal in its function and has to compete for limiting nutrients to survive in its surrounding environment. Although there are some mechanisms how these organisms can communicate with one another, there is no need for physiological mechanisms. However, life is more complex in multicellular organisms. Differentiated cells serve compartmentalized functions and have to collaborate within tissues or organs in order to maintain physiological functions throughout the whole lifespan. Inter- and intracellular communication is required to properly orchestrate the numerous regulatory events of the complex body plan during embryogenesis and to maintain homeostasis. Multicellular organisms therefore need to modulate the repression and activation of target genes at specific times in precise places. This requires a dynamic, adaptive and efficient communication as well as sensory networks[1,2].

1.1 Nuclear receptors

In human, a related but diverse array of 49 nuclear receptors has been identified so far[3]. Their role is not trivial and typically starts with the recognition of hydrophobic molecules which are able to cross the plasma membrane by diffusion. Although these molecules show great differences regarding their chemical structure and biological function, they act in a similar manner[4]: their binding provokes changes in the NR activity and subsequently results in altered target gene expression[4]. NRs hence combine several key functions including signal sensing and transduction as well as interaction with specific DNA motifs and the sequential recruitment of other transcription factors and co-regulators. With this, they provide a direct link between signaling molecules and the regulation of gene transcription. It is thus not surprising that NRs are involved in the regulation of a broad spectrum of physiological functions such as development, cell proliferation, metabolism and reproduction[5].

The way in which a NR orchestrates transcription, however, is diverse. It ranges from initiation and activation to repression of gene expression, either by direct interaction with genomic DNA or indirectly by the recruitment of co-regulatory complexes[6,7]. Besides ligand binding, the activity of NRs can furthermore be modulated by post-translational modifications, which makes NR signaling even more complex[7].

1.1.1 General structure

All nuclear receptors share a phylogenetic relationship and a typical modular organization. They consist of a highly variable amino-terminal activation domain that often carries an activation function 1 (AF1) sequence, a characteristic DNA binding domain (DBD) and a conserved carboxy-terminal ligand-binding domain (LBD) which contains the ligand dependent activation function 2 (AF2) motif (Figure 1)[8-10].

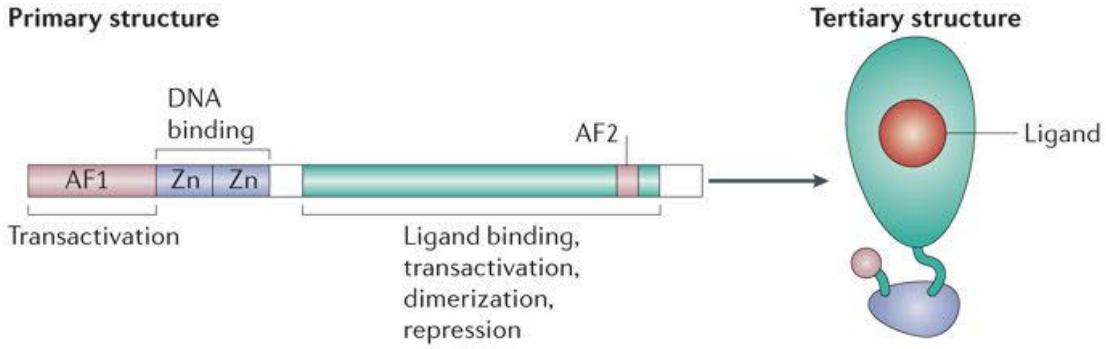

Figure 1: General domain organization of nuclear receptors.

Typically, NRs consist of an N-terminal ligand independent activation function-1 domain (AF1), a central DNA-binding domain (DBD) which is highly conserved and linked by a short hinge region to the ligand binding domain (LBD) which comprises the ligand-dependent activation function-2 motif (AF2). Schematic layout of a nuclear receptor tertiary protein structure after ligand binding is displayed on the right. Image adapted from[8].

Due to their highly conserved DBD, nuclear receptors have the characteristic ability to directly interact with specific sequences of genomic DNA that are localized in immediate vicinity to their target gene promotors or in enhancer regions. Interaction is mediated by two C4 zinc finger motifs: the proximal box region (P-box) which ensures sequence specific binding and the α-helical distal box (D-box), which contributes to protein stability and mediates receptor dimerization[7,11,12]. Despite of

the large diversity within the superfamily of NRs, the recognized DNA consensus sequence is rather conserved and includes RGKTCA hexamers (R = A or G; K = G or T)[5,13]. The flexible hinge region, by which DBD and LBD are linked, can be targeted by post-translational modifications. Located in the LBD, the hydrophobic binding pocket can be found, which greatly varies in size among the NRs and is the place for ligand interaction. However, the LBD furthermore enables ligand-independent interactions with co-activators and co-repressors through allosteric changes in the AF2 region[4,7].

1.1.2 Classification

Despite their conserved structural organization, members of the NR family are extremely flexible in their functionality. Moreover, they can not only exist as monomers but also form homo- or heterodimers. Dimerization is facilitated by sequences which are contained within the DBD and LBD[14-16]. Based on its mode of action and its DNA binding properties, the superfamily of NRs is categorized into three groups[5,8] (Figure 2):

Type I receptors distinguish themselves from other NR family members by their cellular localization as most of them are synthesized in non-active forms and anchored in the cytoplasm by interaction with heat-shock proteins (HSPs). Steroid hormone ligands are produced by endocrine glands. Upon hormone binding, type I NRs are released from their chaperone which allows exposure of the nuclear localization sequence and subsequent translocation into the nucleus. Here, they preferentially bind to palindromic response element sequences as homodimers[5,17,18]. Gene transcription is then regulated by association of the ligand-receptor complex with transcriptional coactivators. This group includes the well characterized steroid hormone receptors such as estrogen receptor and glucocorticoid receptor (GR)[19].

Type II receptors, such as the peroxisome-proliferator-activated receptors (PPARs) and liver X receptors (LXRs), reside in the nucleus and are often permanently bound to their DNA response element, even in the absence of ligand[5,16]. These NRs mostly exert repressive functions and typically form heterodimers with the retinoid X receptor (RXR)[5,20]. Ligand binding evokes the dissociation of co-repressor complexes

and their replacement by co-activator molecules. Co-activators often contain enzymatic functions that help to decondense chromatin. Interestingly, this class of NRs is typically regulated by molecules that are produced in an auto- or paracrine manner. This allows cell-autonomous feedback regulation[5,19,21].

The third type of receptors primarily binds to DNA as monomers. For most of these NRs, endogenous ligands are not yet described which is why they are called "orphans". These NRs regulate gene transcription mainly through changes in their own expression or in response to post-translational modifications[5].

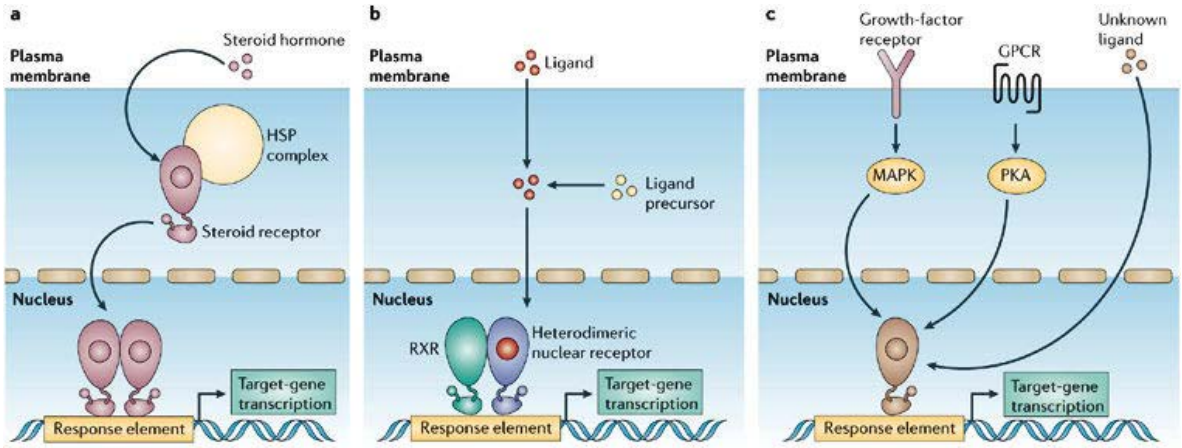

Figure 2: Classification of NRs based on their activation and DNA binding properties.

NRs can be classified into three groups: steroid hormone receptors that bind to their DNA response element as homodimers (**a**), receptors that heterodimerize with retinoid X receptors (RXRs) (**b**) and the orphan NRs, which typically bind to the DNA as monomers (**c**). The orphan receptors might regulate gene transcription in response to post-translational modifications such as phosphorylation or SUMOylation. GPCR: G protein-coupled receptor; MAPK: mitogen-activated protein kinase; PKA: cAMP-dependent protein kinase. Image adapted from[8].

However, other classifications of NRs exist. These are either based on their localization within the cell (cytoplasm versus nucleus), their DNA binding and dimerization properties (homodimers that bind to inverted DNA repeats, heterodimers, homodimers that bind to direct repeats and monomers)[22] or sequence homology (NR class 0 to 6)[23]. Interestingly, apart from their genomic action in the regulation of gene expression, it is reported that some NRs can also exert rapid effects through DNA-independent protein-protein interactions.

1.1.3 Orphan nuclear receptors

For the group of NRs, which are referred to as "orphans", no endogenous ligands have been identified so far and it is not clear if physiologically relevant ligands exist at all. Interestingly, orphan receptors often respond to xenobiotics in the environment and subsequently mediate the transcription of detoxifying enzymes such as CYP molecules. NRs thereby establish a regulatory interface between the environment (external) and the human genome (internal)[24]. Orphan NRs typically show transcriptional activity even in the absence of any ligands. Like the other NR family members, they can be subjected to post-translational modifications by various signaling pathways such as phosphorylation, SUMOylation or acetylation. Importantly, apart from the direct modulation of NR activity these modifications can also influence different other components of the NR-mediated transcriptional regulation machinery including the interaction of NRs with co-regulators or even the NR subcellular localization[25].

Keeping in mind that the expression of co-regulatory proteins might be tissue specific, that there exists a huge range of signaling pathways and a broad spectrum of post-translational modifications which can influence both, NRs and their co-regulatory proteins and that the turnover rate of NR-protein complexes allows combinatorial or sequential interaction with different co-regulators, it becomes clear that the regulation of NR activity is impressively complex.

1.1.4 Nuclear receptors in T cell development and inflammation

It is well known that steroid hormones exert profound influence on the immune system and it is hence not surprising that synthetic glucocorticoids (GC) are among the most commonly prescribed drugs worldwide[26]. Although immunosuppressive when applied in pharmacological concentrations, endogenous GCs seem to rather modulate the immune system. It was observed that upon exposure to prolonged periods of stress, which causes elevated GC levels, immune responses are shifted from a T_H1 promoted cell-mediated type to a more T_H2 type humoral answer[27]. This can be explained by the ability of GCs to repress the transcription of pro-inflammatory

molecules via the glucocorticoid receptor (GR). It is furthermore widely accepted that GCs are linked to apoptosis in the immature T cells of the thymus. However, its concrete role during thymocyte selection remains controversial. While some studies suggest that GCs influence the thresholds for TCR-mediated positive and negative selection[28], thymus-specific GR knockout animals failed to provide any support for this hypothesis[29]. However, the pronounced sensitivity of thymocytes to GCs and their constitutive production in the thymus strongly suggest a critical role of GCs in T cell development.

Another member of the NR superfamily that is involved in the modulation of immune responses is the small heterodimer partner (SHP). SHP is an atypical orphan NR which lacks a DBD and exerts its regulatory role through direct interaction with other NRs mostly by trans-repression. One example is its ability to negatively regulate cell proliferation by repression of cyclin D_1 encoding genes[30]. Several studies suggest a role of SHP in the modulation of innate immune responses via inhibition of the Toll-like receptor (TLR) signaling pathway[31].

The list of NRs that play key roles in T cell development and function is by far not complete but shall be limited to a third example: the orphan NR Nur77. While Nur77 was first identified as an immediate early serum-induced gene, it was then discovered to also become rapidly upregulated upon antigen receptor ligation or phorbol ester plus ionomycin treatment[32]. For maximum induction of Nur77, combined signals from the TCR-CD3 complex as well as additional co-stimulatory signals from ligand-activated CD28 antigens are required. However, detailed molecular mechanisms remain unknown. Besides the transcriptional regulation of target gene expression[33,34], Nur77 in heterodimeric complex with RXRα can also translocate to the mitochondria and directly interact with the anti-apoptotic Bcl2 protein to induce apoptosis[35,36].

1.2 Liver receptor homolog-1 (LRH-1)

Liver receptor homolog-1 (LRH-1) is a transcription factor that belongs to the Nr5a subfamily of NRs. It was originally identified in mouse due to its sequence homology to the Fushi tarazu factor-1 (Ftz-F1) of *Drosophila melanogaster*[37]. However, orthologues were soon found in other vertebrates including fish, rat and humans[38]. The Ftz-F1 box is a conserved stretch of 26 amino acids located at the carboxy-terminus of the DBD where it dictates DNA binding. While most NRs form homo- or heterodimers, it is characteristic for the members of the Nr5a subfamily, namely LRH-1 and steroidogenic factor-1 (SF-1), to bind with high affinity to their cognate target sequence 5′-(Py)CAAGG(Py)C(Pu)-3′ as monomers[37].

1.2.1 Structure of LRH-1

Human LRH-1 has been isolated independently by different research groups and was thus provided with different names such as fetoprotein transcription factor (FTF)[39], human B1-binding factor (HB1F)[40] and CYP7A1 promoter-binding factor (CPF)[41]. Its gene is located on chromosome 1 q32.11[39] and contains eight exons, spanning more than 150 kilobases[42]. The LRH-1 transcription start site is located 310 bp upstream of the translation start site and contains a TATA box motif[42].

Exons 1 and 2 encode the amino-terminal A/B region, followed by a highly conserved DNA binding domain (DBD), or C domain, which is derived from exons 3 and 4 (Figure 3). Exons 3 and 4 each contain one zinc-finger motif and are hence responsible for the DNA-binding specificity and the direct DNA interaction. Exon 5 is the largest exon and covers the conserved Ftz-F1 box, the unusually large and conformationally flexible hinge region and part of the ligand binding domain[43,44]. The other part of the LBD is derived from exons 6-8, of which exon 8 also comprises the AF-II region[42].

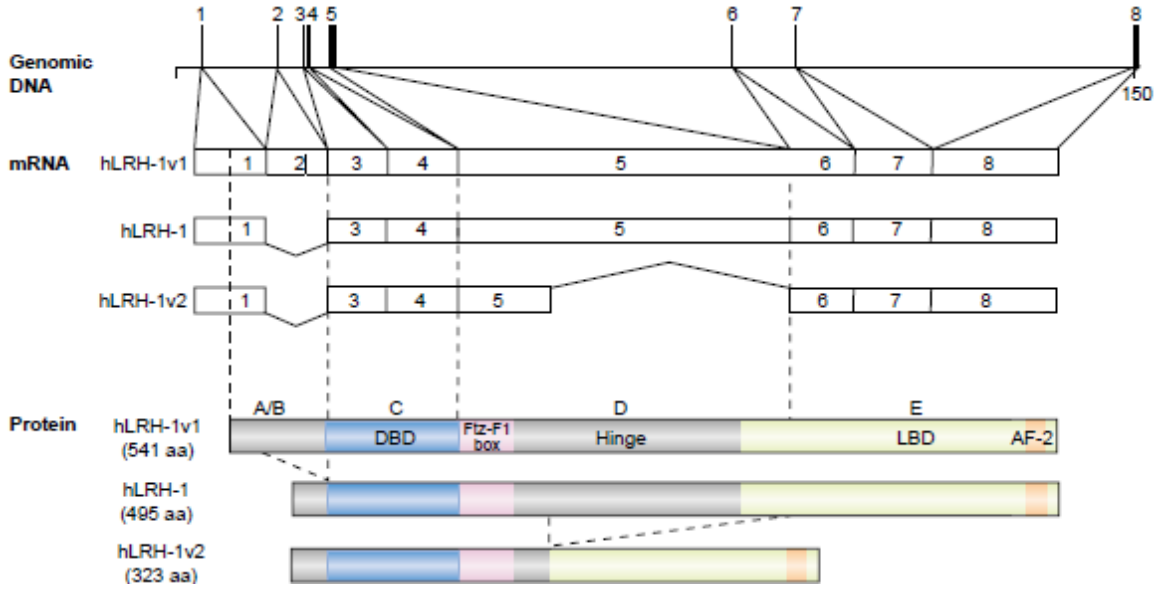

Figure 3: Structure of the human *NR5A2* gene and corresponding mRNA or protein isoforms.

The human LRH-1 gene spans 150 kb and comprises eight exons (represented by black bars), which encode particular protein domains. Alternative splicing results in three different isoforms: LRH-1v1, the most abundant isoform LRH-1 which lacks exon 2 and the dominant negative form LRH-1v2 with an additional splicing of exon 5. Image adapted from[38].

Three different isoforms have been found, which are derived from alternative splicing: the most abundant isoform, which is simply called LRH-1, is identical to the largest isoform LRH-1v1 with the exception that it lacks exon 2 in the amino-terminal A/B domain (Figure 3)[45]. Nevertheless, both isoforms are reported to have similar DNA-binding and transactivation capacities. An additional deletion in the AF2 containing exon 5 results in the smallest and least abundant isoform LRH-1v2, which is a dominant negative protein that cannot activate transcription[46]. Interestingly, while all splicing sites possess the "GT-AG" consensus residues, the size of the introns varies remarkably from 1549 bp (Intron 3) to 62.385 bp (Intron 5)[42].

Mouse and human LRH-1 share a high similarity regarding the amino acid sequence within their DBD and LBD[38]. Although there is by far not as much information about murine LRH-1 in the literature as it is available for its human orthologue, there are some differences that shall be pointed out:

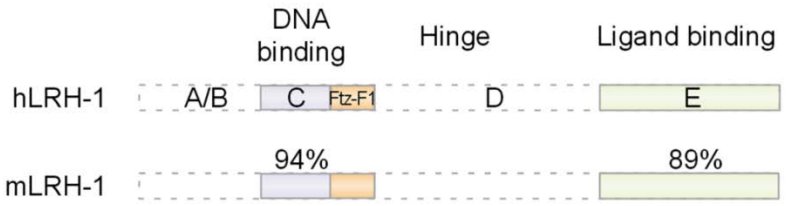

Figure 4: Close homology between human and mouse LRH-1.

The DNA binding domain (DBD) and ligand binding domain (LBD) of human and mouse LRH-1 show a high degree of similarity. Numbers indicate percentage of identity in amino acid alignments. The characteristic Ftz-F1 domain is also conserved between species. Image adapted from[38].

In mice, in which an additional LRH-1 retro-pseudogene has been discovered, LRH-1 maps to cytoband E4 of chromosome 1[47]. The DBD and LBD are highly similar to the human ones[38]. Interestingly, mouse LRH-1 is described to contain 11 exons (NCBI) and six splice variants which seem to use between two and nine exons (ENSEML).

Crystal structures revealed that, in contrast to other NRs, the LBD of mouse LRH-1 contains an Nr5a-specific extended H2 helix which indirectly stabilizes the active conformation of helix H12 and its AF2, leading to ligand independent basal activity. Furthermore, the introduction of bulky side chains and hence the alteration of the shape and size of the large hydrophobic binding pocket did not influence LRH-1 activity. However, human and mouse LHR-1 both seem to be targeted by phospholipids[48,49]. Although SF-1 and LRH-1 are both able to bind phospholipids in their LBD, physiological ligands are not yet known. However, the orphan members of the Ftz-F1 subfamily are typically constitutively active without ligand binding[50,51].

1.2.3 Regulation of LRH-1 expression

Upstream of the *Nr5a2* gene, various regulatory sequences and transcription factor binding sites are located which are able to modify the expression of LRH-1. Conserved between human and mouse are three binding sites for GATA transcription factors and Nkx homeodomain recognition motif[42,47]. Tumor necrosis factor α (TNFα) is also reported to induce the transcription of LRH-1[52]. However, the regulatory network that controls the expression of LRH-1 seems to be complex[38].

Besides the regulation on a transcriptional level, LRH-1 activity can also be modulated through the binding of small hydrophobic molecules such as steroid hormones, nutrients and xenobiotics[53]. Although no physiological ligand is known so far, synthetic phospholipids were shown to influence protein conformation and hence activity. In this regard, the antidiabetic dilauroyl phosphatidylcholine (DLPC) was found to increase the activity of human and mouse LRH-1[54,55], while different synthetic compounds including 3d2[56] and SR1848[57] are known to act as LRH-1 inhibitors. While 3d2 was described to stabilize the LBD in an inactive conformational state, SR1848 seems to translocate LRH-1 from the nucleus into the cytosol.

Nevertheless, the activity of LRH-1 is primarily controlled through interactions of co-activator or co-repressor proteins[51]. Co-regulatory proteins include the repressive interaction with Dax-1 (dosage-sensitive, sex reversal adrenal hypoplasia critical region, on chromosome X, gene 1) and SHP (Figure 5). Interestingly, Dax-1 and SHP both are atypical orphan NRs which, in contrast to other family members, lack a DBD. Besides several co-activator molecules, post-translational modifications including SUMOylation[58] and phosphorylation[43] are further described to regulate LRH-1 activity.

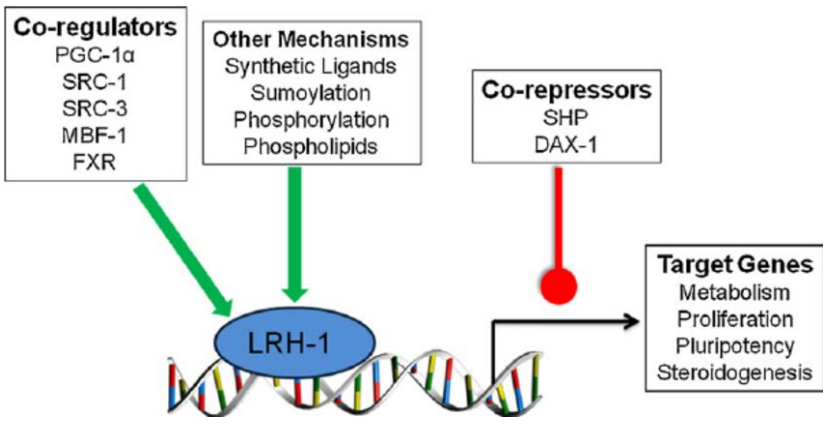

Figure 5: LRH-1 regulatory mechanisms.

The activity of LRH-1 can be modulated by co-regulators and co-repressors, synthetic ligands or post-translational modifications to finally regulate the expression of genes involved in metabolism, proliferation, pluripotency and steroidogenesis. Image adapted from[59].

1.2.4 Function of LRH-1

LRH-1 is predominantly expressed in tissues derived from endoderm[38] where it acts as a key transcriptional regulator in many different biological processes including development, metabolism, reproduction and proliferation (Figure 6).

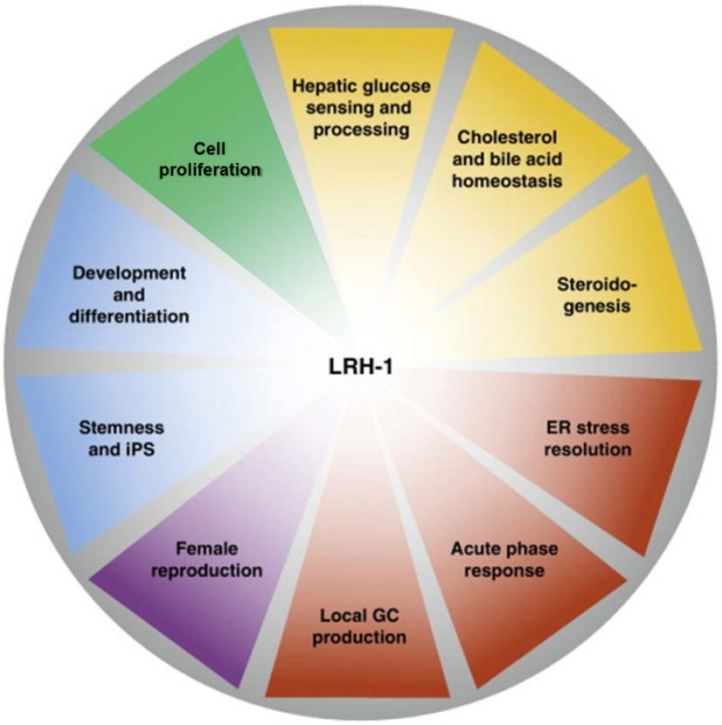

Figure 6: Diverse biological functions of LRH-1.

LRH-1 is a key regulatory factor in metabolic processes (yellow), stress response (red), female reproduction (purple), development (blue) and cell proliferation (green). Image modified from[60].

Development and pluripotency

LRH-1 plays a critical role in the maintenance of stem cell pluripotency as well as the early embryonic development and cell differentiation. It is thus not surprising that homozygous deletion or mutation of genomic LRH-1 leads to death around embryonic day (E) 6.5 - 7.5[61-63]. Embryonic stem cells require an array of several transcription factors, such as Oct4 and Nanog, to maintain pluripotency. Expression of these proteins must be tightly regulated. It is confirmed that LRH-1 is an upstream transcription factor of Oct4[63,64] and that it can further contribute to the maintenance

of pluripotency by controlling Nanog expression in interaction with the β-catenin/Wnt signaling pathway[61]. LRH-1 mRNA is temporally but abundantly expressed during early differentiation of the foregut endoderm[65,66], and shows an adult expression pattern with a characteristic and persistent expression in the liver, exocrine pancreas, intestine, ovaries and crypts[59].

Metabolism

LRH-1 does not just regulate the enterohepatic development but it is also well known for its key regulatory function in the cholesterol metabolism. In hepatocytes, LRH-1 regulates the transcription of Cyp7A1 and Cyp8B1, enzymes which catalyze bile acid synthesis[67]. As it is furthermore involved in the transcription of transporter proteins and the recycling of bile acids, it is an important regulator of bile acid homeostasis[59]. Another process, which is regulated by LRH-1, is the reverse cholesterol transport. To remove excessive cholesterol, it has to be transported from the periphery to the liver, where it is converted into bile and finally can be secreted[68-70].

Diabetes and mild obesity[52,70] are metabolism related diseases which are associated with LRH-1. In the liver, which is the main source of blood glucose, LRH-1 regulates the expression of glucokinase (GCK) and thereby synthesis and breakdown of glycogen as well as fatty acid synthesis[71]. Recent studies show that hepatic glutamine metabolism is also dependent on LRH-1, as it directly controls the expression of the phosphate-activated glutaminase 2 (Gls2)[72].

Steroidogenesis

Glucocorticoids (GC) are steroid hormones that fulfill important functions during lymphocyte development[28,73] and in the regulation of immune responses. They are mainly but not exclusively secreted by the adrenals[74]. Interestingly, extra-adrenal synthesis was also observed in the epithelium of the intestine, which hosts the largest population of immune cells within the body[75]. In the intestine, transcription of GCs in response to immunological stress is indirectly controlled by LRH-1 via transcriptional regulation of cytochrome P450 family members (CYP)[38,76]. These local GCs exert

immunosuppressive functions such as the attenuation of antigen-specific T cell activation during viral infections[75].

Cell proliferation

Besides the regulation of local glucocorticoid synthesis, LRH-1 was found to contribute to the epithelial cell renewal by controlling cell proliferation in the intestinal crypts. More precisely, LRH-1 is described to coordinate the cell cycle transition from G_1- to S-phase via the regulation of cyclins D_1, E_1 and c-myc[77,78]. While the cyclin D_1 promoter lacks an obvious LRH-1 response element, a perfect LRH-1 binding site was found within the cyclin E_1 promoter, which is conserved between mouse and human[78]. Further experiments showed that, in the intestine, cyclin D_1 and c-myc are indirectly regulated by LRH-1 via crosstalk with the Wnt/β-catenin signaling pathway irrespectively of DNA binding. The transcription of cyclin E_1, in contrast, is directly controlled by LRH-1 on a genomic level[78]. As dysregulated cell proliferation promotes tumor formation, it is not surprising that aberrant LRH-1 expression is observed in many human tumors including breast[79-82], gastrointestinal tract[83-85] and pancreas[86-88].

1.2.5 Role of LRH-1 in immune cells

Although the current knowledge concerning the expression and function of LRH-1 in immune cells is enigmatic, there are some reports which are to be mentioned. During a study correlating LRH-1 expression with cancerogenous cell proliferation, Benod et al. observed specific LRH-1 immunostaining in tumor-infiltrating lymphocytes[86]. Later, Lefèvre et al. described LRH-1 expression and an anti-inflammatory role in alternatively activated macrophages[89]. A third observation was just reported recently by Schwaderer et al., who found that LRH-1 regulates the transcription of Fas (CD95) ligand[90] and that inhibition of LRH-1 attenuated the expression of pro-inflammatory cytokines in macrophages[91].

1.3 The adaptive immune system

The immune system comprises two parts, which work closely together but have different tasks: the innate and the adaptive defense. While the innate immune response is a first and general reaction against pathogens, the adaptive immune response enables the body to recognize and remember specific pathogens. In the latter one, B and T lymphocytes are the main type of cells that is involved.

A typical adaptive immune response starts with an immature antigen-presenting cell (APC) that captures an antigen somewhere in the body, subsequently matures and migrates to secondary lymphatic organs. This is the place, where immature B or T lymphocytes can best interact with the APC and, in case of matching antigen, activation is induced. While B cells can defeat pathogens in the blood and body fluids by differentiation into antibody producing plasma cells upon encountering a specific antigen, T cell-mediated immune responses are necessary to eliminate pathogens from within the tissue or cancerous cells. T lymphocytes therefore require the ability to discriminate between healthy and infected cells.

In contrast to healthy cells that only express their own proteins, infected cells also contain pathogen derived proteins. These proteins are broken down into small fragments which can then be loaded onto minor histocompatibility complexes (MHC) on the T lymphocyte surface to form peptide-MHC complexes (pMHC). T cells have the unique ability to recognize foreign pMHCs, while they do not respond to self-MHC/self-peptide arrangements. This is called antigen-discrimination and T cells are specially trained for this in the thymus[92,93].

1.3.1 T cell development

The development of peripheral αβ T lymphocytes starts with bone-marrow-derived, hematopoietic stem cells that enter the thymus via blood vessels (Figure 7). Due to their lack of CD4 and/or CD8 expression they are termed double negative (DN). These lineage negative thymocytes can further be subdivided into four stages of differentiation (DN1 – DN4) according to their CD25 and CD44 expression pattern

(DN1: $CD44^+CD25^-$; DN2: $CD44^+CD25^+$; DN3: $CD44^-CD25^+$; CD4: $CD44^-CD25^-$) as well as their TCR status[94-97]. Through stage DN2 – DN4, thymocytes interact with cortical thymic epithelial cells (cTECs) and undergo V(D)J re-arrangement of the TCR β-chain. Together with an un-rearranged α-chain it forms the pre-TCR[98]. V(D)J re-arrangement is catalyzed by the recombination activation gene-1 (RAG-1). Due to the lack of functional TCR, RAG deficient mice do not develop mature B or T cells[99].

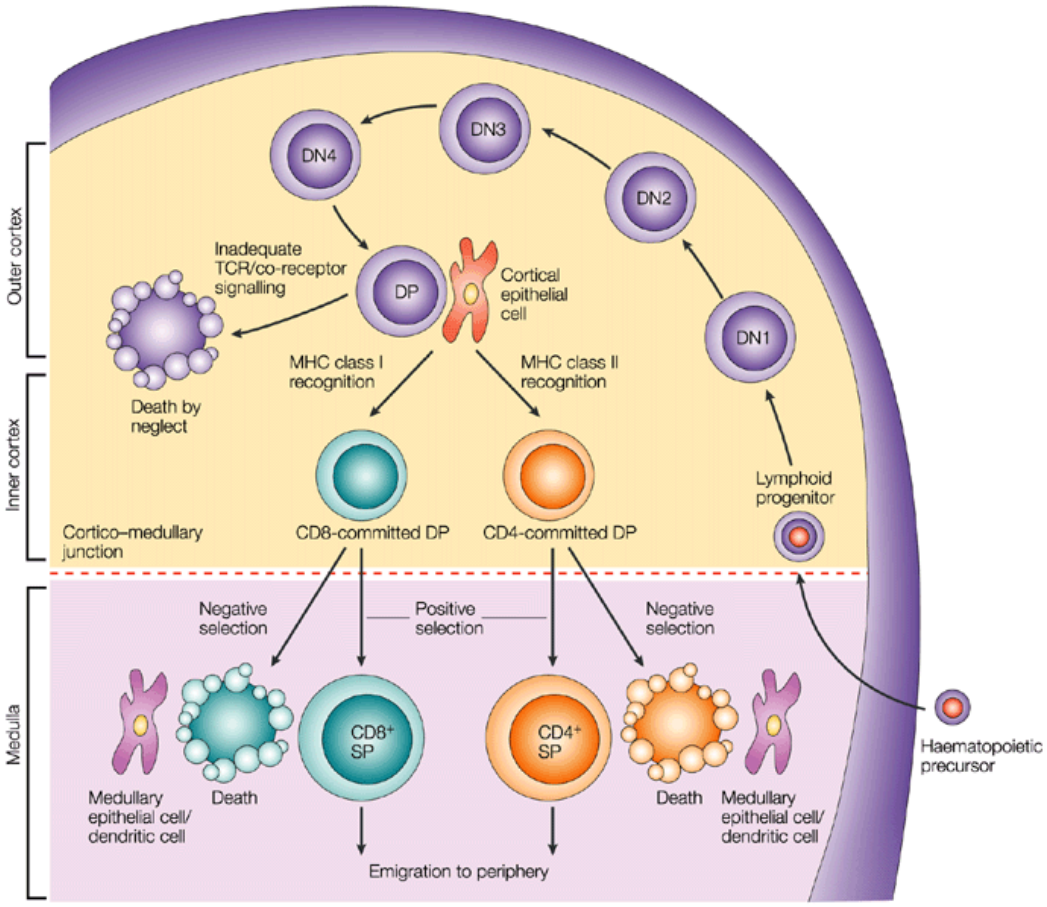

Figure 7: Overview of intra-thymic T cell development.

The thymus is organized in the outer cortex and the inner medulla area. During maturation, thymocytes are characterized phenotypically by the expression of the cell surface markers CD4, CD8, CD44 and CD25. Death by neglect, negative or positive selection result in a subset of self-tolerant single positive lymphocytes which are finally released into the periphery. DN: double negative; DP: double positive; SP: single positive; TCR: T cell receptor; MHC: major histocompatibility complex; Image adapted from[96].

Upon successful TCR re-arrangement, DN4 thymocytes undergo massive expansion, upregulate both CD4 and CD8 molecules on their surface and are now called double positive (DP) lymphocytes. The pre-TCR α-chain is now replaced by a new re-

arranged TCR α-chain and finally yields a mature αβ-TCR. DP thymocytes interact with thymic epithelial cells, which express both MHC class I and II molecules in a high density on their surface[98,99]. Interaction of DP thymocytes with self-pMHC complexes now dictates the fate of the thymocyte and "selects the useful, neglects the useless and destroys the harmful"[100]. Most DP thymocytes express TCR molecules that have no or very low affinity to self-peptide-MHC complexes, so that they do not get any survival signals and die by neglect. In contrast, a very small fraction of DP thymocytes carries a TCR with very strong affinity to self-ligands. These lymphocytes have to be destroyed as they potentially cause autoimmunity. They die by induction of apoptosis in a process called negative selection[96]. Finally, T cells that bind to the self-peptide MHC complexes with intermediate affinity receive survival signals but no apoptosis signals which allows further maturation and lineage-specific differentiation into $CD4^+$ or $CD8^+$ single positive (SP) cells. This process is called positive selection and ensures the generation of self-tolerant $CD4^+$ and $CD8^+$ T cells[96,101,102]. Chemokine-directed migration into the thmyic medulla and interaction with medullary TECs and dendritic cells (DCs) are further important for the induction of central tolerance, before the mature lymphocytes are finally released into the periphery[103,104].

1.3.2 T cell homeostasis

Looking at the total number of mature T cells in an organism it is striking that it is almost stable and comparable between individuals of the same sex and age. Importantly, while a specific pool of T cells undergoes massive expansion during an immune response, most of these cells are eliminated in a subsequent deletion phase to restore T cell numbers to normal levels [105]. On the other hand, if T cells are transferred into an immunodeficient host, such as recombination activating gene (RAG)-deficient animals, naïve T cells are able to spontaneously undergo extensive proliferation to increase T cell numbers[106-108]. It is obvious that there exist mechanisms that are responsible for the maintenance of these constant T cell numbers.

One mechanism to control excessive T cell numbers is activation induced cell death (AICD). This form of cell death is mainly mediated by Fas ligand and induced by the restimulation of already activated and expanded T cells without appropriate co-stimulation[109,110]. *In vitro*, this scenario can be mimicked using TCR activated and IL-2 cultured T cells (T cell blasts)[111].

T cell survival and expansion are furthermore influenced by signals that are received primarily through the TCR, co-stimulatory molecules and cytokines including IL-2 and IL-15[112]. While the activation of a T cell requires specific antigens, homeostatic proliferation does not and thus is polyclonal. It is of particular interest that cells that undergo homeostatic proliferation show a characteristic phenotype that is distinct from the one induced by high affinity to self-MHC/peptide complexes. In comparison to high-affinity ligand recognition, cells that undergo homeostatic expansion proliferate slowly, do not enlarge and lack the up-regulation of acute activation markers including CD25 and CD69[113]. Interestingly, those T cells that underwent homeostatic expansion, also acquire effector functions that are characteristic for memory T cells. In this regard, it was observed that under homeostatic conditions expanded $CD8^+$ T cells were able to mediate CTL activity and mount accelerated functional response to cognate antigens, while naïve $CD8^+$ T cells did not[114,115]. The effector response intensity, however, is lower than that of overtly activated effector T cells stimulated with foreign antigen. In this line, massive secretion of IFNγ in response to *in vitro* anti-CD3 stimulation was observed in homeostasis driven wild type C57BL/6 T cells, while this was not observed in naïve control cells. The ability to secrete IFNγ was reported to increase with each cell division[114,116].

While the physiological importance of homeostatic T cell proliferation might be reduced once the secondary lymphatic organs contain large numbers of naïve T cells, it is a crucial factor for the replenishment of the T cell pool under lymphocytopenic conditions.

1.3.3 Secondary lymphatic organs

While the thymus gland as primary organ is in charge of T cell maturation, secondary lymphoid organs such as the spleen and the lymph nodes are responsible for the initiation of an acquired immune response and lymphocyte activation.

The spleen is a dark red, encapsulated organ which is located in the left abdomen underneath the diaphragm. Although the overall size and appearance of the spleen varies between species and individuals, the ratio of splenic weight to body weight is almost constant[117]. The spleen is the largest secondary lymphoid organ and consists of two compartments that differ greatly in their functionality and their morphology: the red and white pulp. While the red pulp is responsible for blood filtration and antibody trapping, degradation of senescent or damaged erythrocytes as well as storage and recycling of iron, the white pulp is the initial point for immune responses to blood-derived antigens[118,119]. The white pulp is further sub-divided into three compartments, characterized by their specific cell populations: the T lymphocyte rich areas which are also known as periarteriolar lymphoid sheaths (PALS), the B cell follicles and the marginal zone macrophages (Figure 8). Furthermore, dendritic cells (DC), plasma cells and capillaries can be found[120]. In the PALS, T cells interact with professional APCs such as DCs and passing B cells, which allows the recognition of foreign antigen and the subsequent initiation of an immune response. In the B cell follicles, activated B lymphocytes can undergo clonal expansion. The marginal zone is an important transit area, where hematopoietic cells can migrate from the blood stream into the white pulp. However, it also contains a pool of unique resident macrophages including the marginal zone macrophages, which typically form a ring around the B- and T-lymphocyte rich areas[121-123].

An adaptive immune response in the spleen is typically initiated with the entry of an APC to the T cell area, which is located within the white pulp. By migrating through the marginal zone and passing the B cell follicles, the activated APC mediates B cell survival and their differentiation into antibody producing plasma cells. When activated APCs enter the PALS, antigen-specific T cells become activated and subsequently migrate to the edge of the B cell follicles, where B cells receive help from

activated T cells[124]. Activated T cells then loose the expression of the CCR7 chemokine receptor, so that their affinity to the splenic white pulp zone is lost. This allows activated T cells to enter the blood stream and subsequent migration to the site of infection. This might occur through the bridging channels, which are direct contact zones of white pulp areas with the marginal zone[125]. However, the detailed molecular mechanisms are still unclear.

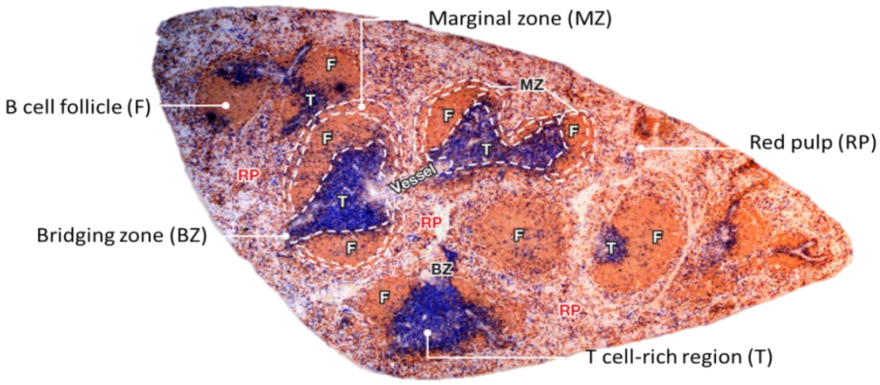

Figure 8: Spleen architecture

Cross-sectional view of a mouse spleen. White pulps are composed of T cell rich areas (anti-CD3; blue), adjacent B cell follicles (anti-B220; intense brown) and the surrounding marginal zone (MZ). Bridging zones (BZ) are regions in which T cell directly interact with the red pulp (RP). Image adapted from[126].

Lymph nodes are bean-shaped encapsulated structures that are distributed along the course of lymphatic vessels. Their structural organization and physiological function is similar to splenic white pulps. However, while the spleen screens for antigens that are present in the blood, lymph nodes drain the lymph from throughout the body. Another difference is the route of lymphocyte entrance. Instead of migration through the marginal zone, lymphocytes enter the lymph nodes via high endothelial venules and afferent lymphatic vessels[127].

1.3.4 Mature T lymphocytes

Depending on their affinity to MHC class I or II molecules during thymic development, T cells develop into $CD8^+$ cytotoxic T cells of $CD4^+$ helper or regulatory T cells[96,128]. While MHC class I transmembrane glycoproteins mainly display fragments of proteins that were intracellularly synthesized and degraded by the proteasome, such as virus particles[129-131],

MHC class II molecules show high affinity to peptides from exogenous sources. These antigens are mainly internalized by various pathways such as phagocytosis, endocytosis and processed in endosomal compartments before association with MHC-II molecules[128,132,133]. However, whenever a T cell encounters its specific antigen delivered on the appropriate MHC molecule and derives co-stimulation by the APC, this T cell quickly undergoes a series of clonal expansion and differentiates.

During an immune response, $CD4^+$ T helper cells provide help for B cells to develop into antibody-producing plasma cells, assist in the activation of cytotoxic T cells as well as macrophages and secrete cytokines[134]. They can furthermore differentiation into different subtypes including regulatory T cells (T_{reg}), T_H1, T_H2 and T_H17 cells to support different types of immune responses by the secretion of appropriate cytokines[135,136]. The major role of T_{regs} is the attenuation of T cell-mediated immunity at the end of an immune reaction and the repression of autoreactive T cells that escaped the selection processes in the thymus. While T_{regs} can develop already in the thymus, they can also be induced in the periphery[137]. However, expression of the transcription factor FoxP3 is mandatory and can hence be used to identify T_{regs}.

To actually eliminate infected or cancerous cells, $CD8^+$ T cells are necessary[138]. Upon appropriate activation, these cells differentiate into cytotoxic effector cells which are capable of eliminating virus-infected or cancerous cells by the release of vesicles containing cytotoxic effector molecules such as granzyme B and perforin. Therefore, $CD8^+$ lymphocytes and target cells have to come to close proximity, this is why this killing mechanism is also known as “kiss of death”[139]. $CD8^+$ T cells can be inactivated by various molecules that are secreted by T_{regs} to prevent autoimmune diseases. Following an immune response elicited by an infection or vaccination, long-term protection against this pathogen is established by the generation of $CD8^+$ but also $CD4^+$ memory T cells. The advantage of memory T cells is that it allows the adaptive immune system to react faster and more efficient to defend the body from pathogens that are already known[138].

All leukocytes express the congenic marker CD45, which belongs to the family of protein tyrosine phosphatases (PTP), on their cell surface. CD45 is a signaling molecule that is involved in the regulation of cell growth and differentiation and in mice, there are two alleles, CD45.1 (Ly5.1) and CD45.2 (Ly5.2) which are identical in their function[140]. As those markers can be distinguished using specific antibodies, CD45 is commonly used as marker to identify the initial source of the T cell in transfer experiments.

1.3.5 T cell activation

Cells that never encountered their specific antigen are called naïve. To proliferate and differentiate into effector T cells, presentation of the specific antigen on the appropriate MHC molecule as well as co-stimulation by APCs are required, which induce a cascade of signaling transduction events (Figure 9)[141].

While the α and β subunits of the TCR are necessary to recognize pMHC, the associated CD3 complex with its subunits γ, δ, ε and ζ is required for intracellular signal transduction[142]. Activation of the co-receptor associated lymphocyte-specific protein tyrosine kinase (lck) leads to phosphorylation of the immunoreceptor tyrosine-based activation motifs (ITAM) of the TCR-CD3 complex. This hence enables binding of ZAP70 (ζ-chain associated protein kinase 70) to the ITAM via two Src-homology (SH2) domains[123,124]. Subsequently, ITAM bound ZAP70 is activated by phosphorylation and in return, phosphorylates the adapter molecules SLP76 (SH2 domain containing lymphocyte protein of 76 kDa) and LAT (linker of activated T cells). These molecules provide a scaffold that allows different signaling molecules to assemble such as phospholipase Cγ1 (PLCγ1), which regulates the hydrolysis of phosphatidyl inositol bisphosphate (PIP2) and generates the second messengers IP3 (inositol 1,4,5-trisphosphate) and DAG (diacylglycerol)[142,143].

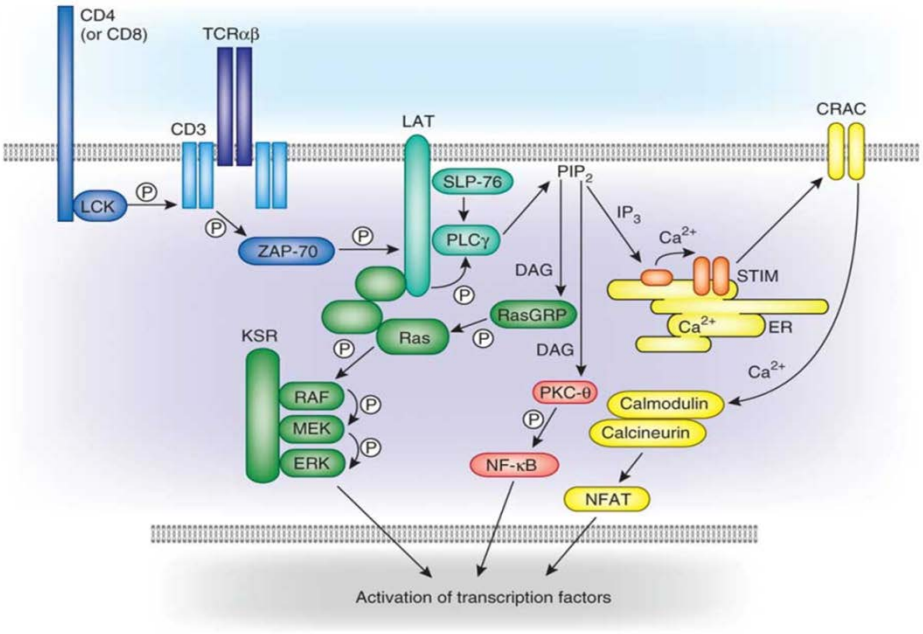

Figure 9: T cell receptor signaling

Signaling is initiated by TCR recognition of pMHC and the subsequent activation of protein tyrosine kinases (blue). Consecutive signaling includes the induction of the Ras-Erk pathways (green), activation of NF-κB (red) and Ca^{2+}-mediated control of NFAT (yellow). Image adapted from[144].

IP3 increases the concentration of intracellular calcium ions (Ca^{2+}) by opening the Ca^{2+} ion channels that are located on the surface of the endoplasmic reticulum (ER). This increase of intracellular Ca^{2+} levels can be mimicked by the pharmacological application of the ionophore ionomycin. Transcription of the nuclear factor of activated T cells (NFAT) can finally be induced via binding of Ca^{2+} to calmodulin and activation of calcineurin[142].

Binding of the other second messenger DAG leads to the activation of the Erk/MAP kinase cascade via activation of RasGRP (Ras guanyl-releasing protein) and NFκB via the activation of protein kinase C (PKC)[145]. PKC can also be activated by the synthetic molecule PMA. T cell activation finally leads to the transcription of genes involved in the survival, homeostasis and effector function of T cells.

1.3.6 Experimental transfer colitis

A typical animal model to study $CD4^+$ effector functions and T cell homeostasis is the induction of experimental colitis by the transfer of naïve $CD4^+CD45RB^{hi}$ T cells into a syngeneic, lymphopenic host. This model allows the control of colitis onset and disease severity as well as the examination of early and late immunological events.

The $CD4^+CD45RB^{hi}$ population of T cells is a naïve subset which is unable to induce the generation of regulatory T cells and, upon activation by intestinal commensal bacteria, undergoes rapid proliferation. Uncontrolled T cell expansion is hence accompanied by colitis and inflammation of the small bowel[146,147]. Colitis is histologically manifested by transmural inflammation, increased bowel thickness, severe leukocyte infiltration, crypt abscesses, loss of goblet cells, damaged epithelial cells and accompanied by diarrhea and body weight loss of the animals[148]. Characteristic for the transfer colitis is the secretion of Th1/Th17 derived cytokines such as IL-2 and IL-17 as well as the up-regulation of TNFα and IFNy in the lamina propria[147].

Another advantage of this animal model is that it can furthermore be extended to study the role of regulatory T cells (T_{regs}). This can be done by the co-transfer of $CD4^+CD45RB^{lo}$ regulatory T cells. $CD4^+CD45RB^{lo}$ cells are able to expand and subsequently suppress inflammation by the secretion of IL-10, TGF-β and IL-35. This leads to the prevention or attenuation of intestinal and colonic inflammation[146,149-151].

1.3.7 Antiviral immune response

Lymphocytic Choriomeningitis Virus (LCMV) is a well characterized enveloped, single-stranded RNA virus of the arenavirus group. This virus is non-cytopathic, which means that it does not lyse its target cells, and known to primarily infect non-lymphocytic cells[152,153]. It is a common natural pathogen of rodents and a typical model to study antiviral immune responses as the T cell response to LCMV is very focused and robust.

Upon infection, LCMV propagates within adult mice and virus titers in the spleen peak around day four. The expansion of virus specific cytotoxic T cells is subsequently

induced and reaches its maximum seven to nine days after infection[154,155]. Around this time, immune competent animals have fully eliminated the virus[156,157]. In mice of the C57BL/6 strain, most cytotoxic T cells recognize the virus specific epitope glycoprotein 33-41 (GP-33) on their MHC class I molecule H-2D_b[158].

While $CD8^+$ T cells are able to kill the virus via perforin-mediated mechanisms, $CD4^+$ T helper cells are not capable to directly eliminate LCMV. However, they are known to orchestrate the effector functions of cytotoxic T cells and influence the anti-viral immune response by inhibition of virus replication[159]. Of particular relevance in the generation of a specific immune response is also an intact splenic micro-architecture[160]. It was observed that especially the marginal zone of the spleen is important for the clearance and retention of LCMV in the spleen as the virus seems to propagate in macrophages and dendritic cells[161-164].

2 Aim of the study

The orphan nuclear transcription factor Liver receptor homolog-1 (LRH-1) is highly expressed in endoderm derived organs such as the liver and intestine. In these tissues, LRH-1 is known to perform key functions in the regulation of development, metabolism, steroidogenesis and cell proliferation. However, the current knowledge about the expression and function of LRH-1 in T lymphocytes is very limited.

The first aim of this thesis was hence to characterize the expression of LRH-1 in immature and mature T cell subsets. Furthermore, the influence of LRH-1 deletion on lymphocyte development was to be examined by the use of animals with LRH-1 deficient T cells.

The second aim addressed to unravel the function of LRH-1 in T cells with a focus on apoptosis induction, T cell activation and cell proliferation using LRH-1 deficient T cells as well as pharmacological inhibitors.

The third goal of this study was to elucidate the role of LRH-1 on T cell effector functions. Different pathogenesis models were therefore chosen to examine the function of LRH-1 in T helper and cytotoxic T cells *in vitro* and *in vivo*.

Altogether, this study aims to gain a better understanding about the importance and role of LRH-1 in T cell development and function and unravel potential applications in the treatment of T cell-mediated inflammatory diseases.

3 Results

3.1 LRH-1 is expressed in the T cell lineage

LRH-1 (encoded by the *Nr5a2* gene) is mainly expressed in tissues of endodermal origin. Knowledge about its expression in cells of the hematopoietic lineage, however, is enigmatic. To reveal the relative abundance of *Nr5a2* expression, gene profiling was performed in different lymphatic organs derived from wild type C57BL/6 mice and related to *Nr5a2* expression in endodermal tissues. Comparison of mRNA levels confirmed the high expression of *Nr5a2* in the liver and the intestine but also revealed transcription in primary and secondary lymphatic organs (Figure 10a).

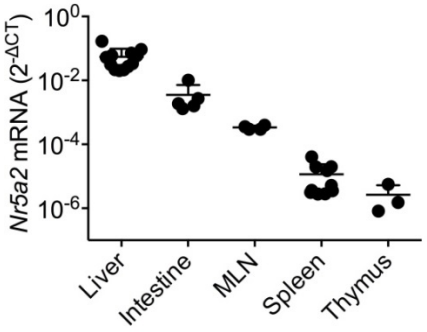

Figure 10: LRH-1 is expressed in lymphoid tissues.

Nr5a2 mRNA expression in endodermal tissue (liver: n = 12; intestine: n = 5) as well as primary and secondary lymphoid organs (thymus: n = 4; spleen: n = 10; mesenteric lymph nodes (MLN): n = 3) derived from C57BL/6 mice. *Actb* was used as reference gene. Mean values ± S.D. are shown.

Although this finding provides a first hint, it does not allow concrete conclusions about the expression of LRH-1 in T lymphocytes. This is because lymphatic organs do not only consist of immune cells but other cell types such as epithelial cells, which are already known to express LRH-1[165]. For a more detailed analysis, T cell subsets derived from thymus or spleen were FACS separated with a purity of more than 98% (Figure 11a-b). Although expression levels were extremely low, *Nr5a2* mRNA was clearly detectable in all immature and mature T cell subsets (Figure 11c-d).

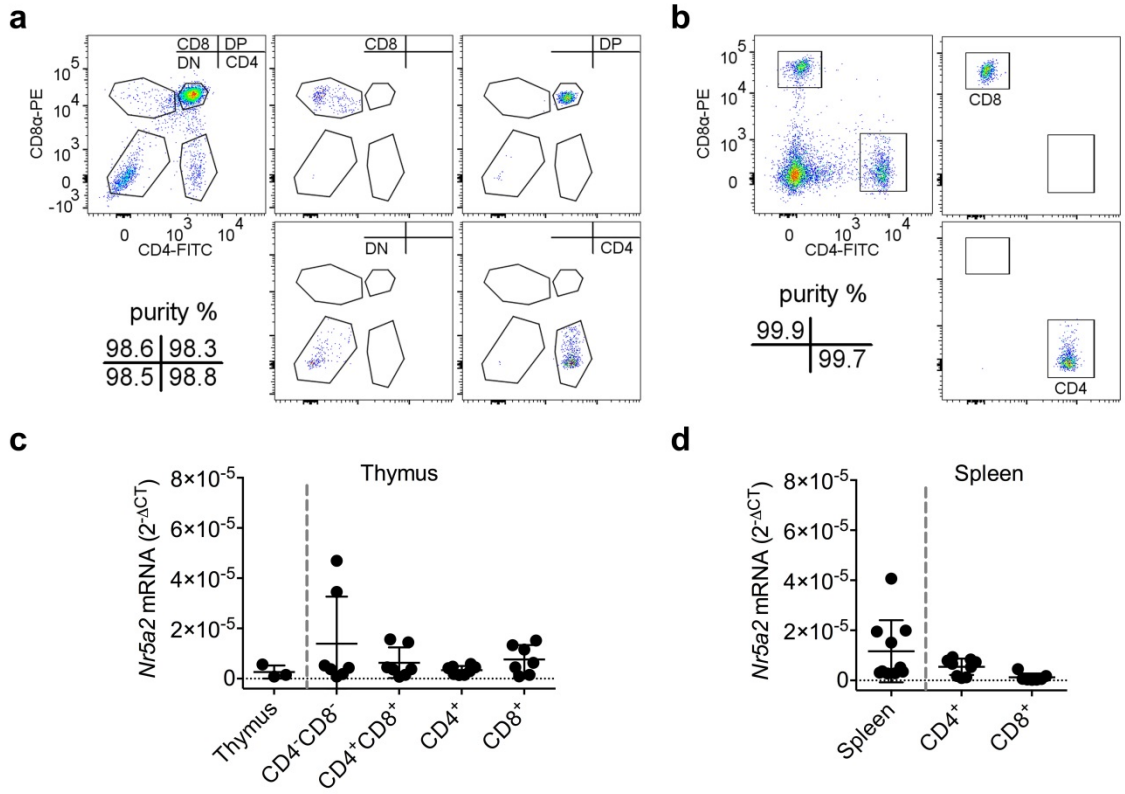

Figure 11: LRH-1 is expressed in immature and mature T cells.

(**a**-**b**) Freshly isolated (a) thymocytes (b) and splenocytes derived from C57BL/6 wt mice were highly purified by cell sorting. Representative plots are shown. (**c**-**d**) *Nr5a2* mRNA expression levels were determined in sorted T cell subsets from thymus (c) ($CD4^-CD8^-$: n = 7; $CD4^+CD8^+$: n = 7; $CD4^+$: n = 8; $CD8^+$: n = 7) and spleen (d) ($CD4^+$: n = 9; $CD8^+$: n = 7). *Actb* was used as reference gene. Mean values ± S.D. are shown in each graph.

To explore if LRH-1 is further expressed in human lymphocytes, acute lymphoblastic leukemia T cell lines as well as freshly isolated peripheral blood mononuclear cells (PBMC) were analyzed. In line with murine T cells, *NR5A2* expression was confirmed in all human cell lines tested (Figure 12a). Again, the quantity of *NR5A2* specific PCR products in T cells was very low compared to the colorectal adenocarcinoma cell line Caco2 and the liver cancer cell line HepG2 (Figure 12a).

Functional LRH-1 protein was confirmed in Jurkat lT cells by luciferase reporter assay. Compared to cells that were transfected with a control plasmid, luciferase activity was about eight times higher in Jurkat lT carrying an LRH-1-response element driven reporter construct (Figure 12b). Due to the low expression levels in T cells and the unavailability of appropriate antibodies, it was not possible to further confirm the expression of LRH-1 on a protein level by western blotting.

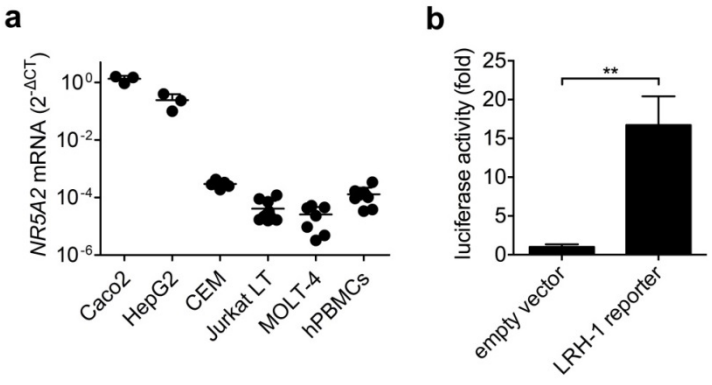

Figure 12: Expression of functional LRH-1 in human T-cells.

(**a**) *NR5A2* expression in human colonic (Caco2: n = 3), hepatic (HepG2: n = 3), T-cell lymphoma (CEM: n = 5; Jurkat lT: n = 11; MOLT-4: n = 7) cell lines and freshly isolated human peripheral blood mononuclear cells (PBMCs: n = 9 biological replicates). *GAPDH* was used as reference gene. (**b**) Transcriptional activity of endogenous LRH-1 in Jurkat lT cells as determined by luciferase reporter assay. Luciferase expression was controlled by five repeats of a LRH-1 response element (5xRE) and normalized to the pGl3 empty vector control (n = 3 independent experiments). Mean values ± S.D. are shown in each graph. ** $p<0.01$

3.2 LRH-1 expression is dependent on cell proliferation and mitogenic stimulation

Under healthy conditions, the majority of peripheral T lymphocytes remains in a quiescent state and does not proliferate. However, upon antigen-specific activation, T cells start to divide rapidly. As LRH-1 is tightly linked with cell proliferation in pancreatic adenocarcinomas[78,86] and intestinal epithelial cells[85], *NR5A2* promoter activity and mRNA expression were compared in resting versus proliferating Jurkat lT cells.

Jurkat lT cells which were transiently transfected with a luciferase expression plasmid under the control of the 1.5 kb human *NR5A2* promoter showed basal activity when compared to transfection with the appropriate MCS3 control vector (Figure 13a). This indicates active *NR5A2* transcription in proliferating Jurkat lT cells and is in line with the observed mRNA and protein expression described in Figure 12a-b. Interestingly, while the luciferase signal was reduced to background levels by serum withdrawal, *NR5A2* promoter activity was clearly enhanced in response to stimulation with PMA plus ionomycin (Figure 13b). As serum withdrawal is known to inhibit cell

proliferation and PMA/ionomycin stimulation leads to polyclonal T cell activation, this observation indicates a relationship between cell division and LRH-1 expression in Jurkat lT cells.

Connection between LRH-1 and the cellular proliferation status was further confirmed by the examination of *NR5A2* mRNA levels of Jurkat lT cells that were cultured under different conditions. Treatment with PMA and ionomycin significantly induced *NR5A2* transcription around five times compared to control cells. Interestingly, transcription was increased even stronger in cells that have been cultivated in serum-free medium for 24 h and hence reversibly arrested in their cell cycle prior to stimulation with PMA and ionomycin (Figure 13c).

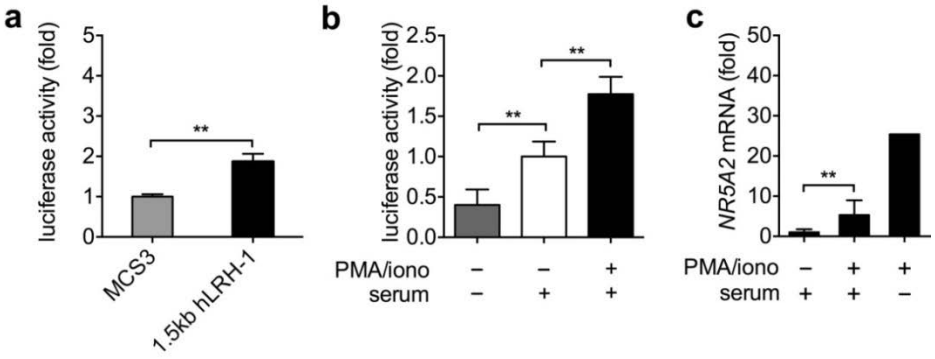

Figure 13: LRH-1 promoter activity is cell cycle dependent.

(**a**) Endogenous *NR5A2* promoter activity in Jurkat lT cells as assessed by luciferase reporter assay. Luciferase expression was assessed by a 1.5 kb sequence derived from the human LRH-1 promoter and normalized to the MCS3 empty vector control (n = 3 independent experiments). (**b**) Effect of serum deprivation and/or stimulation with PMA and ionomycin on *NR5A2* promoter activity in Jurkat lT cells (n = 4 independent experiments). Relative luciferase units were normalized to those derived from unstimulated but serum containing conditions (described in a). (**c**) *NR5A2* mRNA expression levels in response to PMA and ionomycin treatment and/or 12 h of serum withdrawal (+ serum: n = 4; + serum/+ PMA/iono: n = 4; - serum/+ PMA/iono: n = 1 biological replicate). Mean values ± S.D. are shown in each graph. ** $p<0.01$.

To further confirm a rapid, mitogen-induced upregulation of *Nr5a2*/*NR5A2,* C57BL/6 splenocytes or human PBMCs were treated with various activating agents for 3 h prior to mRNA quantification. In both species and for all stimuli tested, a significant increase of *Nr5a2/NR5A2* mRNA expression was determined (Figure 14a-b).

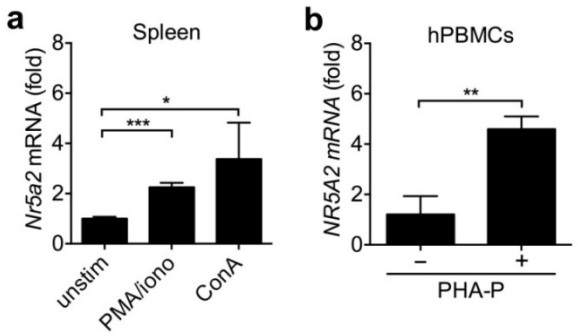

Figure 14: LRH-1 expression is induced early upon mitogenic stimulation.

(**a**) *Nr5a2* mRNA levels in splenocytes after 3 h treatment with PMA plus ionomycin (PMA/iono) or concanavalin A (ConA) normalized to basal expression (unstim) (n = 3 C57BL/6 wt mice per group). *Actb* was used as housekeeping gene. (**b**) *NR5A2* mRNA expression in human PBMCs after 3 h stimulation with phytohemagglutinin P (PHA-P) normalized to basal levels (n = 3 biological replicates). Mean values ± S.D. are shown in each graph. * $p<0.05$, ** $p<0.01$, *** $p<0.001$.

In order to investigate a potential role for LRH-1 in the initiation of cell proliferation, the kinetic of activation-induced *Nr5a2* upregulation was examined in detail and compared to the expression of cell cycle regulating proteins. In response to anti-CD3/anti-CD28 treatment, cell cycle analysis revealed a constant reduction of C57BL/6 splenocytes in the G_0/G_1 phase, while the proportion of cells in the G_2/M phase was increasing over time and reached its maximum around 48 h (Figure 15a-b). This proofs successful activation and initiation of lymphocyte proliferation. CFSE dilution experiments were performed to further track the onset of cell proliferation and distinguish between $CD4^+$ and $CD8^+$ T cell subsets, (Figure 15c-e). Proliferation rate was generally higher in $CD8^+$ T cells compared to $CD4^+$ subsets. In accordance with cell cycle analysis measurements, maximum T cell expansion was monitored between 36 h and 48 h (Figure 15c-e).

Aiming to correlate *Nr5a2* induction with cell cycle progression, mRNA levels of cyclins and *Nr5a2* were analyzed next. As expected, expression of c-myc (encoded by the *Myc* gene), which is a direct regulator of the cell cycle machinery, was induced very early after activation (Figure 14f). Interestingly, also *Nr5a2* transcription was upregulated soon after stimulation, with a peak between three and six hours (Figure 14g). In line with the reported transcriptional control of cyclin E_1 by LRH-1[78], *Ccne1* mRNA expression was induced subsequent to *Nr5a2* (Figure 14h).

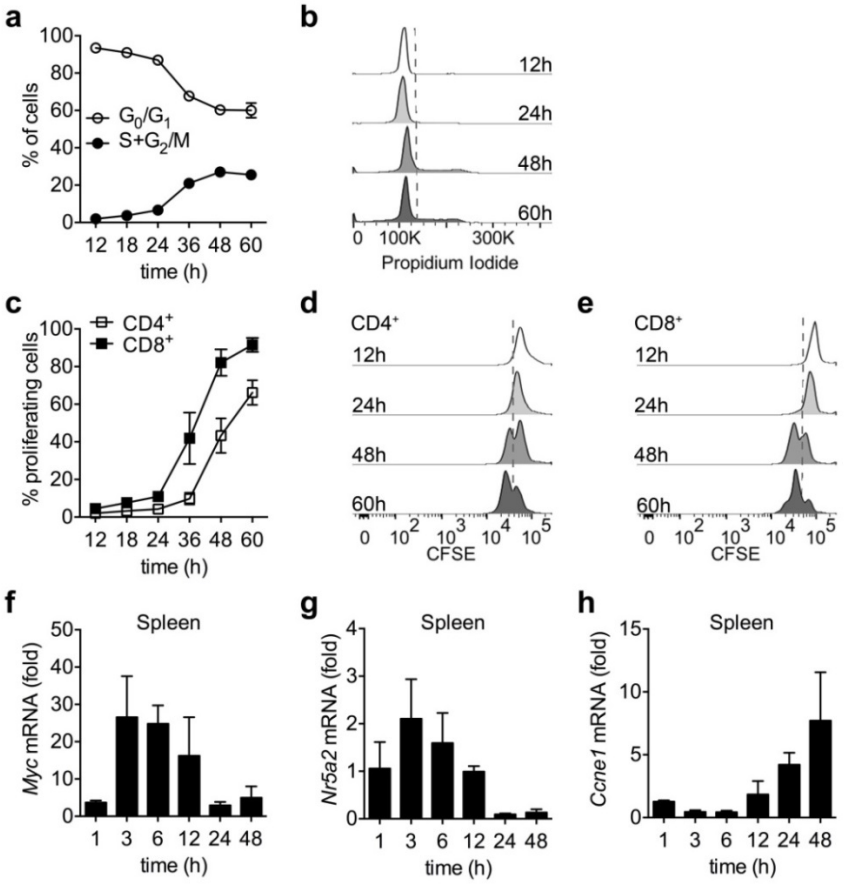

Figure 15: Kinetic correlating T cell activation to cell proliferation and cyclin expression.

(**a-h**) Splenocytes were stimulated with 3 µg/ml plate bound anti-CD3 and 1 µg/ml soluble anti-CD28 antibody (n = 3 C57BL/6 mice). (a) Cell cycle profiles were analyzed by hypotonic propidium staining at different time points following activation. (b) Representative histograms. (c) Proliferation of $CD4^+$ and $CD8^+$ mature T lymphocytes was assessed by CFSE dilution. Representative histograms are shown for (d) $CD4^+$ and (e) $CD8^+$ T cells. mRNA expression levels of (f) *Myc*, (g) *Nr5a2*, and (h) *Ccne1* were determined by quantitative RT-PCR and normalized to the unstimulated control. *Actb* was used as reference gene. Mean values ± S.D. are shown in each graph.

3.3 Conditional deletion of LRH-1 in T cells is specific and efficient

Based on the provided evidence that LRH-1 is expressed in T cells and involved in steps subsequent to activation, a mouse model was generated to further investigate a potential role of LRH-1 in T cells. As the complete deletion of LRH-1 is known to be embryonically lethal, a conditional knockout system based on the Cre/lox strategy was chosen in which T cell specific deletion by CD4 promoter-driven Cre recombinase.

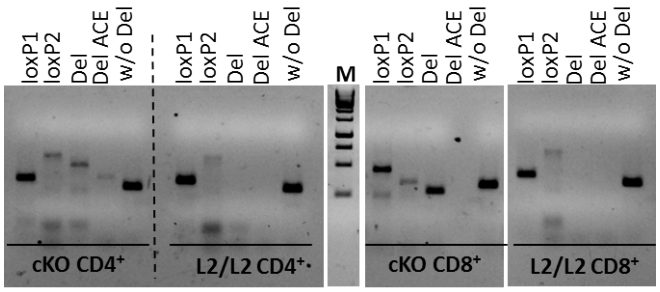

Figure 16: Verification of genomic deletion.

Deletion-specific or control fragments were amplified by PCR and subjected to agarose gel electrophoresis. loxP1/loxP2: P1 or P2 site of the *Nr5a2* gene that is flanked by the loxP sequence; Del: deletion-specific fragment; Del ACE: deletion-specific PCR product using primer ACE 225; w/o Deletion: control product that is formed if deletion did not occur; M: marker (GeneRuler™ 1kb DNA ladder; Thermo Scientific)

In purified T cell subsets, deletion of LRH-1 was verified by the detection of a specific PCR product (Figure 16). Low basal expression in T cells as well as the lack of appropriate antibodies impeded further verification on a protein level. However, presence of deletion-specific amplification fragments alone does not allow conclusions concerning the efficiency of Cre-mediated LRH-1 deletion. Unfortunately, determination of knockout efficiency by qPCR also failed as different selected primer combinations led to unspecific SYBR green melting curves.

To overcome this problem, a second mouse line was generated which, additionally to floxed LRH-1 and CD4-driven Cre recombinase, carries two alleles of the double-fluorescent mTmG reporter. These mice are named LRH-1 mTmG CD4-Cre. Membrane-targeted tandem dimer Tomato (td-mTomato) is ubiquitously expressed in all cells of these mice and exhibits red fluorescence when examined under the microscope or by flow cytometry. Cre-driven excision of loxP flanked tandem dye segments leads to the conversion from red to green (GFP) fluorescence[166]. As the CD4 promoter becomes activated during the double positive stage of thymocyte maturation, specific LRH-1 deletion was first quantified in immature T cells.

As expected, conversion to green fluorescence was minimal in the very immature double negative population of thymocytes, indicating that LRH-1 is not yet deleted at this stage (Figure 17a-b). Concurrent with the expression of CD4, double positive thymocytes were found to express mGFP already in around 90% of cells

(Figure 17a, c). Same tendencies were observed in single positive CD4⁺ thymocytes (Figure 17a, d-e). Although slightly reduced in CD8⁺ T cells, deletion was still very efficient with an overall rate of approximately 80% (Figure 17e).

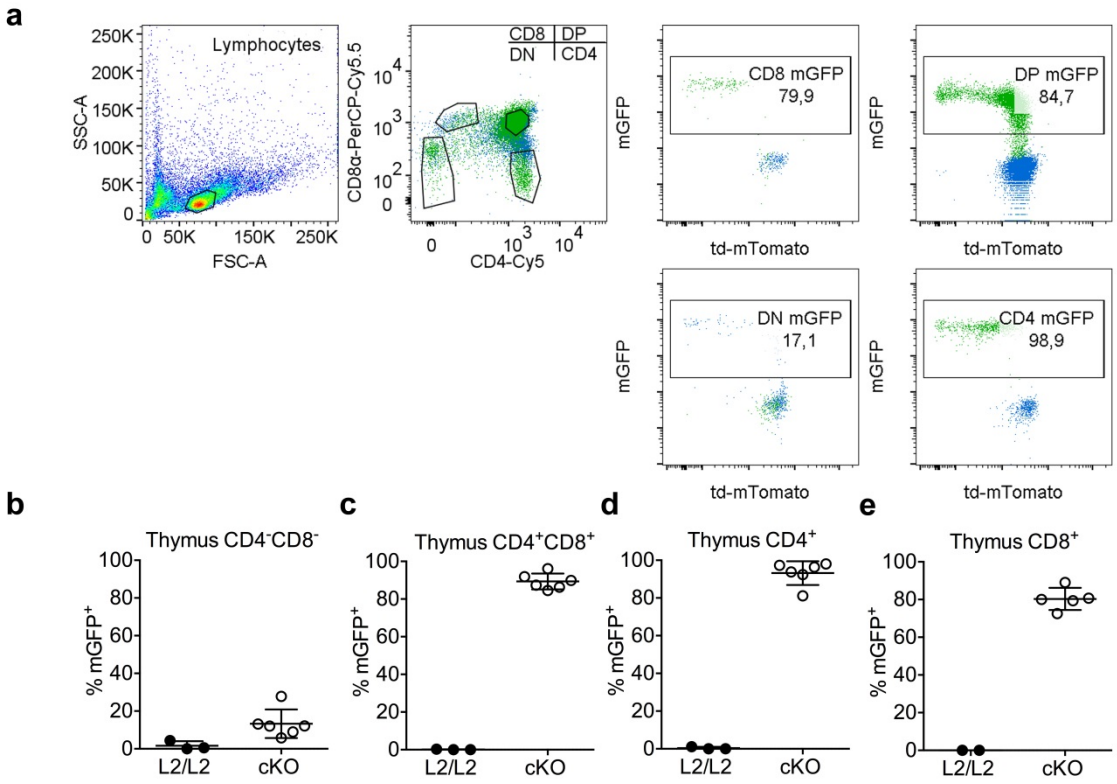

Figure 17: Efficiency of CD4-Cre mediated LRH-1 deletion in immature T lymphocytes.

(**a**) Representative overlays showing the distribution of mGFP⁺ and td-mTomato⁺ thymocytes in CD4-Cre negative (L2/L2; blue) or CD4-Cre positive (cKO; green) *Nr5a2*$^{L2/L2}$ mTmG mice as assessed by flow cytometry. Numbers indicate percentages of mGFP⁺ cells in the corresponding T cell subset. (**b-e**) Quantitation of mGFP reporter expression indicating LRH-1 deletion in (b) CD4⁻CD8⁻, (c) CD4⁺CD8⁺, (d) CD4⁺ and (e) CD8⁺ thymoctes (L2/L2: n = 3; cKO: n = 6). Mean values ± S.D. are shown in each graph.

Verification and quantitation of LRH-1 deletion were next extended to the mature T cells of the periphery. Therefore, LRH-1 mTmG CD4-Cre splenocytes were analyzed for fluorescence conversion. In line with the observation in single positive thymocytes, deletion was almost complete in peripheral CD4⁺ T cells and slightly lower but still very efficient in CD8⁺ lymphocytes (Figure 18a-b). Specific deletion was also confirmed and visualized by microscopy of unstained spleen sections (Figure 18c). Green fluorescence is clearly and specifically visible in the T cell zones of the splenic white pulp areas while other cell types express the mTomato protein and

hence were not targeted by Cre recombinase. Surprisingly, red fluorescence is generally not very bright within the white pulp areas (Figure 18c). Consistent with these findings, Cre was activated in cells of the axial (Figure 18d) and mesenteric lymph nodes (Figure 18e).

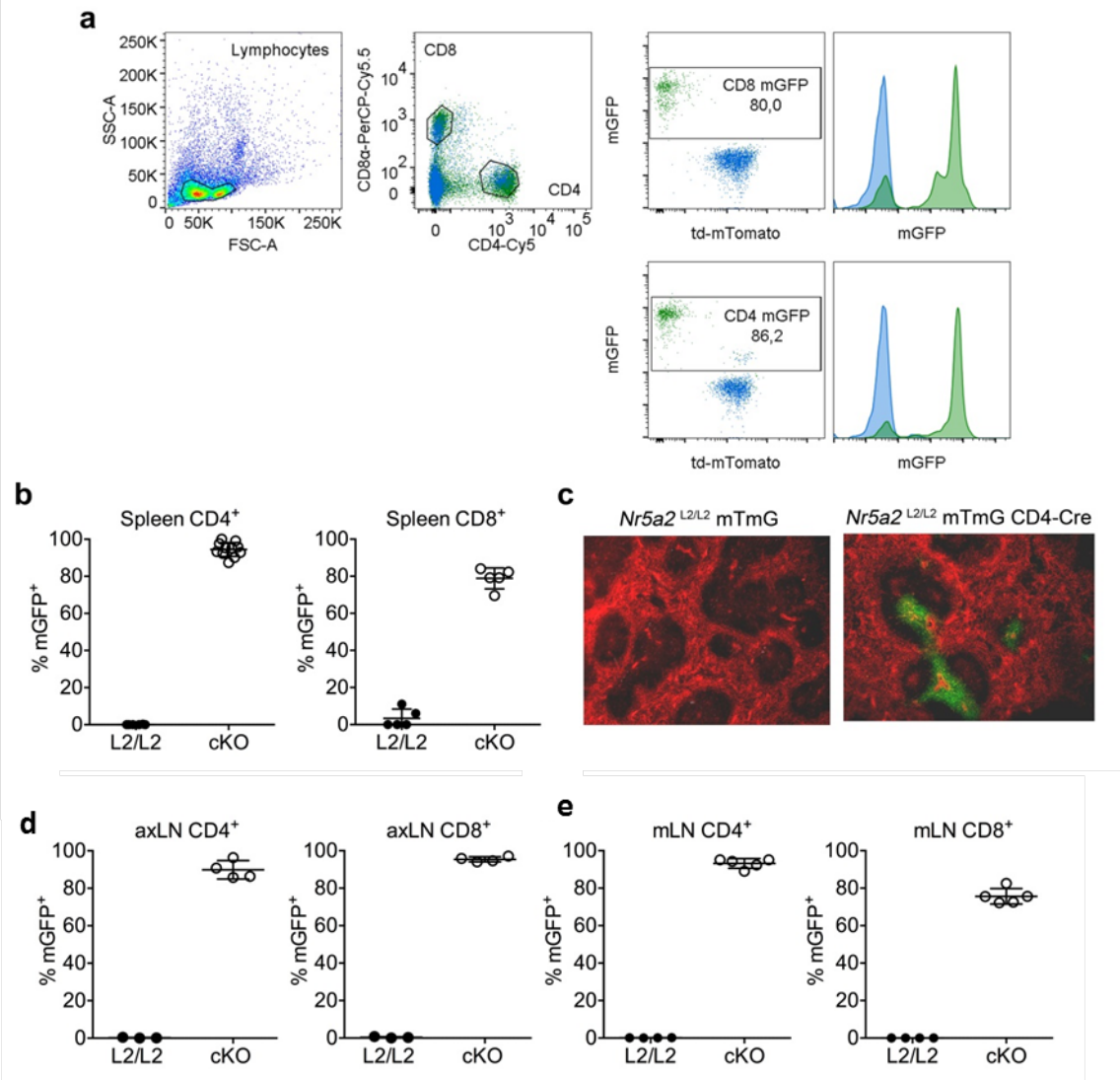

Figure 18: Efficiency of CD4-mediated Cre recombinase activity controlled in mature T cells.

(**a**) Representative overlays showing the distribution of mGFP⁺ and td-mTomato⁺ splenocytes in L2/L2 (blue) or cKO (green) mice as assessed by flow cytometry. Numbers indicate percentages of mGFP⁺ cells in the corresponding T cell subset. (**b**) Quantitation of mGFP reporter expression, indicating LRH-1 deletion in CD4⁺ and CD8⁺ splenocytes. (**c**) Representative pictures of untreated spleen sections showing basal td-mTomato and mGFP fluorescence in CD4-Cre negative (L2/L2) or CD4-Cre positive (cKO) *Nr5a2*$^{L2/L2}$ mTmG reporter mice. Scale bar = 300 µm. (**d-e**) Quantitation of mGFP reporter expression in lymphocytes derived from (d) axial lymph nodes (axLN) or (e) mesenteric lymph nodes (mLN). Each data point represents one mouse. Mean values ± S.D. are shown in each graph.

3.4 LRH-1 deletion affects thymocyte maturation

To investigate the consequences of LRH-1 deletion on immature T cells, thymi of *Nr5a2*$^{L2/L2}$ CD4-Cre conditional knockout (cKO) animals was compared to organs derived from *Nr5a2*$^{L2/L2}$ littermate controls (L2/L2).

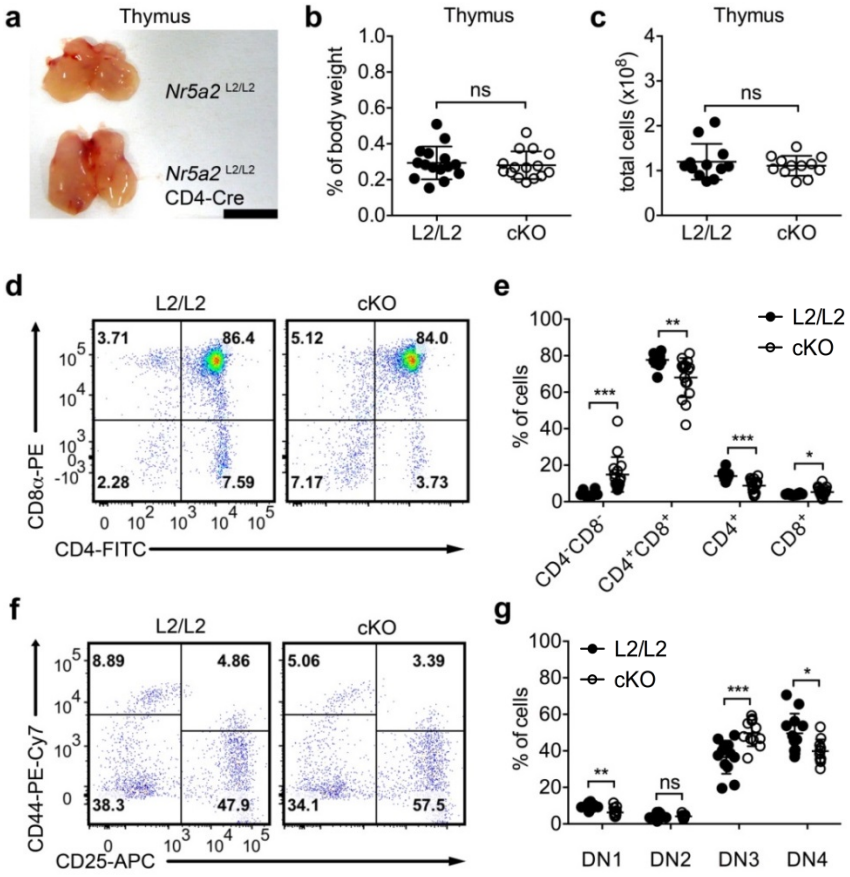

Figure 19: Deletion of LRH-1 impairs T cell maturation.

(**a**) Representative picture of *Nr5a2*$^{L2/L2}$ (L2/L2, ctrl) and *Nr5a2*$^{L2/L2}$ CD4-Cre (cKO) thymi. (**b**) Thymus organ weight relative to body weight (n = 15 mice per group). (**c**) Thymus cellularity (n = 12 mice per group). (**d**) Representative density plots of CD4$^+$ and CD8$^+$ thymocyte distrubtion in L2/L2 and cKO mice. Numbers indicate percentage of cells. (**e**) Relative distribution of T cells subsets in the thymus analyzed by flow cytometry (L2/L2: n = 11; cKO: n = 15). (**f**) Representative density plots of CD4$^-$CD8$^-$ thymocytes in L2/L2 and cKO mice. Numbers indicate percentage of cells. (**g**) Relative distribution of T cell populations within the double negative (DN) subset of thymocytes (n = 12). Mean ± S.D. are shown in each graph. * p<0.05, ** p < 0.01, *** p<0.001, ns: not significant.

At first view, no big difference was observed in thymus size (Figure 19a), weight (Figure 19b) or cellularity (Figure 19c). However, detailed analysis of thymocyte subset distribution revealed a significant reduction of double positive lymphocytes,

while the amount of double negative T cells was elevated (Figure 19c-d). Significant reductions were also observed in the single positive $CD4^+$ subset and minor increases in the $CD8^+$ lymphocyte subsets (Figure 19d-e). Closer characterization of the double negative T cell subset showed an accumulation of thymocytes in the DN3 stadium and an according reduction in DN1 and DN4 (Figure 19e-f).

To further investigate the impact of LRH-1 on thymocyte maturation, another mouse strain was generated. In this strain, Cre recombinase is controlled by the lck-promoter which is induced during early DN thymocyte development. LRH-1 lck-Cre mice also carry the mTmG reporter construct to facilitate the quantitation of deletion efficiency.

Interestingly, while some of the examined animals did not show dramatic differences in thymus size (Figure 20a) and cellularity (Figure 20b), the thymus of other conditional knockout animals was extremely small. Analysis of deletion efficiency revealed, that the deletion was not comparable between analyzed lck-cKO animals. While those organs that macroscopically did not differ much from the littermate controls, only showed minimal fluorescence conversion, tissues with high GFP expression showed dramatic reduction of thymus size and cellularity (Figure 20c). This observation indicates that LRH-1 is indispensable for thymocyte maturation. However, it seems that those cells that escaped the deletion were able to compensate the loss of LRH-1 deficient thymocytes.

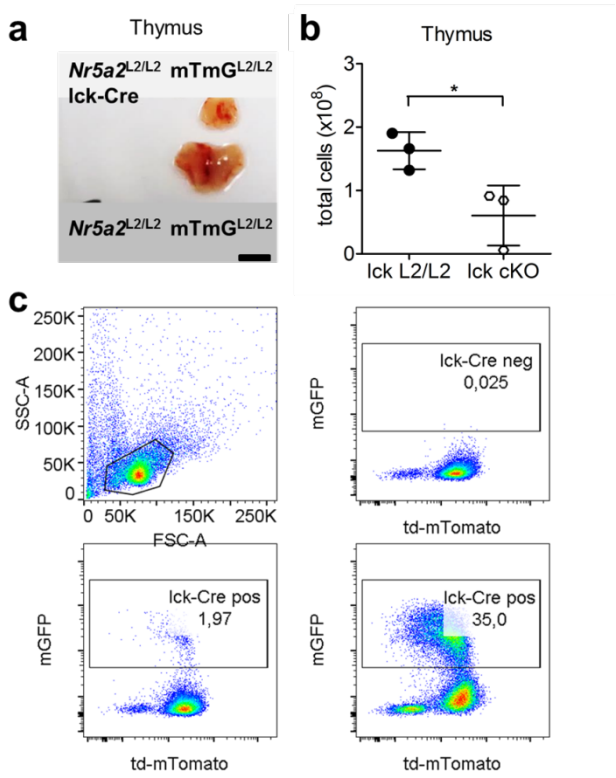

Figure 20: LRH-1 deletion impairs thymocyte maturation.

(**a**) Picture of *Nr5a2*$^{L2/L2}$ mTmG$^{L2/L2}$ lck-Cre (lck cKO) or *Nr5a2*$^{L2/L2}$ mTmG$^{L2/L2}$ (lck L2/L2) thymi. Scale bar = 0.5 cm. (**b**) Thymus cellularity (n = 3 mice). Mean values ± S.D. are shown. (**c**) Representative density plots showing the distribution of mGFP and td-mTomato expressing thymocytes in *Nr5a2*$^{L2/L2}$ mTmG$^{L2/L2}$ lck-Cre (lck-Cre pos) or *Nr5a2*$^{L2/L2}$ mTmG$^{L2/L2}$ (lck-Cre neg) mice as assessed by flow cytometry. Numbers indicate percentages of mGFP^{+} cells.

3.5 LRH-1 deletion leads to a loss of mature T cells

In addition to thymocytes, consequences of LRH-1 deletion were also addressed in mature T cells. Therefore, spleens of age and sex matched *Nr5a2*$^{L2/L2}$ CD4-Cre (cKO) and *Nr5a2*$^{L2/L2}$ (L2/L2) control animals were compared. A prominent reduction of spleen size was observed in LRH-1 deficient animals (Figure 21a) which was supported by significant reduction of organ weight (Figure 21b) and cellularity (Figure 21c).

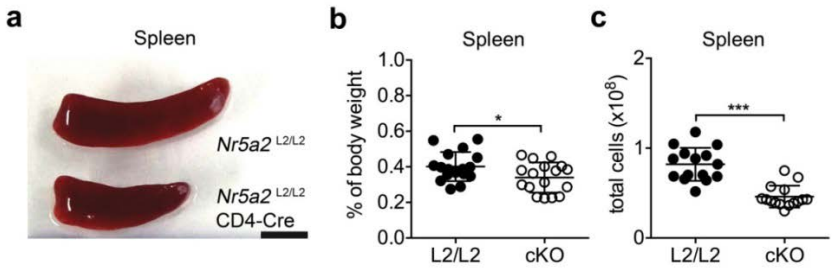

Figure 21: Conditional deletion of *Nr5a2* leads to reduced spleen size and cellularity.

(**a**) Representative picture of L2/L2 and cKO spleens. Scale bar: 0.5 cm. (**b**) Spleen organ weight relative to body weight (L2/L2: n = 17; cKO: n = 18 mice). (**c**) Spleen cellularity (n = 15 mice). Mean values ± S.D. and individual values are shown in each graph. * p<0.05, *** p<0.001.

Detailed flow-cytometric analysis further revealed that reduced cell numbers were particularly caused by the loss of $CD3^+$ cells (Figure 22c-d), while the relative distribution of $B220^+$ cells was only slightly enhanced (Figure 22a) and the percentage of $NK1.1^+$ cells was unaltered (Figure 22b). Examination of $CD4^+$ and $CD8^+$ lymphocyte subsets revealed a characteristic loss of 50% $CD3^+CD8^+$ T cells and an even more substantial reduction of $CD3^+CD4^+$ lymphocytes by approximately 80% (Figure 22e). These findings were confirmed when analyzing total cell numbers (Figure 22f-g).

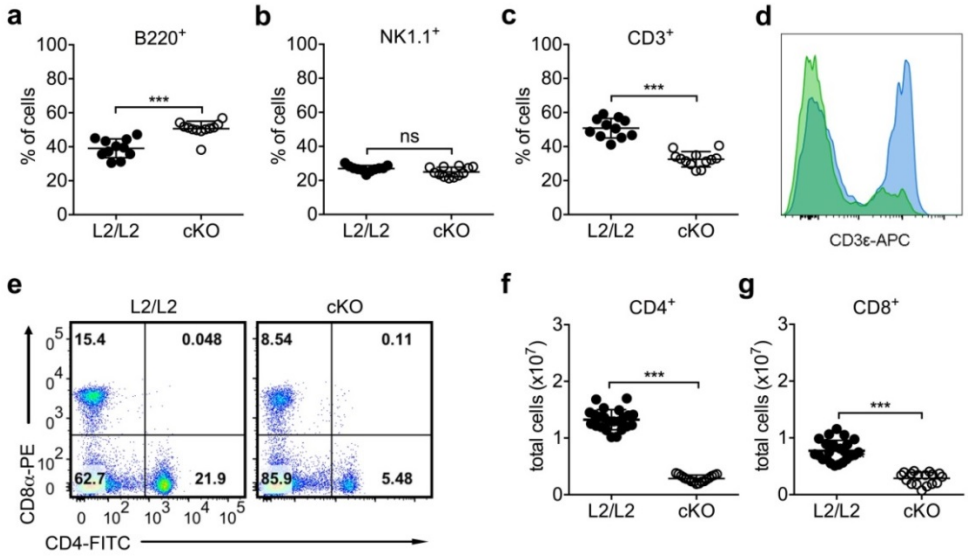

Figure 22: Conditional deletion of *Nr5a2* leads to a loss of mature splenocytes.

(**a**-**c**) Relative distribution of splenic (a) $B220^+$, (b) $NK1.1^+$ or (c) $CD3^+$ lymphocytes as analyzed by flow cytometry (L2/L2: n = 11; cKO: n = 12 mice per group). (**d**) Representative histogram illustrating the distribution of $CD3^+$ cells in control (L2/L2; blue) and LRH-1 deficient (cKO; green) spleens. (**e**) Representative pseudocolor plots of splenic $CD4^+$ and $CD8^+$ cells. Numbers indicate percentages of cells. (**f**-**g**) Absolute numbers of splenic $CD3^+CD4^+$ and $CD3^+CD8^+$ T lymphocytes (L2/L2: n = 23; cKO: n = 17). Mean values ± S.D. and individual values are shown in each graph. *** p<0.001, ns: not significant.

To elucidate if this phenotypic loss of mature T cells can also be observed in other secondary lymphatic organs, axial (axLN) as well as mesenteric lymph nodes (mLN) were subjected to flow cytometric analysis. Along these lines, $CD3^+$ T cell numbers were found to be significantly reduced (Figure 23c; i) while the relative abundance of $B220^+$ B cells was increased (Figure 23a; g).

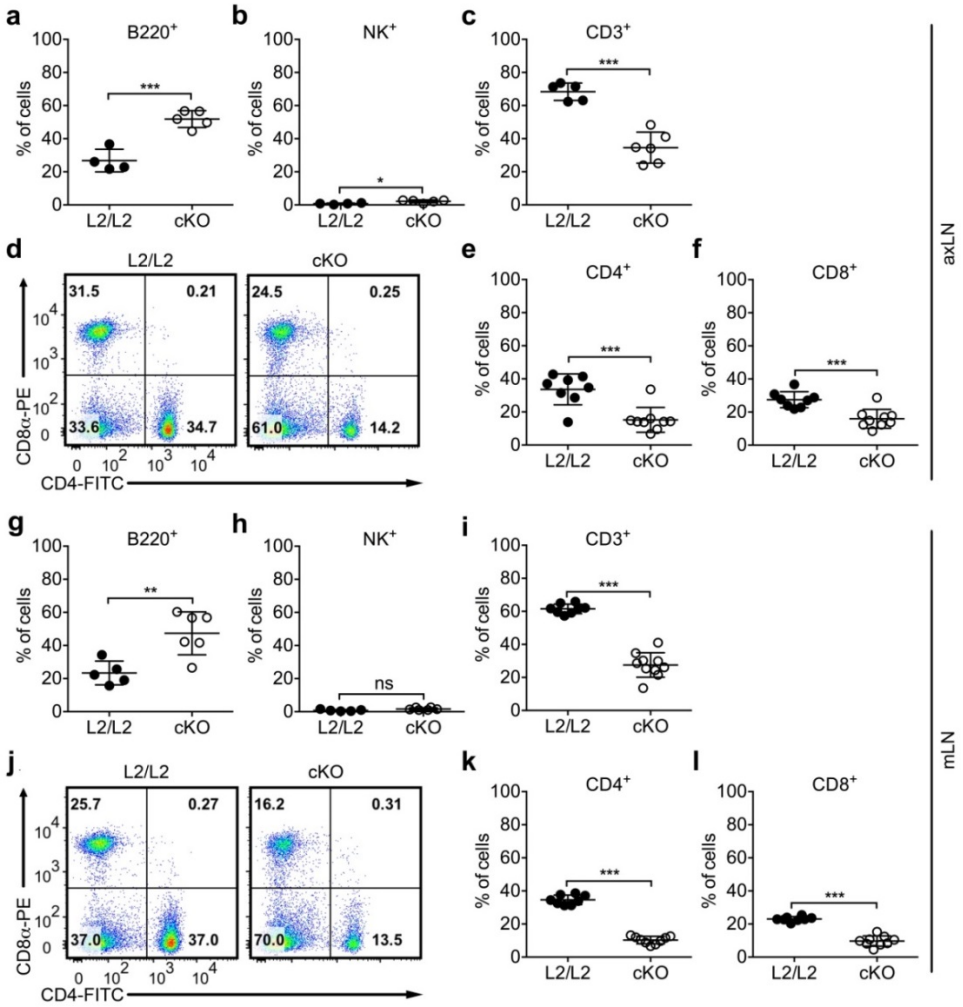

Figure 23: Loss of mature T cells in axial and mesenteric lymph nodes of conditional KO mice.

(**a-c**) Cells derived from axial lymph nodes of age and sex matched L2/L2 or cKO mice were analyzed for their cell surface expression of (a) B220, (b) NK1.1 and (c) CD3 markers. (**d**) Representative dot plot showing the distribution of $CD8\alpha^+$ and $CD4^+$ T cells in axial lymph nodes. (**e-f**) Quantification of (e) $CD3^+CD4^+$and (f) $CD3^+CD8^+$ lymphocytes derived from axial lymph nodes. (**g-i**) Mesenteric lymph nodes were analyzed for (g) B220 (h) NK1.1 and (i) CD3 marker expression. (j) Representative dot plots showing the distribution of $CD8\alpha^+$ and $CD4^+$ lymphocytes in mesenteric lymph nodes. (**k-l**) Quantitation of $CD3^+CD4^+$ and $CD3^+CD8^+$ lymphocytes in tissue derived from mesenteric lymph nodes. Mean values ± S.D. and individual values are shown in each graph. Each symbol represents one animal. *** $p<0.001$, ns: not significant.

Minor but significant differences regarding the distribution of $NK1.1^+$ T cells were monitored in axial lymph nodes (Figure 23b) while $NK1.1^+$ lymphocyte subsets were not affected in mesenteric lymph nodes (Figure 23h). Analysis and quantitation of $CD3^+CD4^+$ and $CD3^+CD8^+$ T cell subsets confirmed a significant reduction of mature T cells in peripheral lymph nodes (Figure 23d-f) which was in accordance to the loss of mature T cells observed in the spleen. Interestingly, a big amount of $CD3^+CD4^-CD8^-$ T cells was detected in all cKO derived secondary organs. Altogether, these findings suggest an important, indispensable role for LRH-1 in peripheral lymphocyte homeostasis.

3.6 T cell specific deletion of LRH-1 does not alter splenic organ structure

Conditional deletion of LRH-1 in T cells evoked an impressive loss of mature T cells. To reveal if this loss is accompanied by disruption of splenic organ structure, the overall spleen architecture was analyzed in detail.

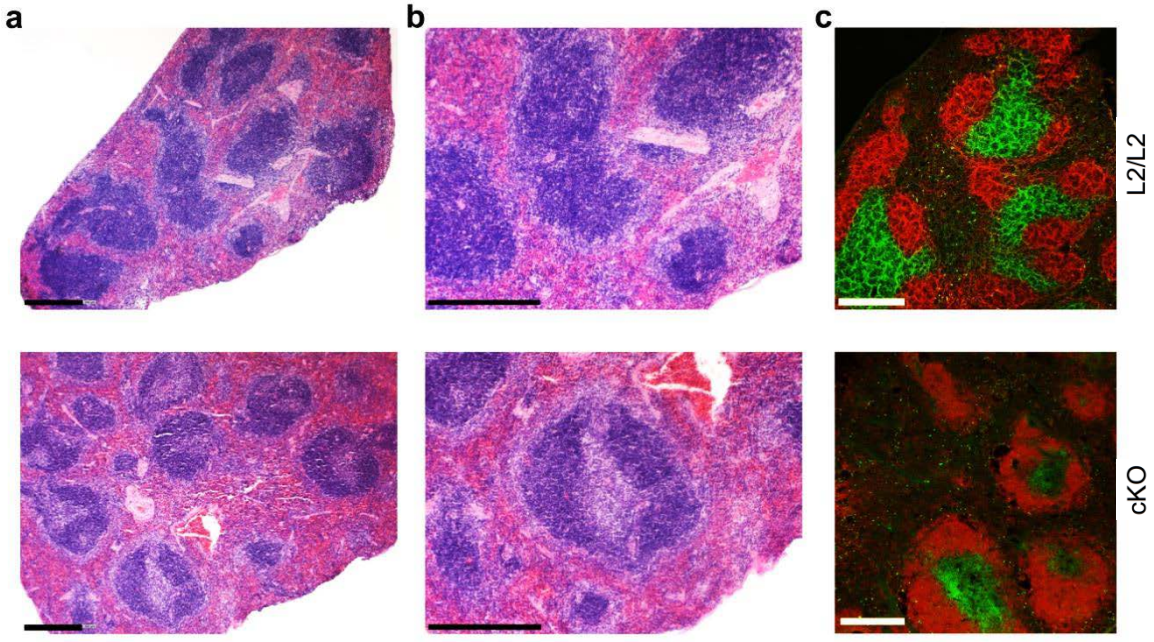

Figure 24: Spleen organ structure of *Nr5a2* deficient and control mice.

(**a**-**b**) Representative cross-sectional view of L2/L2 (upper panel) and cKO (lower panel) mouse spleens with hematoxylin and eosin (H/E) staining. Scale bar: 300 µm (b) Detailed view with focus on a white pulp zone. (**c**) Representative immunohistology showing the distribution of T cells (anti-CD3, green) and B cells (anti-B220, red) expression.

Histological hematoxylin/eosin (H/E) staining of splenic paraffin sections revealed integer organization within cKO organs as defined by confined white pulp follicles (Figure 24a). However, lymphoid white pulps appeared to be significantly smaller in size and more roundish (Figure 25). Interestingly, the inner zones of the white pulp cords were obviously packed less densely as indicated by reduced hematoxylin staining, which suggests a lack of cells within these areas (Figure 24a-b).

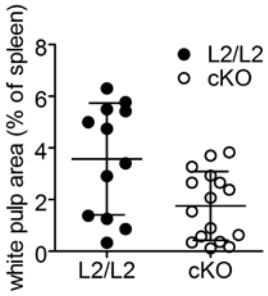

Figure 25: Relative quantitation of splenic white pulp area.

Splenic white pulp area was measured using PalmRobo software (Zeiss) and related to total spleen size. One experiment counting L2/L2: n = 12 white pulps; cKO: n = 16 white pulps of one spleen per group.

To further allow discrimination between B and T lymphocytes, spleen sections were stained for T cells ($CD3^+$, green) and B cells ($B220^+$, red) (Figure 24c). Central, T cell-rich regions were surrounded by B cell follicles in organs derived from both, L2/L2 and cKO animals and bridging zones were observed in both genotypes (Figure 24a-c). While the distribution of B cells was not altered in cKO spleen sections, lack of T cells in the central white pulp core was remarkable (Figure 24c). This is in line with the severe loss of mature T cells that was observed by the flow-cytometric analysis of spleens derived from cKO animals.

For a more detailed analysis of the splenic architecture, staining targeting the macrophage cell surface marker F4/80 was performed. Specific immunoperoxidase staining revealed no obvious difference in the distribution of macrophages within the red pulp or marginal zone of L2/L2 or cKO mice (Figure 26a). These findings were confirmed by immunohistochemistry (Figure 26b-c). It is hence concluded that conditional deletion of LRH-1 in T cells does not affect the overall spleen structure.

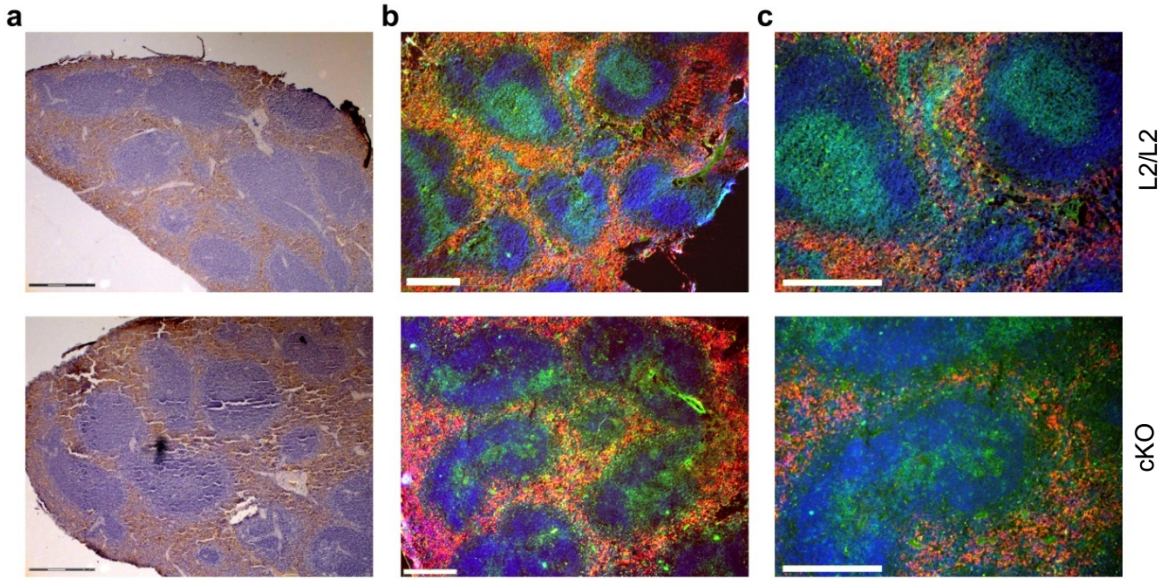

Figure 26: Spleen organ structure with focus on macrophages.

(**a**) Representative immunoperoxidase staining of L2/L2 (upper panel) and cKO (lower panel) mouse spleens showing the macrophage (F4/80; brown) distribution in the red pulp. Additional hematoxylin and eosin (H/E) staining was performed. (**b-c**) Representative staining for CD3 (green), F4/80 (red) and DAPI (blue). (**c**) Detailed view of (b); Scale bars: 300 µm.

3.7 LRH-1 deficient T cells are not hypersensitive to apoptotic stimuli

To elucidate the reasons that are causing the dramatic loss of mature T lymphocytes, sensitivity of quiescent T cells towards different apoptotic stimuli was examined. In the immature thymocyte population, no increased cell death was observed in $CD4^+CD8^+$ thymocytes when subjected to increasing doses of the glucocorticoid dexamethasone (Figure 27a), the topoisomerase II inhibitor etoposide (Figure 27b), the unselective apoptosis inducing PKC inhibitor staurosporine (Figure 27c) or plate bound anti-CD3 antibody (Figure 27d). However, enhanced cell death was observed in thymocytes derived from cKO animals under basal, non-stimulatory conditions (Figure 27a-d).

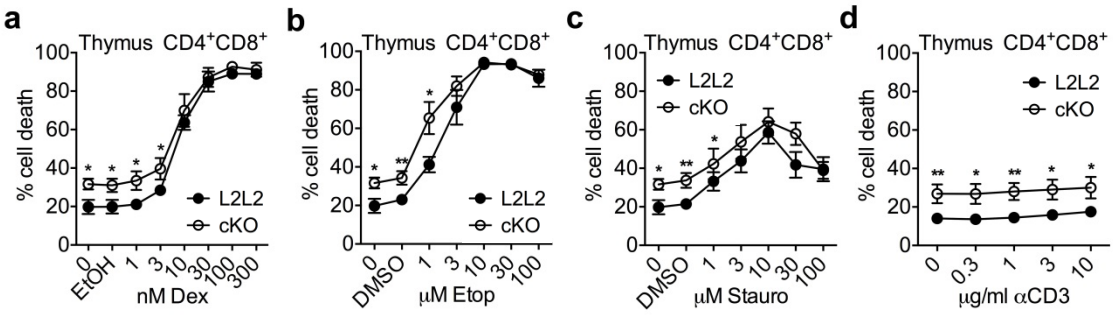

Figure 27: Apoptosis sensitivity is not altered in LRH-1 deficient thymocytes.

(**a-d**) CD4+CD8+ thymocytes from L2/L2 (filled symbols) or cKO (empty symbols) mice were subjected to increasing doses of (a) dexamethasone (Dex), (b) etoposide (Etop), (c) staurosporine (Stauro) or (d) plate bound anti-CD3 antibody (αCD3) for 8 h. Apoptosis was analyzed by Annexin V staining. Mean values ± S.D. of one representative experiment are shown (n = 3 mice per group). * p<0.05, ** p<0.01

Apoptosis sensitivity was further examined in quiescent, mature splenocytes. No hypersensitivity of naïve, LRH-1 deficient CD4+ or CD8+ T cells was observed after treatment with increasing doses of various apoptosis inducing agents (Figure 28a-d). In line with thymocytes, basal cell death rates were significantly enhanced in CD4+ and CD8+ T cells under non-stimulatory conditions (Figure 28a-d).

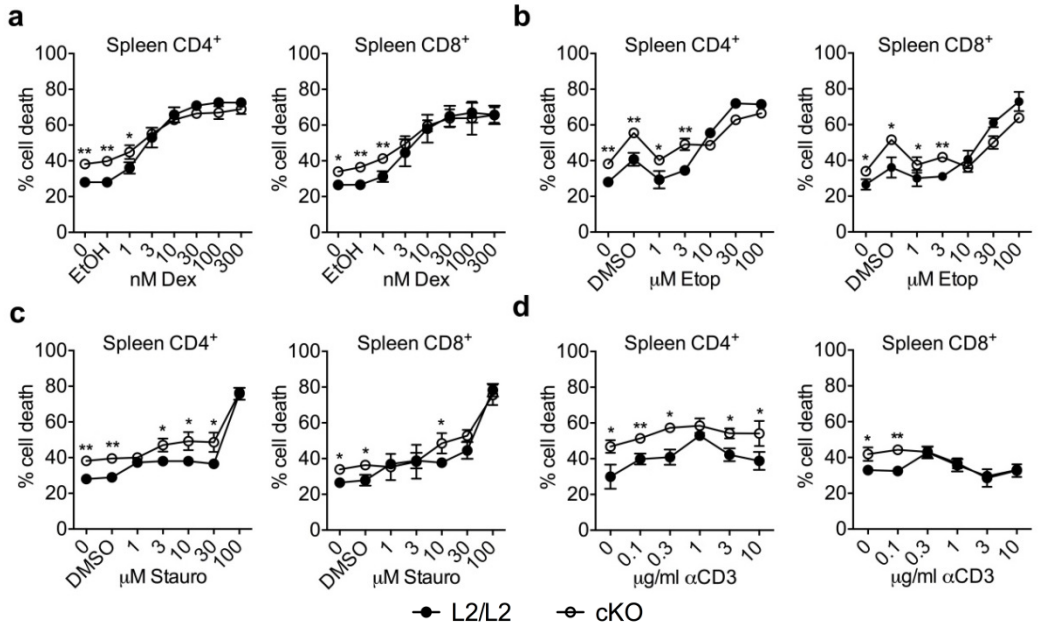

Figure 28: Sensitivity of mature T cells to apoptosis inducing stimuli.

(**a-d**) L2/L2 (filled symbols) and cKO (empty symbols) splenocytes were treated with increasing doses of (a) dexamethasone (Dex), (b) etoposide (Etop), (c) staurosporine (Stauro) or (d) plate bound anti-CD3 antibody (αCD3) for 8 h. Apoptosis in CD4+ or CD8+ T cells was analyzed by Annexin V staining. Mean values ± SD of one representative experiment are shown (n = 3 mice). * p<0.05, ** p<0.01

As T cells are generally more susceptible to cell death after activation[167] and because LRH-1 is tightly linked with cell proliferation[78], apoptosis induction was next assessed in proliferating cells. Therefore, concanavalin A (ConA) induced T cell blasts were generated. Unexpectedly, while cells derived from L2/L2 mice were nicely activated and formed T cell blasts, nearly all CD4+ T cells with cKO background died. Due to this exhaustive cell death, almost no viable cKO blasts were available for investigation and subsequently, apoptosis sensitivity of T cell blasts could not be examined. Therefore, attention was turned to analyze apoptosis induction during blast formation.

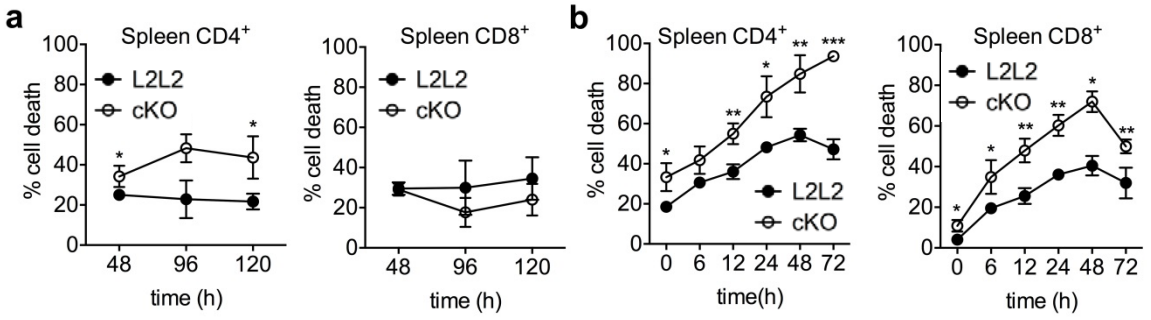

Figure 29: Enhanced mitogen-induced cell death in mature LRH-1 deficient T cells.

(**a**) Kinetic of apoptosis induction during the generation of T cell blasts using concanavalin A (ConA) treatment. Apoptosis in CD4+ and CD8+ T cells from L2/L2 (filled symbols) and cKO (empty symbols) animals was analyzed by Annexin V staining. (**b**) Analysis of apoptosis induction in response to stimulation with plate bound anti-CD3/anti-CD28 antibody. Cell death was examined in CD4+ and CD8+ T cells by Annexin V staining at the indicated time points. Mean values ± S.D. of one representative experiment are shown (n = 3 mice). * $p<0.05$, ** $p<0.01$, *** $p<0.001$.

Close examination of cell death in response to ConA stimulation revealed that apoptosis induction was significantly enhanced in CD4+ T cells with increasing stimulation duration, while this effect was not detected in the CD8+ subsets (Figure 29a). This observation was confirmed by activation with plate-bound anti-CD3 antibody and subsequent cell death analysis at different time points. Starting with an enhanced basal cell death, CD4+ cKO splenocytes dramatically died in response to anti-CD3 treatment, while cell death was moderate in L2/L2 T cells (Figure 29b). cKO derived CD8+ T lymphocytes showed also significantly higher rates of cell death induction compared to the control, however, this rate was attenuated over time (Figure 29).

Generation of T cell blasts was further monitored by microscopic analysis. As expected, wt C57BL/6 splenocytes as well as L2/L2 cells showed polarization and increased their cytoplasm volume. Cells with cKO background also exhibited signs of activation, however to a much lesser extent (Figure 30). While stimulation-induced rosette formation was comparable between L2/L2 and C57BL/6 mice, it was obviously diminished in samples derived from cKO mice (Figure 30). T cell aggregates were smaller in size and less abundant under LRH-1 deficient conditions (Figure 30).

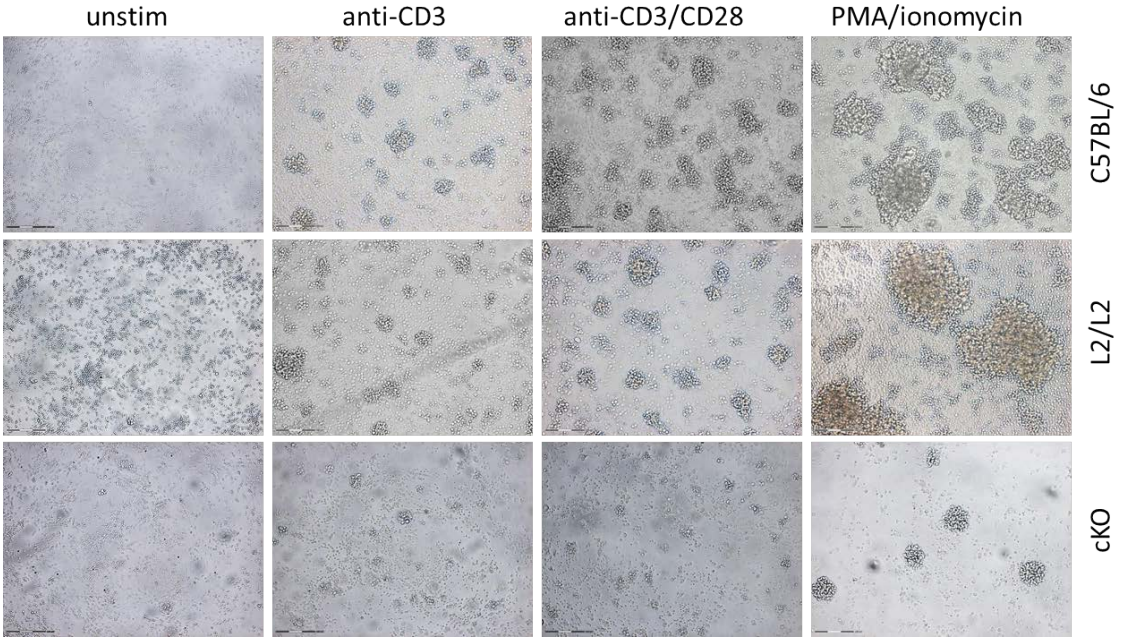

Figure 30: Microscopic evaluation of T cell blast formation.

Splenocytes from C57BL/6 as well as L2/L2 and cKO mice were subjected to PBS (unstim), plate bound anti-CD3, anti-CD3/anti-CD28 or PMA plus ionomycin treatment for 72h. Scale bar: 150µm.

Altogether, these findings suggest that the prominent loss of mature T cells is not caused by hypersensitivity of cKO T cells to apoptosis inducing stimuli but rather a defect related with lymphocyte activation.

3.8 LRH-1 deficient T cells are not anergic

In response to activating stimuli, T cells express activation markers on their cell surface. One of these markers, the leukocyte activation molecule CD69, is induced very early upon stimulation. To investigate if cKO T cells are anergic and fail to become

activated, the kinetic of CD69 upregulation in response to stimulation with plate-bound anti-CD3/anti-CD28 antibody was tracked at different time points. Compared to the L2/L2 control, LRH-1 deficient T cells revealed significantly delayed and decreased levels of CD69 expression in $CD4^+$ (Figure 31a) as well as $CD8^+$ lymphocytes (Figure 31b). However, although the expression was significantly diminished, CD69 leukocyte activation molecules were clearly detectable and upregulated over time with a similar kinetic as in the control. Hence, unresponsiveness of cKO T cells does not explain the dramatic cell death induction and failure to initiate proliferation in mature cKO T cells.

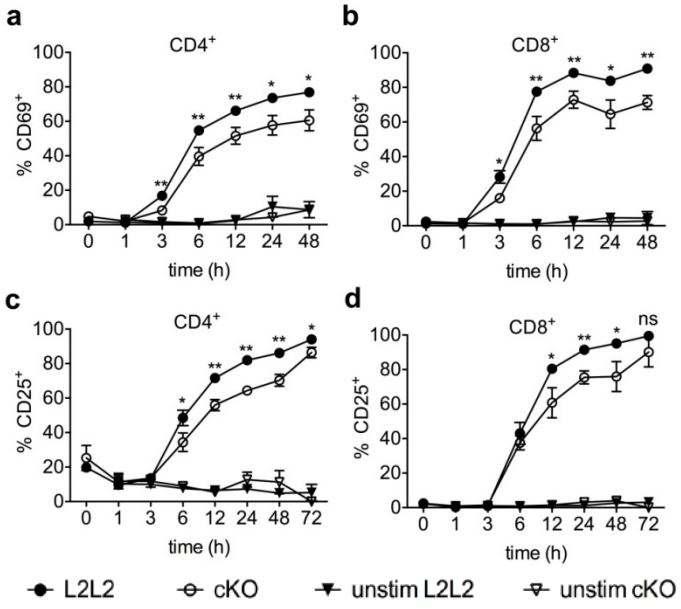

Figure 31: Kinetic showing the stimulation-induced upregulation of activation markers.

(**a**-**b**) Splenocytes were treated with plate bound anti-CD3/anti-CD28 antibodies or left unstimulated (unstim). Expression of (a) CD69 or (b) CD25 was assessed by flow cytometry at the time points indicated. Mean values ± S.D. of one representative experiment are shown (n = 3 mice). * $p<0.05$, ** $p<0.01$, *** $p<0.001$

In order to get a complete picture and confirm that cKO T cells are not anergic, induction of the later activation molecule CD25 (IL-2Rα) was observed over time. As expected, activation molecules were not upregulated in the absence of stimulatory reagents (Figure 31a-d). However, here again, significant differences in the rate and kinetic of CD25 expression were observed between cKO and L2/L2 T cell subsets under stimulatory conditions (Figure 31c-d).

T cell activation is not only accompanied by the upregulation of specific cell surface molecules but also characterized by the secretion of different cytokines including IL-2 and IFNγ. To analyze the capacity of cytokine production and secretion in cKO T cells, highly purified $CD4^+$ and $CD8^+$ lymphocytes were activated and cytokine levels were subsequently quantified by ELISA. Both, $CD4^+$ and $CD8^+$ cKO T cells produced surprisingly high amounts of IFNγ that exceeded the one from L2/L2 T cells significantly (Figure 32a). Especially pronounced was this effect in $CD8^+$ T cells (Figure 32a). Interestingly, secretion of IL-2 was also slightly enhanced in $CD8^+$ T cells while it was similar to control cells in $CD4^+$ lymphocytes (Figure 32b). However, differences were not as prominent as for IFNγ.

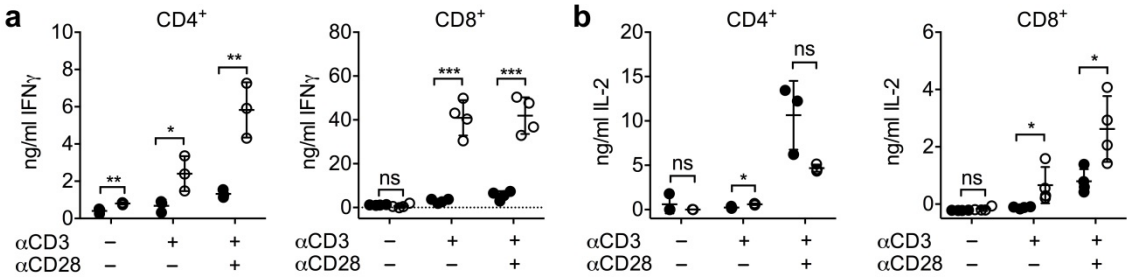

Figure 32: Activation-induced cytokine expression.

(**a**-**b**) Sort-purified $CD4^+$ or $CD8^+$ splenic T cells were stimulated as indicated for 48 h. Secretion of (a) IFNγ or (b) IL-2 was determined by ELISA. n = 4 individual experiments. Mean ± S.D. are shown. * $p<0.05$, ** $p<0.01$, *** $p<0.001$, ns: not significant

Altogether, the upregulation of activation markers and cytokine secretion exclude anergy as the underlying reason for the massive loss of mature T cells in cKO animals.

3.9 LRH-1 deficient T cells exhibit defects in cell proliferation

Experiments showed that the dramatic loss of mature T cells can neither be explained by hypersensitivity of cKO T cells to apoptosis induction nor by anergy. In accordance with the stimulation-induced upregulation of *Nr5a2* mRNA expression and the observation that LRH-1 deficient T cells mainly died upon T cell activation, LRH-1 is reported to be linked to cell proliferation. Hence, the proliferation capacity of cKO T cells was next examined.

Therefore, incorporation of radioactive labeled thymidine was analyzed upon activation with plate-bound anti-CD3/anti-CD28 antibody and compared between splenocytes derived from L2/L2 and cKO animals. While stimulation clearly induced cell proliferation in L2/L2 splenocytes, hardly any incorporation of radioactive thymidine was measured in cKO T cells, indicating that cKO T cells have disadvantages concerning cell proliferation (Figure 33).

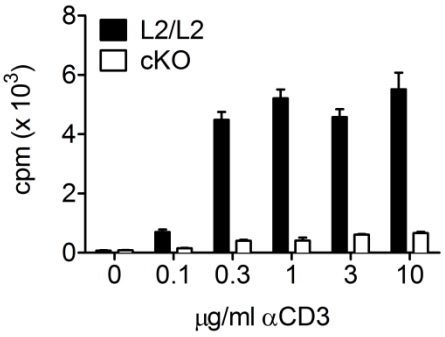

Figure 33: Impaired cell proliferation in LRH-1 deficient T cells.

L2/L2 or cKO Splenocytes were treated with increasing concentrations of plate bound anti-CD3/anti-CD28 antibodies for 72 h. Incorporation of ^{3}H-thymidine was monitored. Mean values ± S.D. of one representative experiment with n = 3 technical replicates are shown. cpm: counts per minute.

However, as the relative abundance and mature T cell number are strongly reduced in cKO animals, starting conditions are not comparable between whole spleen isolates. To normalize this difference and further differentiate between $CD4^{+}$ and $CD8^{+}$ populations, cell division was further tracked by CFSE dilution.

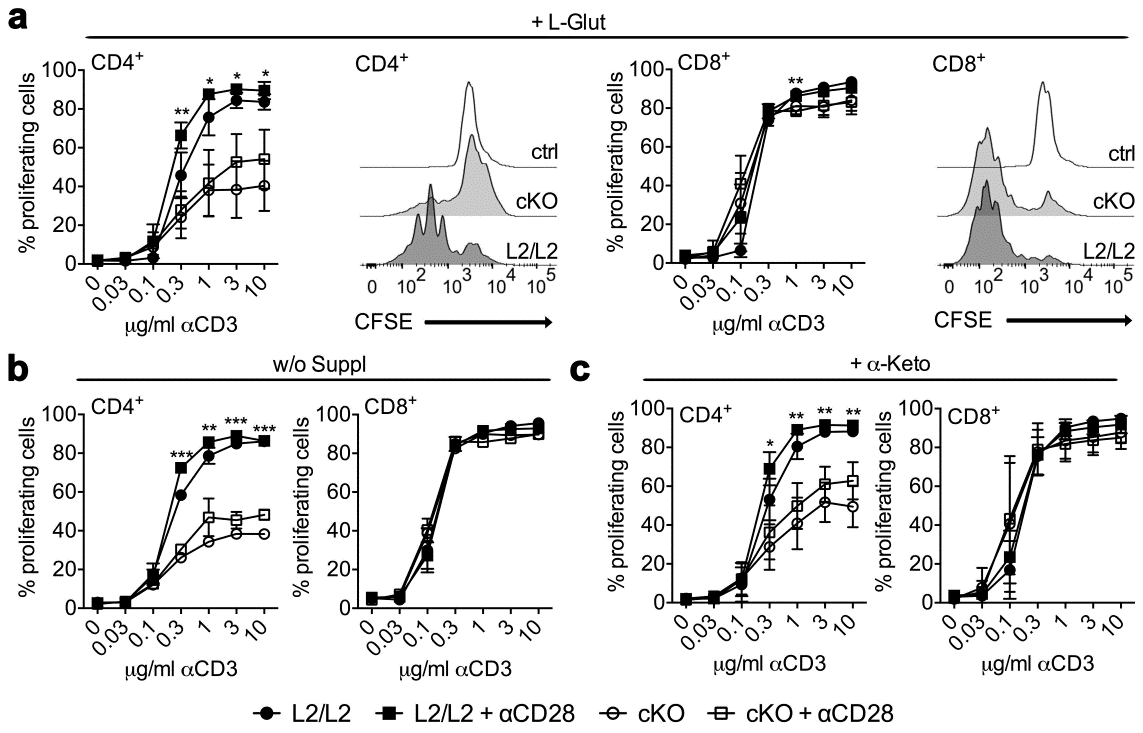

Figure 34: Impact of LRH-1 on cell proliferation and glutamine metabolism.

(**a-c**) Proliferation of CD4+and CD8+ splenocytes in response to increasing doses of anti-CD3 plus (filled symbols)/or without (empty symbols) antiCD28 antibody was assessed by CFSE dilution after 72 h. Culture medium was supplemented with (a) 2 mM l-glutamine (L-Glut), (b) left unsupplemented (w/o Suppl) or (c) with 2 mM α-ketoglutarate (α-Keto). Unstimulated cells were used as control (ctrl). Mean values ± S.D. of 3 individual experiments are shown. * p<0.05, ** p<0.01, *** p<0.001

Cells cultivated under common conditions underwent cell division in response to anti-CD3 ± anti-CD28 stimulation (Figure 34a). As expected, stimulation with anti-CD3 only evoked a proliferation rate that was slightly lower compared to co-stimulatory conditions and proliferation rate was generally higher in CD8+ T cells (Figure 34a). Interestingly, while proliferation was significantly reduced in CD4+ cKO T cells, no difference was observed in the CD8+ lymphocyte population (Figure 34a).

As LRH-1 was recently described to control glutamine metabolism in liver cells[72], it was investigated whether defective cell proliferation is caused by metabolic defects. Therefore, CFSE dilution was tracked in cells that were cultivated without additional supplementation of stable l-glutamine. However, these sub-optimal culture conditions lead to similar results. Here again, CD4+ T cells showed strongly reduced cell proliferation which was even more pronounced compared to l-glutamine

supplemented conditions while CD8+ T cells were not affected (Figure 34b). To circumvent glutamine dependent metabolism block, cells were next cultured in α-ketoglutarate containing medium. While the proliferation defect of cKO CD4+ subsets was still significant, it was slightly attenuated and cell proliferation was facilitated in cKO T cells (Figure 34c). In line with the previously tested culture conditions, LRH-1 deficient CD8+ T cells did not show any signs of proliferation defect (Figure 34c).

As α-ketoglutarate is a rather hydrophilic molecule, the administration of α-ketoglutarate and its ability to cross the plasma membrane are discussed controversially. Hence, the influence of α-ketoglutarate supplementation on cell proliferation was investigated. Therefore, ^{3}H-thymidine incorporation was examined in cells cultured under different conditions.

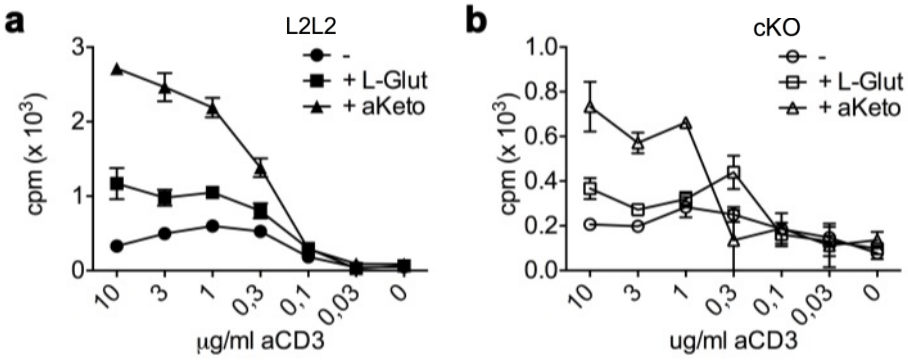

Figure 35: Impact of α-ketoglutarate supplementation on cell proliferation.

(**a**-**b**) Splenocytes derived from (a) L2/L2 or (b) cKO animals were treated with increasing doses of anti-CD3/anti-CD28 in cell culture medium without further supplementation (-), 2mM l-glutamine (L-Glut) or 2mM α-ketoglutarate (α-Keto). Cell proliferation was assessed after 72 h by analyzing the incorporation of radioactive thymidine. cpm: counts per minute. Mean values ± S.D. of one representative experiment are shown. n = 3 technical replicates.

As expected, L2/L2 splenocytes cultured without supplementation of stable l-glutamine showed least ^{3}H-thymidine incorporation while cell proliferation was clearly enhanced by the addition of l-glutamine (Figure 35a). However, cell division was further supported by the supplementation of α-ketoglutarate, indicating its uptake in the cell (Figure 35a). Same tendencies were observed in cKO splenocytes. However, the overall cell proliferation rate was much lower in LRH-1 deficient T cells (Figure 35b).

Cell proliferation was further investigated under sub-optimal conditions (5% FBS, no stable l-glutamine supplementation). As expected, proliferation rate was generally rather low and reduced in CD4+ cKO cells (Figure 36). Interestingly, while proliferation was not reduced in cKO CD8+ T cells under the conditions examined before, FBS reduction now decreased cell division rates also in the CD8+ population (Figure 36).

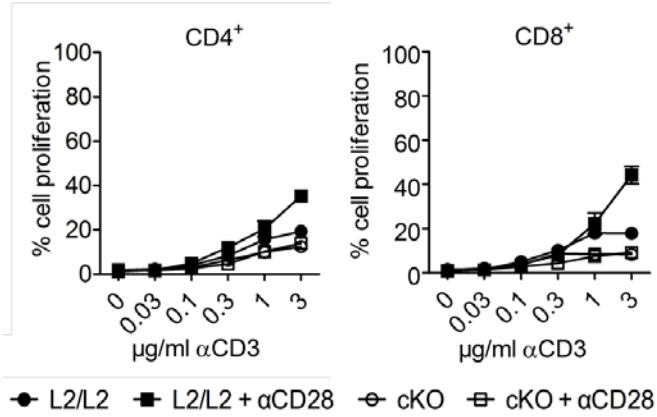

Figure 36: Cell proliferation under sub-optimal culture conditions.

Splenocytes were cultured in medium with 5% FBS and without supplementation of stable l-glutamine for 72 h. Cell proliferation was assessed by CFSE dilution. Mean values ± S.D. of one representative experiment are shown. n = 3 technical replicates.

These findings lead to the assumption that LRH-1 contributes to cell proliferation but also functional metabolism in T cells, most likely via the regulation of glutamine metabolism. FBS further seems to contain substances that facilitate proliferation in LRH-1 deficient CD8+ T cells. However, these substances are not able to compensate for the loss of LRH-1 in CD4+ lymphocytes. Altogether, the strong proliferation defects cannot be explained alone by a role of LRH-1 in cell metabolism as none of the supplementations was able to rescue proliferation in cKO CD4+ T cells.

To further investigate the dependence of T cell proliferation on LRH-1, specific pharmacological inhibitors were applied to mimic the loss of LRH-1 protein.

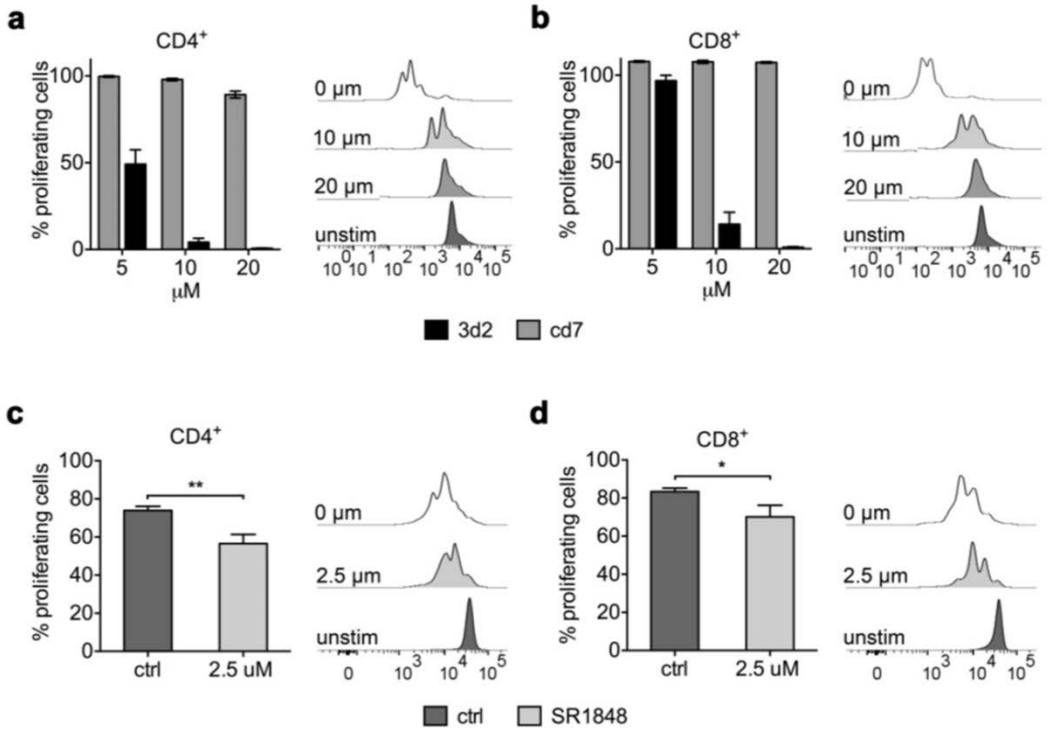

Figure 37: Impact of LRH-1 specific inhibitors on cell proliferation.

(**a**-**b**) Splenocytes were treated with anti-CD3/anti-CD28 antibodies and increasing doses of the LRH-1 inhibitor 3d2 or the control substance cd7. Proliferation in (a) $CD4^+$ or (b) $CD8^+$ T cells was assessed after 72 h by CFSE dilution. Representative histograms are shown. (**c-d**) Splenocytes were subjected to anti-CD3/anti-CD28 treatment ± the LRH-1 inhibitor SR1848. Cell proliferation was analyzed in (a) $CD4^+$ or (b) $CD8^+$ T cells after 72 h using CFSE dilution. Representative histograms are shown. Mean values ± S.D. are shown in each graph. n = 3 independent experiments. * $p<0.05$, ** $p<0.01$, *** $p<0.001$

Application of the selective LRH-1 inhibitor 3d2 significantly reduced CFSE dilution in a dose dependent manner within the $CD4^+$ subset of L2/L2 splenocytes (Figure 37a). No inhibition of cell proliferation was observed in response to treatment with the control substance cd7 (Figure 37a). Interestingly, $CD8^+$ T cells also showed reduced proliferation rates, although higher concentrations of the inhibitor were necessary (Figure 37b). Application of a second LRH-1 inhibitor SR1848 further confirmed these results. In response to SR1848 administration, cell proliferation was diminished in $CD4^+$ L2/L2 T cells and to a lesser extent, but still significant, also in $CD8^+$ T cells (Figure 37c-d).

In a next approach, cell proliferation was examined in highly purified T cell subsets to exclude any influence of accessory cells and confirm a specific role of LRH-1 in T cells.

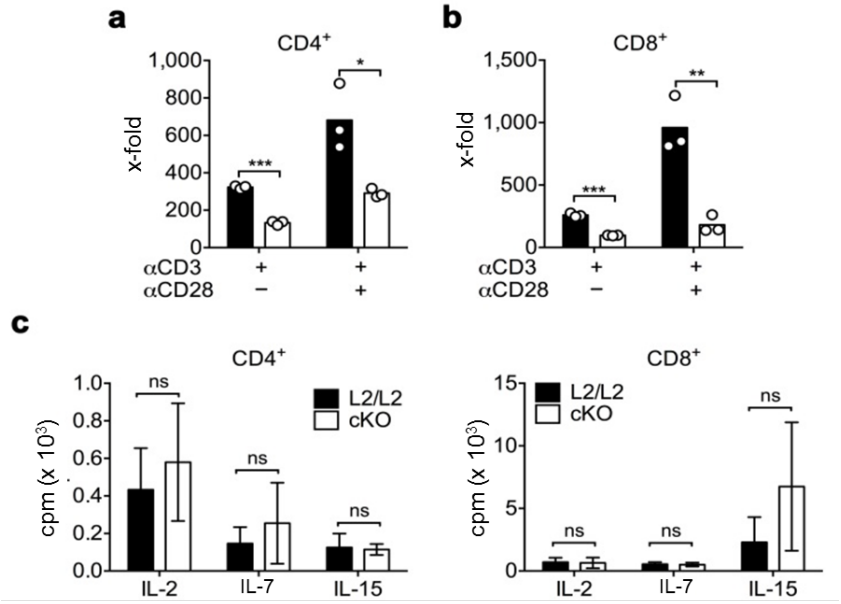

Figure 38: Reduced cell proliferation in highly purified cKO T cell subsets.

(**a**-**b**) Sort-purified (a) CD4+ or (b) CD8+ splenocytes were stimulated as indicated for 72 h and incorporation of ^{3}H-thymidine was monitored to analyze cell proliferation. cpm values were normalized to untreated control (x-fold). (**c**) Purified CD4+ or CD8+ splenic T cells were treated with IL-2 (200 U/ml), IL-7 (10 ng/ml) or IL-15 (10 ng/ml) for 72 h before proliferation was determined by ^{3}H-thymidine incorporation. cpm: counts per minute. Mean values ± S.D. are shown in each graph. n = 3 independent experiments. * $p<0.05$, ** $p<0.01$, *** $p<0.001$, ns: not significant.

Incorporation of ^{3}H-thymidine was analyzed in sort-purified T cell subsets after stimulation. As expected, CD4+ cKO T cells showed significantly reduced thymidine incorporation compared to L2/L2 cells (Figure 38a). Surprisingly, however, reduction of cell proliferation was most prominent in the CD8+ subsets (Figure 38b), which is in contrast to previous observations.

To further investigate the response to proliferation-inducing cytokines, purified CD4+ or CD8+LRH-1 deficient T cells were subjected to stimulation with IL-2, IL-7 and IL-15. While proliferation of CD4+ lymphocytes was slightly but not significantly enhanced after stimulation with IL-2 and IL-7, homeostatic expansion driving cytokine IL-15 clearly facilitated cell division of CD8+ T cells (Figure 38c). However, none of the applied cytokines was able to rescue cell proliferation in CD4+ T cells while only IL-15 showed tendencies to substitute for LRH-1 deficiency in the CD8+ subset (Figure 38c).

To confirm a central role of LRH-1 in the regulation of human T cell proliferation, LRH-1 inhibitors were next applied to freshly isolated PBMCs.

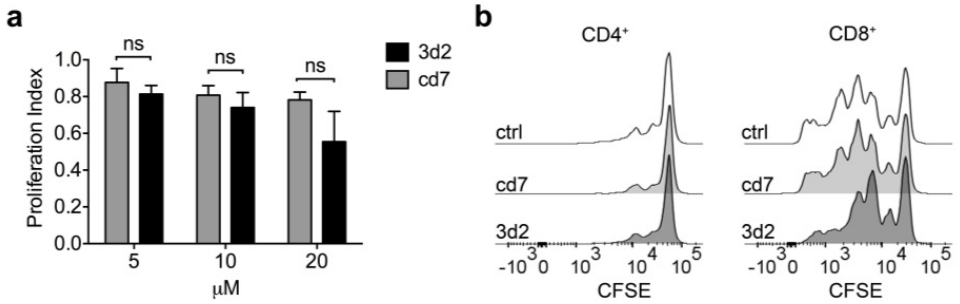

Figure 39: Impact of LRH-1 inhibition on cell proliferation in human PBMCs.

(**a**) Freshly isolated human PBMCs were stimulated with PHA-P and increasing doses of the LRH-1 inhibitor 3d2 or the control substance cd7. Proliferation was normalized to cells without inhibitor. (**b**) Representative histograms are shown. Mean values ± S.D. of one experiment are shown. n = 3 biological replicates. PBMC: peripheral blood mononuclear cell; ns: not significant.

Administration of 3d2 but not cd7 clearly reduced the proliferation of human PBMCs in studies analyzing ^{3}H-thymidine incorporation (Figure 39a) or CFSE dilution (Figure 39b). However, reduction was not significant. Interestingly, in contrast to the findings in mice, human CD8^{+} lymphocytes seem to be more affected by the loss of LRH-1 than CD4^{+} T cells (Figure 39b). Altogether, these experiments confirm an important role of LRH-1 in the regulation of T cell proliferation in both, mouse and human species.

3.10 LRH-1 deficient T cells fail to undergo homeostatic expansion *in vivo*.

Cell proliferation plays a central role during homeostatic expansion of T cells upon thymic maturation. Released into the periphery, these cells have to expand and populate secondary lymphatic organs. As LRH-1-deficient T cells, especially CD4^{+}, showed severe defects in cell proliferation, it was investigated if deficits in homeostatic expansion account for the loss of mature T cells.

A model system to analyze homeostasis-driven expansion of T lymphocytes is the transfer of T cells into lymphopenic recipient mice[114]. In the absence of antigenic stimulation, naïve T cells undergo cell proliferation and are hence able to repopulate the lymphocyte lacking secondary lymphatic organs of the host. Those processes that lead to homeostatic cell proliferation are independent of IL-2 or co-stimulation via CD28 and do not induce the differentiation into effector cells[114].

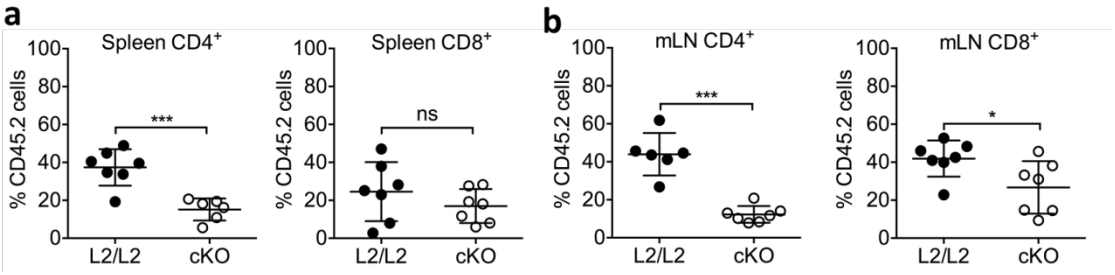

Figure 40: Homeostatic expansion is impaired in LRH-1 deficient T cells.

(**a-b)** Adoptive transfer of sort-purified CD45.2$^+$ CD4$^+$ and CD8$^+$ L2/L2 or cKO T cells plus equal numbers of CD45.1$^+$ wild type T lymphocytes into Rag 1$^{-/-}$ animals. Distribution of CD45.2$^+$ CD4$^+$ or CD8$^+$ T cells was analyzed in (a) spleen or (b) mesenteric lymph nodes (mLN) after 21 days. n = 6-7 mice. Mean values ±S.D. are shown. * $p<0.05$, *** $p<0.001$, ns: not significant

For the adoptive transfer, sort purified CD4$^+$ and CD8$^+$ T cells derived from either cKO or L2/L2 animals were mixed with equal numbers of wild type T cells carrying the CD45.1 isoform on their cell surface. Cells were then transferred into Ly5.1$^+$ Rag 1$^{-/-}$ lymphopenic hosts by Anna-Lena Geiselhöringer. In close collaboration with Anna-Lena Geiselhöringer, secondary lymphatic organs were isolated after an incubation period of 21 days and analyzed for the abundance of cKO or L2/L2 derived T cells. Donor cells were identified by the expression of CD45.2. Confirming the hypothesis that homeostatic expansion is impaired in LRH-1 deficient T cells, the relative abundance of cKO T cells in the spleen (Figure 40a) and mesenteric lymph nodes (Figure 40b) was significantly lower compared to control cells. In line with the pronounced reduction of mature CD4$^+$ T cell numbers in cKO animals, expansion of CD4$^+$ lymphocytes was reduced more severely than the expansion of CD8$^+$ T cells (Figure 40a-b).

3.11 CD4$^+$ effector functions are impaired in LRH-1 deficient T cells

As CD4$^+$ T cells failed to undergo homeostatic expansion, impact of LRH-1 deficiency on the effector function of CD4$^+$ helper T cells was studied next. Therefore, cKO or L2/L2 littermate control mice were injected with ovalbumin protein in incomplete Freund's adjuvans (IFA). After an incubation phase of 14 days, splenocytes of immunized mice were subjected to ovalbumin protein *in vitro* and restimulation-

induced proliferation of antigen-specific T cells was assessed by incorporation of radioactively labeled thymidine.

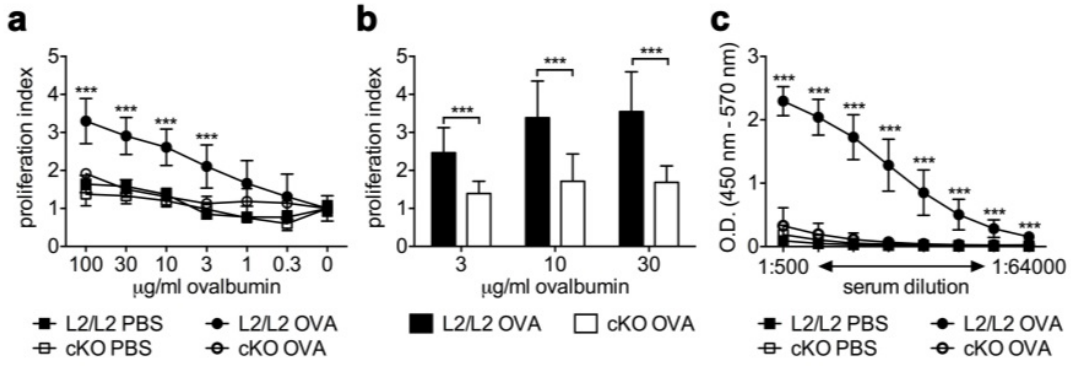

Figure 41: Ovalbumin-induced T cell expansion and antibody production are impaired in LRH-1-deficient mice.

(**a**) L2/L2 or cKO mice were immunized with ovalbumin protein in incomplete Freund's adjuvant for 14 days and proliferation was assessed by incorporation of ^{3}H-thymidine after *in vitro* re-stimulation with ovalbumin for 72 h. Mean values ± S.D. of one representative experiment is shown (L2/L2 PBS: n = 1; cKO PBS: n = 1; L2/L2 OVA: n = 4; cKO OVA: n =2). (**b**) Pooled results of three individual experiments are shown (L2/L2 PBS: n = 3; cKO PBS: n = 3; L2/L2 OVA: n = 13; cKO OVA: n = 11 mice). (**c**) Anti-ovalbumin ELISA of serum dilutions derived from control (PBS) or ovalbumin-injected L2/L2 or cKO animals at day 14 post immunization. L2/L2 PBS: n = 6; cKO PBS: n = 6; L2/L2 OVA: n = 13; cKO OVA: n = 11. Mean values ± S.D. are shown. * $p<0.05$, ** $p<0.01$, *** $p<0.001$.

As expected, control immunization with PBS did not induce the expansion of ovalbumin specific T cells in cKO and L2/L2 animals (Figure 41a). In contrast, L2/L2 mice immunized with ovalbumin antigen exhibited strong proliferation which can be attributed to the *in vivo* expansion of antigen specific T cells (Figure 41a-b). Interestingly, ovalbumin-specific proliferation was almost undetectable and around the background levels in splenocytes derived from cKO animals (Figure 41a-b).

To further evaluate the ability of LRH-1 deficient T cells to provide B cell help, titers of anti-ovalbumin antibodies were measured in the serum of immunized mice. While the amount of anti-ovalbumin antibodies was very high in ovalbumin challenged L2/L2 animals, titers were almost undetectable in cKO mice (Figure 41c). This indicates that T cell dependent B cell activation is defective in cKO mice and with this an important function of T helper cells.

One controversial aspect about the ovalbumin immunization experiment is, that cKO animals already start with significantly reduced T cell numbers in general and

particularly reduced numbers of mature CD4+ T cells. To exclude that the defective CD4+ effector function originates from the overall lack of T helper cells and to further examine CD4+ effector functions *in vivo*, the pathogenesis model of transfer colitis was applied. All transfer colitis experiments were performed by Anna-Lena Geiselhöringer during her master thesis with minimal support and hence reported here only briefly.

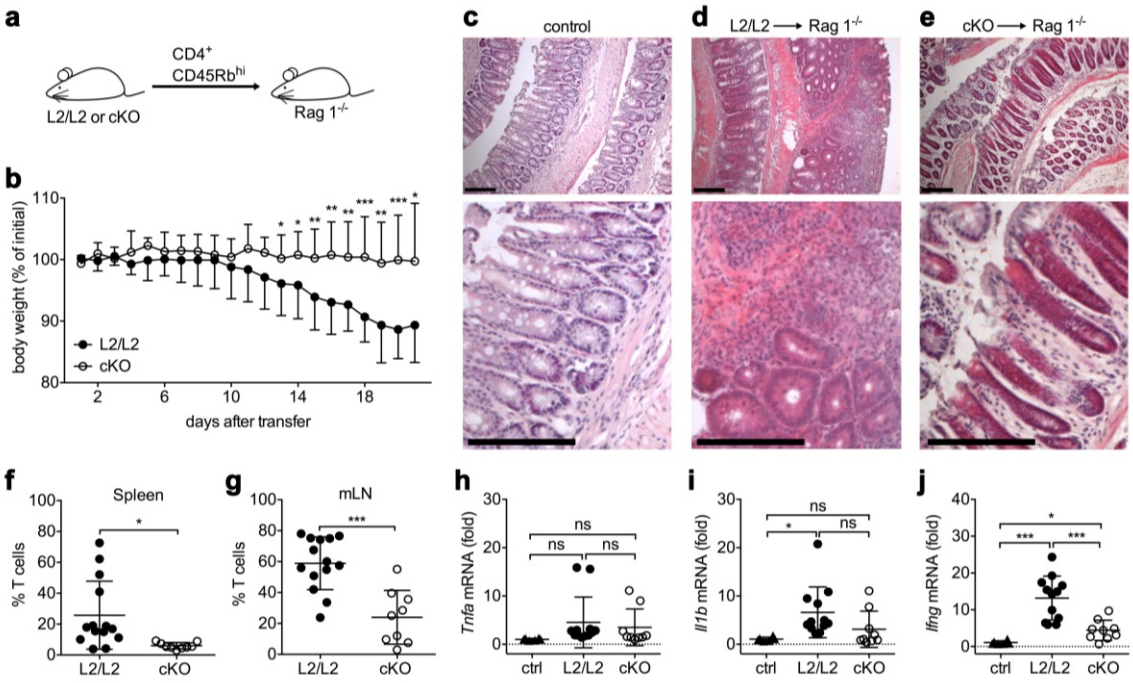

Figure 42: Induction of transfer colitis is impaired in LRH-1 deficient CD4+ T cells.

(**a**) Schematic representation illustrating the induction of transfer colitis in Rag 1-/- recipient mice. (**b**) Colitis-induced loss of body weight in Rag 1-/- mice injected with L2/L2 or cKO CD4+ CD45Rbhi T cells (L2/L2 donor: n = 14; cKO donor: n = 9). (**c-e**) Representative hematoxylin/eosin (H/E) colon sections derived from a Rag 1-/- mouse which was (c) untreated or received CD4+ CD45Rbhi T cells from (d) L2/L2 or (e) cKO donors. Upper panel: lower magnification; lower panels: higher magnification. Scale bar = 300 µm. (**f-g**) Relative abundance of naïve L2/L2 or cKO T cells after repopulation of (f) spleen or (g) mesenteric lymph nodes (mLN). (**h-j**) mRNA expression levels of the pro-inflammatory cytokines (h) *Tnfa* (i) *Il1b* or (j) *Ifng* in colon samples derived from control mice or Rag 1-/- animals transferred with L2/L2 or cKO T cells. Mean values ± S.D. of n = 9-14 mice are shown. * p<0.05, ** p<0.01, *** p<0.001, ns: not significant.

The colitis pathogenesis model is based on the transfer of naïve CD4+ CD45Rbhi T cells into syngeneic lymphopenic Rag 1-/- hosts. In the B- and T cell lacking recipient animal, naïve T cells encounter antigens derived from the gut microbiota. The lack of regulatory T cells (T_{reg}) leads to uncontrolled activation and proliferation of the transferred T cells which finally results in the induction of pancolitis and inflammation of the small bowel[146,148,168] (Figure 42a).

In contrast to L2/L2 T cells, which induced a characteristic, time-dependent loss of body weight (Figure 42b) and severe colonic inflammation (Figure 42d), Rag $1^{-/-}$ recipient mice, failed to promote body weight loss and caused significantly less colonic inflammation after the transfer of cKO T cells (Figure 42b; e). Histological colon sections were compared to those derived from untreated Rag $1^{-/-}$ animals (Figure 42c).

In line with the attenuated colitis induction by cKO donor cells, significantly reduced expansion and repopulation of spleen (Figure 42f) and mesenteric lymph nodes (Figure 42g) was observed. Furthermore, reduced expression of pro-inflammatory cytokines was measured in the colon of Rag 1-deficient mice after the transfer of naïve, LRH-1 deficient T cells (Figure 42h-j).

As T cell-mediated colitis induction is subject to uncontrolled cell proliferation, co-transfer of T_{reg} containing $CD4^+$ $CD45Rb^{lo}$ lymphocytes usually results in complete protection or at least attenuation of disease severity[148] (Figure 43a). While the transfer of CD45.1 $CD4^+$ $CD45Rb^{hi}$ T cells evoked pronounced colitis accompanied by body weight loss (Figure 43b) and colonic inflammation (Figure 43c), transfer of L2/L2 derived $CD4^+$ $CD45Rb^{lo}$ lymphocytes resulted in restored body weight (Figure 43b) and attenuated colonic inflammation (Figure 43d). Purified cKO $CD4^+$ $CD45Rb^{lo}$ T cells, however, were unable to protect the animals from disease development (Figure 43b; e).

Consistently, relative abundance of cKO donor T cells in the spleen (Figure 43f) and mesenteric lymph nodes (Figure 43g) of recipient mice indicate that this defect in colitis protection is based on an impaired expansion of regulatory T cells *in vivo*.

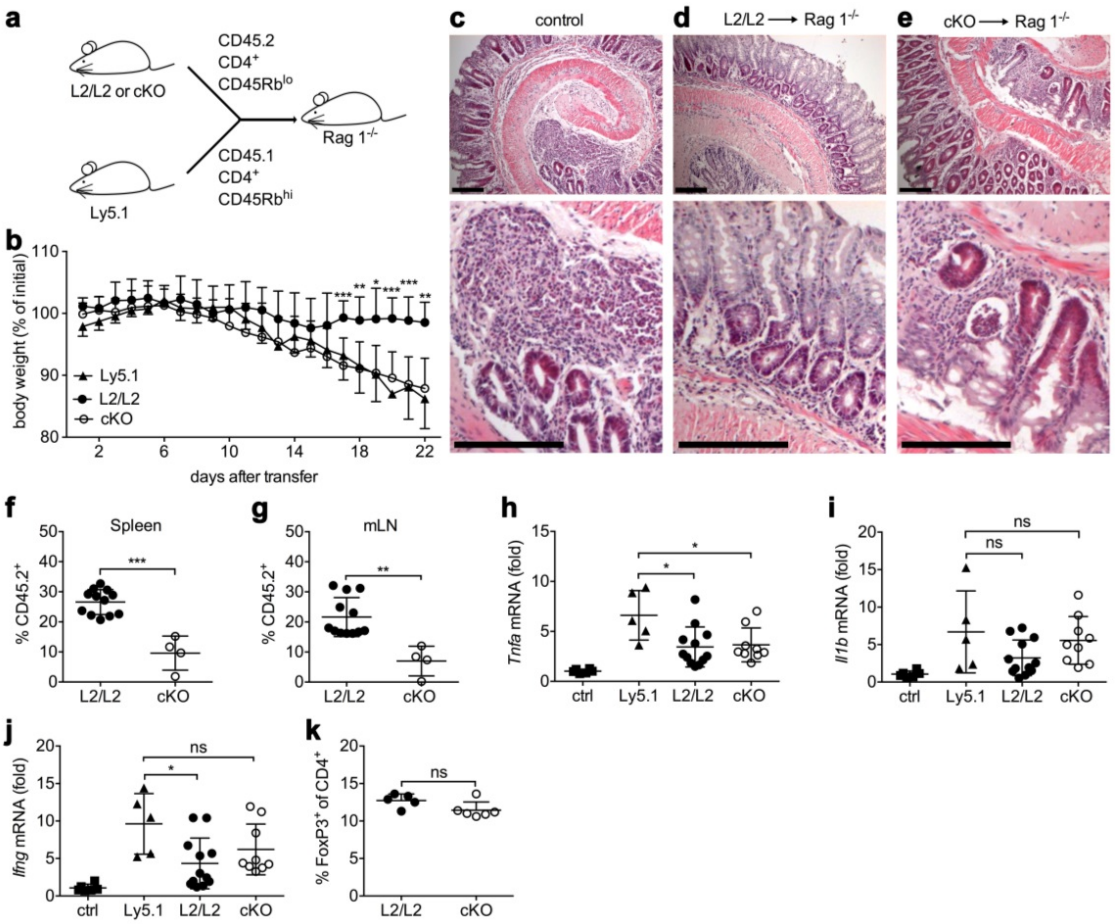

Figure 43: Defective function of LRH-1 deficient regulatory T cells.

(**a**) Model illustrating the experimental setup for the induction and protection of transfer colitis in Rag $1^{-/-}$ recipient mice. (**b**) Colitis-induced loss of body weight after transfer of naïve Ly5.1 wild type cells only or the co-transfer of $CD4^+CD45Rb^{lo}$ regulatory T cells derived from L2/L2 or cKO animals. (**c-e**) Representative hematoxylin and eosin (H/E) stainings of colon sections (c) upon colitis induction by naïve Ly5.1 wild type cells or upon the transfer of (d) L2/L2 or (e) cKO derived $CD4^+CD45Rb^{lo}$ T cells. Upper panel: lower magnification; lower panels: higher magnification. Scale bar = 300 µm. (**f-g**) Relative abundance of L2/L2 or cKO regulatory T cells after repopulation of (f) spleen or (g) mesenteric lymph nodes (mLN). (**h-j**) mRNA expression levels of the pro-inflammatory cytokines (h) *Tnfa* (i) *Il1b* or (j) *Ifng* in colon samples of untreated mice (ctrl), after the transfer of naïve Ly5.1 wild type cells only or the co-transfer of L2/L2 or cKO regulatory T cells. ctrl: n = 6; Ly5.1: n = 5; L2/L2: n = 12; cKO: n = 9 animals. (**k**) Relative abundance of $FoxP3^+$ cells in the $CD4^+$ population of T cells. n = 5-6 mice. Mean values ± S.D. are shown. * $p<0.05$, ** $p<0.01$, *** $p<0.001$, ns: not significant; dpi: days post infection.

While L2/L2 donor cells were able to reduce colonic expression on *Ifng* mRNA significantly, cKO T cells were not (Figure 43j). Cells from both, cKO and L2/L2 donors significantly reduced *Tnfa* mRNA levels (Figure 43h), however, *Il1b* expression was not altered (Figure 43i). To confirm that the failure in colitis protection is derived from defective $CD4^+$ effector functions and not caused by a reduced frequency of T_{reg} within the population of $CD4^+$ $CD45Rb^{lo}$ cKO T cells, the relative abundance of splenic

Foxp3⁺ CD4⁺ lymphocytes was determined in L2/L2 and cKO mice. Importantly, the abundance of Foxp3⁺ CD4⁺ cells was comparable, confirming the dependence of CD4⁺ effector functions on LRH-1 (Figure 43k).

3.12 LRH-1 deficiency impairs virus clearance by cytotoxic T cells

Interested, if the effector function of cytotoxic T cells is also dependent on LRH-1, the CD8⁺ immune response towards LCMV infection was compared between cKO and L2/L2 animals. In close collaboration with Juan Huang, mice were injected with virus derived from the LCMV-WE strain and expansion of CD8αβ⁺TCRαβ⁺ was monitored at different time points post infection. In line with previous observations, cKO animals started with a decreased number of cytotoxic T cells. However, these cells expanded with a similar kinetic as control cells did (Figure 45a). Along these lines, expression of the activation markers CD69 (Figure 45b) and CD25 (Figure 45c) was upregulated in cKO T cells similar to cells derived from L2/L2 mice.

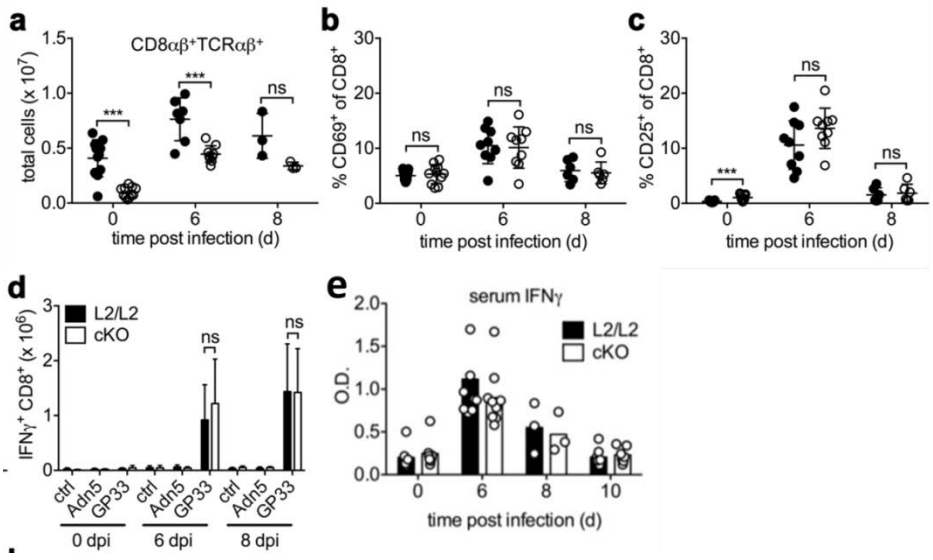

Figure 44: LCMV-specific expansion of cytotoxic T cells.

(**a**) LCMV-induced expansion of CD8αβ⁺ TCRαβ⁺ T cells (0 dpi: n = 11; 6 dpi: n = 9; 8 dpi: n = 3 mice). (**b-c**) Upregulation of the activation marker (b) CD69 or (c) CD25 in CD8⁺ T cells after LCMV infection (0 dpi: n = 11; 6 dpi: n = 9; 8 dpi: n = 6 mice). (**d**) Relative abundance of virus-specific IFNγ-producing CD8⁺ lymphocytes after *in vitro* restimulation with buffer control, Adn5 control peptide or LCMV-specific GP33 peptide assessed by intracellular staining (0 dpi: n = 8; 6 dpi: n = 9; 8 dpi: n = 6 mice). (**e**) Serum IFNγ levels in L2/L2 and cKO mice after LCMV infection (0 dpi: n = 8; 6 dpi: n = 9; 8 dpi: n = 3; 10 dpi: n = 7 mice). Mean values ± S.D. are shown. * p<0.05, ** p<0.01, *** p<0.001, ns: not significant; dpi: days post infection.

To enumerate the relative abundance of LCMV-specific cytotoxic T cells, splenocytes of cKO and L2/L2 animals were restimulated *in vitro* with the virus-specific GP33 peptide before they were subjected to intracellular IFNγ staining. Specificity was confirmed by the absence of IFNγ positive cells in subsets treated with irrelevant adenovirus antigen Adn5 or untreated control cells (Figure 44d). Interestingly, in L2/L2 as well as cKO splenocytes, similar abundance of LCMV-specific IFNγ positive cells was observed at days 6 and 8 post infection (Figure 44d). Comparison of IFNγ levels in the serum of these animals also revealed no significant differences (Figure 44e).

Detailed investigations were further performed to assess virus titers in different tissues of L2/L2 and cKO animals and to confirm efficient elimination of LCMV virus by cytotoxic T cells. Unexpectedly, while the virus load was reduced over time in L2/L2 animals and virus was almost deleted on day 8, cKO animals completely failed to eliminate the virus in all tissues examined (Figure 45a-d). Immunohistochemical staining of the LCMV nucleoprotein VL4 in liver sections further confirmed defective effector functions of LRH-1 deficient cytotoxic T cells and the presence of virus protein in cKO animals on day 10 (Figure 45e). Hence, although cytotoxic T cells expanded and became activated in a similar manner as control cells did, $CD8^+$ cKO cells completely failed to eliminate LCMV virus.

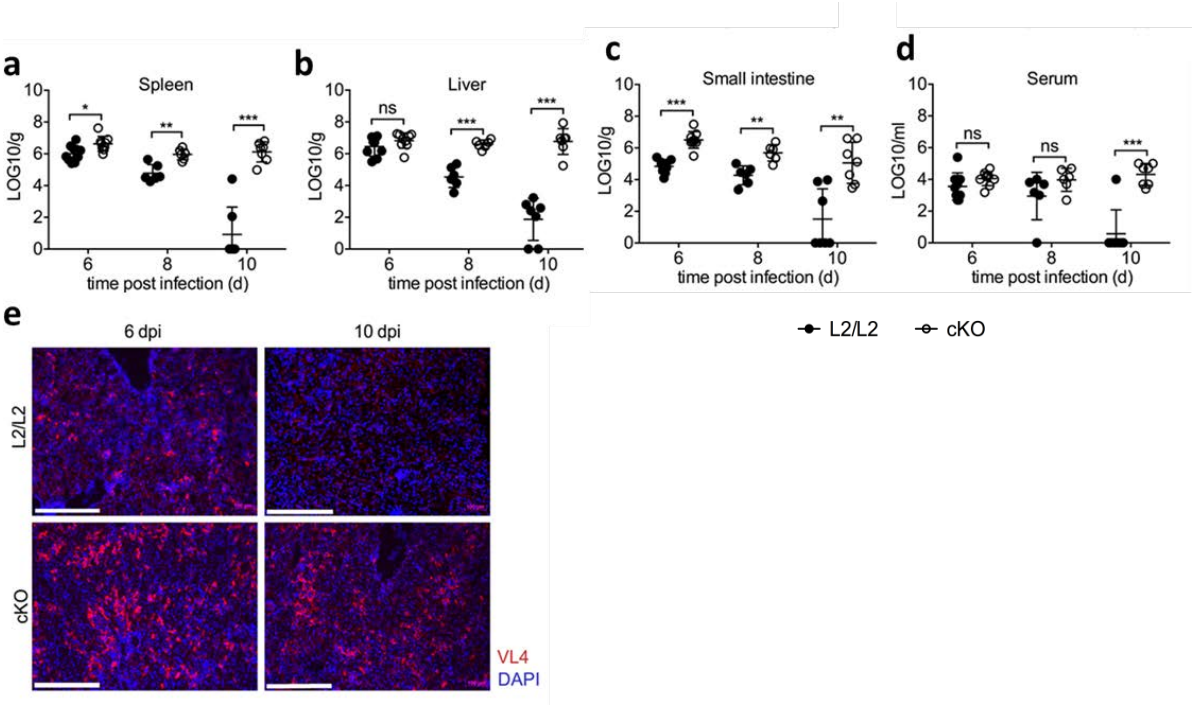

Figure 45: Impaired elimination of LCMV virus in LRH-1 deficient cytotoxic T cells.

(**a-d**) LCMV titers after infection of L2/L2 (filled symbols) or cKO (empty symbols) observed in (a) spleen, (b) liver, (c) small intestine or (d) serum (6 dpi: n = 9; 8 dpi: n = 6; 10 dpi: n = 7 mice). (**e**) Immunohistological staining of LCMV-infected liver sections derived from L2/L2 or cKO animals at day 6 and day 10 post infection (dpi). VL4 LCMV nucleoprotein: red; nuclei: blue (DAPI). Representative pictures are shown. Scale bar = 300 µm. Mean values ± SD are shown. * $p<0.05$, ** $p<0.01$, *** $p<0.001$, ns: not significant.

To investigate if LRH-1 deficient T cells fail to control LCMV expansion due to defective production or secretion of cytotoxic effector molecules, the expression of perforin (encoded by the *Prf1* gene), granzyme B (*Gzmb*) and FasL (*Faslg*) were examined. Importantly, *Prf1* as well as *Gzmb* and *Faslg* were transcribed in both, L2/L2 and cKO animals with minimal difference (Figure 46a-c). Expression was furthermore upregulated with similar kinetics (Figure 46a-c). Lack of effector molecule production can hence be excluded as main reason for the defective cytotoxic immune response.

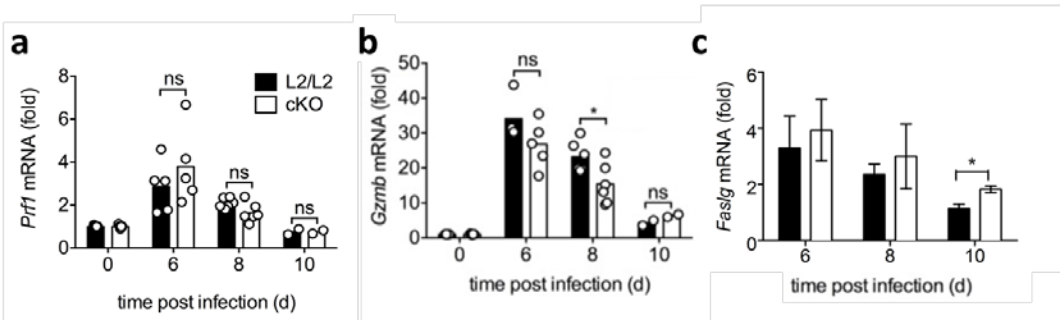

Figure 46: LRH-1 deficient CD8⁺ T cells express cytotoxic effector molecules.

(**a-b**) mRNA expression of the cytotoxic T cell effector molecules (a) perforin (*Prf1*) or (b) granzyme B (*Gzmb*) (0 dpi: n = 5; 6 dpi: n = 5; 8 dpi: n = 6; 10 dpi: n = 2 mice). dpi: days post infection. Mean values ± SD are shown. * p<0.05, ns: not significant.

As the transcription of genes encoding for the effector molecules alone does not provide evidence for the secretion and functionality of cytotoxic molecules, the ability of CD8⁺ T cells to fragment the DNA of target cells was analyzed and compared between cKO and L2/L2 animals. It was observed that, in whole splenocytes, both cKO and L2/L2 derived LCMV specific cytotoxic T cells were able to kill GP33-loaded target cells. Cells coated with the Adn5 peptide, in contrast, were not subjected to cell death induction in either genotype (Figure 47a). This finding was further confirmed in sort-purified CD8⁺ T cells (Figure 47b), excluding impaired secretion and confirming the integrity of cytotoxic molecules.

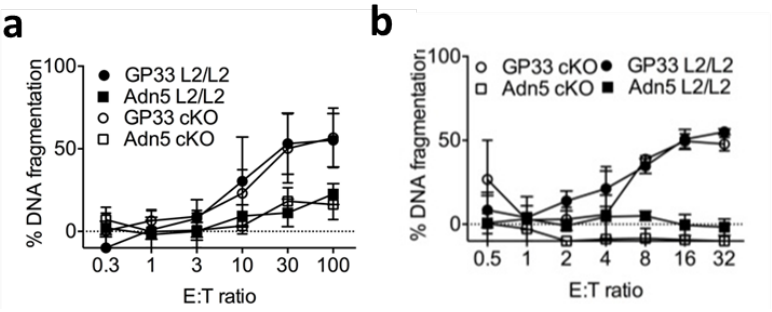

Figure 47: Cytotoxicity is not impaired in LRH-1 deficient CD8⁺ T cells.

(**a-b**) DNA fragmentation of GP33 or Adn5-coated EL-4 cells induced by LCMV-specific T cells derived from (a) whole splenocytes or (b) purified CD8⁺ T cells as assessed by the loss of ^{3}H-thymidine at 8 days post infection. (a): n = 3 mice; one representative experiment out of 2 is shown; (b): n = 3 technical replicates of pooled cells derived from 3 mice. Mean values ± SD are shown. E:T ratio = effector : target ratio. * p<0.05, ** p<0.01, *** p<0.001, ns: not significant.

4 Discussion

4.1 LRH-1 expression and mitogen-induced upregulation

Although the nuclear transcription factor LRH-1 is subject of extensive research in endodermal tissues, there is enigmatic knowledge about its expression and role in other tissues including hematopoietic cells. First, indirect report for a role of LRH-1 in T cells came from Benod et al.[86]. During studies on human pancreatic tumors, Benod and colleagues reported specific LRH-1 staining in tumor infiltrating lymphocytes. Expression of LRH-1 in immune cells was then first described by Lefèvre et al.[89] who examined the role of LRH-1 during cytokine-induced differentiation of macrophages and by Schwaderer et al.[91,169] who investigated the role of LRH-1 in the transcriptional control of FasL. Apart from these reports, the expression and function of LRH-1 in cells of the hematopoietic lineage, especially T lymphocytes, is unexplored.

Gene profiling studies revealed *Nr5a2* gene transcription in primary and secondary lymphatic organs (Figure 10) and confirmed expression in purified T cell subsets (Figure 11c). Presence of *NR5A2* mRNA was further confirmed in the human context (Figure 12). However, detected expression levels were extremely low and about 100 to 1000 times lower compared to the intestine and liver (Figure 11). This might explain why the expression and function of LRH-1 in T cells has been largely ignored until now.

Interestingly, LRH-1 expression in human leukemia cells was dependent on the cell proliferation status (Figure 13) and inducible by mitogenic stimulation in human and murine T cells (Figure 15). These findings demonstrate that LRH-1 expression is regulated in a rather dynamic manner and suggest a link between LRH-1 and T cell proliferation. The observation that LRH-1 is induced very early after T cell activation (Figure 14) emphasizes a critical role for LRH-1 in the initiation of T cell proliferation. This is in line with the well described function of LRH-1 in the regulation of cyclin expression and hence cell proliferation as described in stem cells of the intestinal epithelium as well as cancer cells[78].

A critical role for LRH-1 in context of T cell activation was supported by pronounced apoptosis induction after mitogenic stimulation (Figure 29). Difficulties to enter the cell cycle might account for this pronounced cell death in T cells. Similar to cells that are treated with anti-mitotic drugs for a prolonged period and hence undergo apoptosis, cell death might be caused by conflicting signals that induce cell proliferation but at the same time do not allow cell cycle progression. This hypothesis is supported by the early onset of cell death induction, especially in $CD4^+$ lymphocytes. Interestingly, also the basal levels of cell death were enhanced in LRH-1 deficient T cells. This might be explained by a possible role of LRH-1 in the regulation of cell death which is subject of current research.

4.2 LRH-1 in T cell development

While macroscopically similar, the thymus of *Nr5a2*$^{L2/L2}$ CD4-Cre animals contained significantly reduced $CD4^+CD8^+$ and $CD4^+$ lymphocyte populations. Relative amounts of $CD8^+$ and especially $CD4^-CD8^-$ T cells were consistently increased (Figure 19). Reduced $CD4^+$ T cell numbers are in line with the pronounced loss of mature $CD4^+$ T cells (Figure 21-23) as well as their particular dependence on LRH-1 for cell proliferation (Figure 34) and possibly also survival (Figure 28). The relative increase in $CD8^+$ T cells might be explained by the fact that this T cell subset is less dependent and hence also less affected by the deletion of LRH-1. As thymocytes undergo massive proliferation during the transition from DN to DP stages to ensure diversification of the T cell receptor reservoir[170], the lack of DP thymocytes confirms a critical role for LRH-1 in cell division. Increased levels of DN thymocytes might be explained by the attempt of the body to counterbalance the loss of DP and $CD4^+$ thymocytes, as total numbers were comparable between L2/L2 and cKO thymi (Figure 19). Furthermore, LRH-1 is not yet deleted within the DN subset (Figure 17). Relative accumulation of cells in the DN3 stage can either be caused by defective TCRβ-re-arrangement and subsequent failure to undergo cell division or by the enhanced cell death of DN4 thymocytes due to impaired cell proliferation. However, LRH-1 deficiency seems to affect T cells whenever they become activated and are pushed for division.

Preliminary experiments further revealed that efficient deletion of LRH-1, driven by the lck promoter, caused the loss of approximately 95% thymocytes (Figure 20). It is unclear why the deletion efficiency varied strongly between animals. Nevertheless, together these data suggest a critical role of LRH-1 during T cell development.

4.3 Loss of mature T cells in cKO animals

CD4 promoter-driven deletion of LRH-1 caused dramatic loss of mature T cells and had severe impacts on the distribution of lymphocyte subsets (Figure 21-23). While $CD4^+$ T cells were deleted by approximately 80%, $CD8^+$ lymphocytes were affected less with a reduction of 50% (Figure 22-23). This loss of T cells can also be explained by defective proliferation such as during homeostatic expansion. Once single positive lymphocytes are released from the thymus, they undergo proliferation to populate secondary lymphoid organs. Adoptive transfer studies showed that LRH-1 deficient $CD4^+$ T cells are not able to proliferate *in vivo*, while $CD8^+$ lymphocytes were not affected to the same extent (Figure 40). This might account for the reduced lymphocyte number.

Interestingly, cKO $CD8^+$ T cells were shown to secrete massive amounts of cytokines, especially IFNγ (Figure 32). It is reported that naïve $CD8^+$ T cells acquire phenotypic and functional characteristics of antigen-induced memory T cells when they undergo homeostasis-driven proliferation[114]. This memory-like phenotype includes acceleration of IFNγ secretion. It thus seems likely that most of the $CD8^+$ T cells that made it to the secondary lymphoid organs underwent homeostatic expansion. Together with the observation that proliferation of $CD8^+$ T cells is less dependent on LRH-1, this might explain the difference in the severity of T cell reduction between $CD4^+$ and $CD8^+$ lymphocytes.

.

4.4 LRH-1 regulates cell proliferation in T lymphocytes

A key role for LRH-1 in the regulation of cell proliferation was confirmed by the incapability of T cells to undergo cell division after genetic deletion (Figures 33-34) or pharmacological inhibition of LRH-1 (Figure 37). Although LRH-1 seems to be involved in T cell metabolism, substitution of cell culture medium was not sufficient to rescue the proliferation defects and hence cannot explain the incapability of cKO T cells to divide (Figure 34).

Proliferation defects were particularly prominent in $CD4^+$ lymphocytes, not only *in vitro* (Figures 34, 37-38) but also *in vivo (*Figure 40-43*).* It is unlikely that these proliferation deficiencies result from improper T cell activation as upregulation of early activation markers (Figure 31) and cytokine secretion (Figure 32) were unremarkable. Furthermore, proliferation defects of $CD4^+$ T cells correlate well with the observed inability of $CD4^+CD45Rb^{hi}$ lymphocytes to induce colitis (Figure 42) as well as the failure of $CD4^+CD45Rb^{lo}$ T cells to protect Rag $1^{-/-}$ animals from experimental colitis (Figure 43). The abundancy of regulatory T cells was similar in L2/L2 and cKO mice.

When splenocytes were examined for their ability to divide by CFSE dilution (Figure 34), only $CD4^+$ T cells showed defects while $CD8^+$ T cells were not affected. This phenomenon can neither be explained by incomplete deletion nor by LRH-1 independent proliferation in $CD8^+$ lymphocytes. In theory, CD4 promoter-driven Cre recombinase is activated during the double positive stage of thymocyte maturation and hence expected to target $CD4^+$ and $CD8^+$ lymphocytes in a comparable manner. In line, knockout efficiency was only slightly lower but with approximately 80-90% still almost complete in the $CD8^+$ subset as shown by fluorescence conversion in mTmG reporter mice (Figures 17-18). Insufficient deletion can hence not account for the reduced impact of LRH-1 deletion on $CD8^+$ T cell proliferation. Furthermore, $CD8^+$ T cells developed severe proliferation defects when purified (Figure 38), treated with specific LRH-1 antagonists (Figure 37) or cultured under sub-optimal conditions (Figure 36). It rather seems that in $CD8^+$ T cells, LRH-1 can be replaced by compensatory signals distinct from B7-CD28 interaction. One indication for this

theory is that CD8+ T cells did not show proliferation defects in presence of accessory cells (Figure 34). Furthermore, inhibitors were applied to mixed splenocyte populations. Thus, LRH-1 was not only deleted in T cells but also accessory cells which subsequently might lead to decreased amounts of macrophage secretory factors and other cytokines. Lack of compensatory signals might then unveil proliferation defects in CD8+ T cells. Another aspect that has to be considered is that CD8+ T cells showed proliferation defects when cultured under reduced FBS conditions (Figure 36). As FBS contains not only small molecules such as lipids, amino acids and hormones but also a myriad of growth factors[171], it is likely that it also provides signals that compensate for the loss of LRH-1 in CD8+ T cells. In line with this hypothesis, exogenous addition of IL-15 tended to restore cell proliferation in CD8+ T cells (Figure 38).

4.5 Role of LRH-1 in T cell-mediated cytotoxicity

While all results concerning CD4+ effector functions can be explained by impaired cell proliferation, the situation seems to be more complex in CD8+ T cells. During LCMV infection, LRH-1 deficient CD8+ T cells showed normal expansion with a kinetic comparable to L2/L2, although cKO animals started with reduced levels of CD8+ T cells (Figure 44). Intracellular IFNγ staining after *in vitro* restimulation with virus specific peptides further confirmed the expansion of LCMV-specific CD8+ lymphocytes. Along these lines, upregulation of activation markers and cytokine expression were comparable between L2/L2 and cKO animals (Figure 44).

It was hence surprising that cKO CD8+ T cells clearly failed to control the spreading of LCMV (Figure 45). While LCMV titers were barely detectable on day 10 post infection in L2/L2 animals, they remained high in animals with deleted LRH-1 expression (Figure 45). As neither expansion nor activation of virus-specific T cells seems to be affected by the loss of LRH-1, this observation is rather difficult to interpret. In addition, gene expression analysis ruled out that LRH-1 deficient T cells fail to produce cytotoxic effector molecules and confirmed the expression and virus-specific induction of perforin, granzyme B and FasL at least on an mRNA level (Figure 46). As perforin is the critical effector molecule in the clearance of LCMV and its expression

was comparable between cKO and L2/L2 animals, lack of cytotoxic molecules cannot account for defective virus clearance. Furthermore, integer spleen architecture in cKO animals rules out that disturbed distribution of marginal zone macrophages, which are important in the etiopathology of LCMV infection, are the cause for impaired virus clearance.

Alternative explanations include the possibility that $CD8^+$ T cells do not reach critical numbers for the efficient elimination of LCMV or T cell exhaustion. The most probable reason, however, might be the lack of functional $CD4^+$ T cell help in the coordination of the anti-viral immune response. It is known that $CD4^+$ lymphocytes orchestrate the recruitment and expansion of cytotoxic T cells, so the lack of mature T helper cells in cKO animals could result in defective effector functions. This is in line with the observation that cytotoxic T cells were able to specifically fragment the DNA of target cells *in vitro* (Figure 47).

4.6 Translation to human applications

An interesting aspect of this study is its high potential to transfer the knowledge for future application in humans. Expression of LRH-1 was not only confirmed in human PBMCs and T cell leukemia lines (Figure 12), but also activation-induced upregulation (Figures 13, 15) was described. In mice, two inhibitors (3d2, SR1848) that follow different mechanisms of action were furthermore used for the transient inhibition of LRH-1. Both antagonists were able to significantly reduce cell proliferation and could easily be administered to human cells Treatment of human PBMCs with 3d2 already confirmed a potential modulation of LRH-1 in T cells (Figure 39). As the activity of nuclear transcription factors can be modified by synthetic ligands, they are an interesting pharmaceutical target. Although no endogenous ligands for LRH-1 are identified so far, there are synthetic compounds developed which are known to activate or inhibit is activity. The low expression of LRH-1 in T cells in comparison to endodermal tissues may further open an interesting therapeutic window for the application of synthetic LRH-1 ligands. While low doses of these drugs could potentially inhibit T cell mediated immunopathologies or enhance the function of

vaccines, vital functions of other tissues might not be affected. It was shown by Schwaderer et al.[90] that administration of 3d2 was tolerated by mice with minor damage observed in the liver of the animals, while concanavalin A induced hepatitis was reduced.

5 Outlook

This study focuses on the impact of conditional LRH-1 deletion in the more mature T cells, as CD4 promoter driven Cre recombinase expression is first induced in $CD4^+CD8^+$ thymocytes. However, first examinations of LRH-1 mTmG lck-Cre animals revealed a critical function already during earlier stages of thymocyte development. Many questions remain unsolved concerning the function of LRH-1 during T cell maturation. Apart from the examination of increased animal numbers, also the effect on double negative thymocytes should be further explored. Unclear remain the reasons concerning varying efficiencies of lck-Cre mediated deletion between animals and the expansion of escape mutants in those mice, which did not show an obvious phenotype.

While this study focuses on the function of LRH-1 in murine T cells, it also confirms mRNA expression and upregulation in human PBMCs and inhibition of cell proliferation in response to LRH-1 antagonists. However, these proliferation studies were only performed once with blood derived from three independent donors. Experiments should be repeated and could be extended to the siRNA- or CRISPRS/Cas-mediated downregulation/deletion of LRH-1 to provide deeper insights and confirm these findings. Methods of LRH-1 downregulation/deletion could further be applied to mouse T cells. Alternatively, mature T cells could be studied after the adenoviral introduction of Cre-recombinase into mature L2/L2 T cells, to avoid any effects that LRH-1 has on T cell maturation and circumvent problems caused by the low number of mature T cells in cKO mice.

LCMV infection experiments revealed the inability of $CD8^+$ T cells to control virus expansion. However, based on the normal upregulation of activation markers, virus-specific expansion of cytotoxic T cells and expression of effector molecules the concrete reason remains unclear. Besides the hypotheses of T cell exhaustion or insufficient $CD8^+$ T cell numbers, missing $CD4^+$ T cell based orchestration of the immune response was stated as a possible reason. To proof this concept, LCMV

infection could be repeated in cKO animals with an additional transfer of L2/L2 $CD4^+$ lymphocytes. cKO $CD8^+$ lymphocytes should then be able to clear the virus.

Another way of approaching to unravel the function of LRH-1 in T cells is the deletion of LRH-1 coregulatory proteins. Amongst these, small heterodimeric partner (SHP) is one of the best characterized LRH-1 repressors. Thus, deletion of SHP hypothetically enhances cell proliferation. SHP $^{-/-}$ animals are available in the laboratory and could be used to further confirm the regulatory role of LRH-1 on T cell proliferation.

Room for discussion is also available concerning the molecular mechanisms that lead to the regulation of LRH-1 expression and activity as well as those that are induced by LRH-1 itself. While LRH-1 most likely controls cell cycle progression via the described transcriptional regulation of cyclins D_1 and E_1, there is no proof for this hypothesis in T cells, yet. This question could be targeted by the selective inhibition of signaling pathways and the detailed examination of cyclin induction in LRH-1 deficient T cells. Along these lines, inhibitors could be used to unravel the signaling pathways that are involved in the regulation of LRH-1 expression.

An interesting way to confirm the proliferation defects during homeostatic expansion and further address cell proliferation *in vivo* is the transfer of CFSE stained T cells into lymphopenic hosts where these cells can proliferate and subsequent can be reanalyzed using flow cytometry. CFSE staining allows differentiation between $CD4^+$ and $CD8^+$ T cells and allows the specific tracking of cell division rather than the examination of live cells. In this regard, histological sections could be stained for Ki67 expression to evaluate the distribution of proliferating cells and determine cell proliferation rates.

As the tight regulation of T cell proliferation and effector functions is critical for the prevention of immunopathological diseases, it would be interesting to examine the effect of LRH-1 inhibitors on T cell-mediated or autoimmune disorders. Therefore, LRH-1 antagonists could be applied to human leukemia cell lines or leukemia pathogenesis models. The effect or LRH-1 inhibition on the replication of highly proliferating cancer T cells would be of particular interest to evaluate its relevance for

a possible application in human patients. Another very interesting approach could be the application of LRH-1 inhibitors to modulate the spread of human immunodeficiency virus (HIV). Based on the observation that pathogenic HIV infection positively correlates with $CD4^+$ T cell proliferation[172], inhibition of LRH-1 and hence cell proliferation could hypothetically attenuate virus replication and with this, disease severity. A conceivable application for synthetic LRH-1 agonists could be the enhancement of T cell vaccinations with bacterial or tumor antigens.

6 Conclusion

This study describes the so far unknown and underestimated role of LRH-1 in T lymphocytes and illustrates a critical role for LRH-1 in the regulation of T cell proliferation. LRH-1 expression was confirmed in immature and mature murine T cells as well as human PBMCs and T cell specific deletion of LRH-1 revealed dramatic changes in the number and effector functions of mature lymphocytes.

The observations that LRH-1 was upregulated in response to mitogenic stimuli in human and mouse and that LRH-1 deficient or inhibited T cells failed to proliferate *in vivo* and *in vitro,* emphasize the importance of LRH-1 in lymphocytes. Moreover, LRH-1 deficient $CD4^+$ T cells were neither able to provide B cell help, nor induce or prevent experimental colitis. Similarly, while virus-specific $CD8^+$ T cells were nicely activated, expanded normally and produced cytotoxic effector molecules, these cells were completely unable to eliminate LCMV. This study hence contributes to understanding the role of LRH-1 in T cell effector functions.

The confirmation of LRH-1 in human T cells as well its transient inhibition by several specific antagonists further suggest an application of synthetic LRH-1 ligands in the treatment of T cell-mediated diseases in humans. These findings might thus provide not only the basis to a deeper understanding in the regulation of immune cells and immune responses but also for pharmacological drug targeting.

7 Materials and Methods

7.1 Materials

Table 1: Cell lines

Name:	Organism:	Cell type:	Tissue:	Disease:
Jurkat lT	human	T lymphocyte	peripheral blood	acute T cell leukemia
MOLT-4	human	T lymphoblast	peripheral blood	acute lymphoblastic leukemia
CEM	human	T lymphoblast	peripheral blood	acute lymphoblastic leukemia
Caco2	human	epithelial	colon	colorectal adenocarcinoma
HepG2	human	epithelial	liver	hepatocellular carcinoma
EL-4	mouse	T lymphocyte	ascitic fluid	lymphoma

Notes:

Jurkat lT cells are stably transfected with a plasmid carrying the simian virus 40 (SV40) large T antigen. All cell lines were originally derived from ATCC; EL-4 cells were a kind gift from M. Groettrup (University of Konstanz) and have a C57BL/6 background.

Table 2: Cell culture maintaining reagents

Name:	Abbreviation:	Source:
Roswell Park Memorial Institute 1640	RPMI 1640	Sigma Aldrich
Dulbecco's Modified Eagle's Medium	DMEM	Sigma Aldrich
Phosphate buffered saline	PBS	Sigma Aldrich
Fetal bovine serum (heat inactivated)	FBS	Sigma Aldrich
L-glutamine	l-glut	Sigma Aldrich
gentamycin	genta	Sigma Aldrich
β-mercaptoethanol	2-ME	Roth
α-ketoglutarate	α-keto	Sigma Aldrich

Table 3: Cell culture reagents

Name:	Abbreviation:	Supplier:	Annotations:
stimulating reagents:			
concanavalin A	ConA	Sigma Aldrich	
phytohemagglutinin A	PHA-P		
phorbol 12-myristate 13-acetate	PMA	Enzo Life Sciences	
ionomycin	iono	Enzo Life Sciences	
cell death inducing reagents:			
dexamethasone	Dexa		
staurosporine	Stauro		
etoposide	Etop		
LRH-1 antagonists:			
compound 3 derivative 2	3d2	ChemBridge Corp.	published[56]
compound 7	cd7	ChemBridge Corp.	
SR1848		Sigma Aldrich	published[57]
Cytokines:			
murine interleukin 2	IL-2		eBioscience
murine interleukin 7	IL-7		
murine interleukin 15	IL-15		

Table 4: Antibodies

Primary antibody:	Clone:	Source:	Cat. number:	Lot:
Mouse (labeled):				
anti-CD3ε-APC	145-2C11	BD Pharmingen	553066	4280649
anti-CD45.1-BV421	A20	BD Pharmingen	563983	4042686
anti-CDCD45.2-APC	104	BD Pharmingen	558702	4021564
anti-CD8α-PerCP-Cy5.5	53-6.7	BD Pharmingen	551162	3130665
anti-CD45Rb-FITC	16A	BD Pharmingen	553099	4227847
anti-CD44-PE-Cy7	IM7	BD Pharmingen	560569	
anti-CD4-FITC	GK1.5	eBioscience	11-0041	E00079-1633
anti-CD8α-PE	53-6.7	eBioscience	12-0081	E01038-1634
anti-CD4-Cy5	GK1.5	eBioscience	19-0041	E0435-1482
anti-CD25-APC	PC61.5	eBioscience	17-0251	E07106-1633
anti-F4/80-APC	BM8	eBioscience	17-4801	E07285-1633
anti-NK1.1-PE	PK136	eBioscience	12-5941	E034024

anti-B220-PerCP-Cy5.5	RA3-6B2	eBioscience	45-0452	
anti-CD4-PE	GK1.5	eBioscience	12-0041	E01008-1638
anti-CD8β-FITC	eBioH35-17.2	eBioscience	11-0083	E00122-1632
anti-FoxP3-PE	FJK-16s	eBioscience	12-5773	4279536
anti-TCRβ-PE-Cy7	H57-597	eBioscience	25-5961	E17000-101
anti-IFNγ-FITC	XMG1.2	BioLegend	505806	B191877
anti-CD69-PE	H1.2F3	BioLegend	12-0691	B214527
anti-CD3ε-FITC	145-2C11	self-purified		
anti-VL4		M. Basler		
Annexin-V-FITC		self-purified		

Mouse (unlabeled)

anti-CD3ε	145-2C11	self-purified		
anti-CD28 (azide free)	37.51	Biolegend		

Human (labeled):

anti-CD4	FITC	BioLegend	357406	
anti-CD8α	PE	BioLegend	300908	

Secondary antibody:	**Conjugate:**	**Source:**	**Cat. number:**	**Lot:**
goat anti-rat IgG	Alexa 568	Invitrogen	A11031	48029A
goat anti-hamster IgG	FITC	BD Pharmingen	554011	84885
goat anti-mouse	HRP	Jackson Immuno Research	115-035-003	

mouse ELISA antibody:

	Clone:	**Supplier:**	**Cat. number:**	**Lot:**
IFNγ (capture)	R4-6A2	BioLegend	505702	B193420
IFNγ detection)	XMG1.2	BioLegend	505804	B144560
IL-2 (capture)	JES6-1A12	BioLegend	503702	B163369
IL-2 (detection)	JES6-5H4	BioLegend	503804	B187183
IL-1β (capture)	B122	BioLegend	503501	B190842
IL-1β (detection)	Poly5158	BioLegend	515801	B140263
TNFα (capture)	TN3-19.12	BioLegend	506102	B145868
TNFα (detection)	Poly5160	BioLegend	516003	B197425

Note: anti-CD3 antibody was purified from cell culture supernatant and conjugated with FITC. anti-VL4 antibody was a kind gift from M. Basler (University of Konstanz).

Table 5: Primer sequences

Gene		primer sequence
Nr5a2	fwd	5' – TTG AGT GGG CCA GGA GTA GT – 3'
	rev	5' – ACG CGA CTT CTG TGT GTG AG – 3'
Actb	fwd	5' – TAT TGG CAA CGA GCG GTT CC – 3'
	rev	5' – GCA CTG TGT TGG CAT AGA GG – 3'
Myc	fwd	5' – CTA GTG CTG CAT GAG GAG AC – 3'
	rev	5' – TTT GCC TCT TCT CCA CAG AC – 3'
Ccne1	fwd	5' – TTC TGC AGC GTC ATC CTC TC – 3'
	rev	5' – TGT GCC AAG TAG AAC GTC TC – 3'
Tnfa	fwd	5' – TAG CCC ACG TCG TAG CAA AC – 3'
	rev	5' – ACA AGG TAC AAC CCA TCG GC – 3'
Il1b	fwd	5' – TGC CAC CTT TTG ACA GTG ATG – 3'
	rev	5' – ATG TGC TGC TGC GAG ATT TG – 3'
Ifng	fwd	5' – CGG CAC AGT CAT TGA AAG CC – 3'
	rev	5' – TGT CAC CAT CCT TTT GCC AGT – 3'
Prf1	fwd	5' – TCT TGG TGG GAC TTC AGC TTT – 3'
	rev	5' – TCC ATA CAC CTG GCA CGA AC – 3'
Gzmb	fwd	5' – GCT GCT AAA GCT GAA GAG TAA GG – 3'
	rev	5' – TCA CAT TGA CAT TGC GCC TG – 3'
NR5A2	fwd	5' – GGG CAA CAA GTG GAC TAT TC – 3'
	rev	5' – CCA GCT GGA AGT TTT CAA GG – 3'
GAPDH	fwd	5' – ATG GAG AAG GCT GGG GCT CA – 3'
	rev	5' – AGT GAT GGC ATG GAC TGT GGT CAT – 3'
Faslg	fwd	5' – TTC CAC CTG CAG AAG GAA C – 3
	rev	5' – TAA ATG GGC CAC ACT CCT C – 3

Table 6: Plasmids

Plasmid	Backbone	Insert
pcDNA 3.1 Myc-His b-Gal	pcDNA 3.1 Myc-His	β-galactosidase
hLRH-1 Luciferase 1.5kb	pGl3 MCS3	1.5 kb hLRH-1 promoter
TKpGl3 LRH-1-RE5x	pGl3 basic	5x LRH-1 response elements
pGl3 MCS3	pGl3 basic	multiple cloning site 3
pGl3 basic	pGl3 basic	

Note: The 1.5kb human LRH-1 promoter luciferase reporter and control constructs have been described previously[66]. To test endogenous LRH-1 activity, Jurkat lT cells were transfected with a luciferase reporter construct containing 5 x LRH-1 response elements derived from the SHP promoter[173].

7.2 Methods

7.2.1 Animals

For all *in vitro* and *in vivo* experiments, male and female animals on C57BL/6 background carrying the leukocyte marker CD45 isoform 2 were used at an age between 7–15 weeks, unless otherwise stated. For experiments describing the abundance and upregulation of *Nr5a2* mRNA, wild type (wt) C57BL/6 mice were used.

Nr5a2$^{L2/L2}$ (L2/L2) mice[174] were bred with CD4-Cre$^{wt/tg}$ transgenic mice[175] to obtain *Nr5a2*$^{L2/L2}$ CD4-Cre (conditional knockout, cKO) animals. Animals were kept for heterozygous Cre expression. Transgenic mTmG reporter mice were kindly provided by U. Koch (EPFL Lausanne) and crossed with *Nr5a2*$^{L2/L2}$ CD4-Cre to obtain *Nr5a2*$^{L2/L2}$ mTmG CD4-Cre mice or with *Nr5a2*$^{L2/L2}$ lck-Cre to obtain *Nr5a2*$^{L2/L2}$ mTmG lck-Cre animals. In all experiments, cKO mice were compared to their corresponding, Cre-deficient littermate controls. Ly5.1 animals express the leukocyte marker CD45.1. Rag 1$^{-/-}$ animals were kindly provided by M. Basler (University of Konstanz) and bread on a Ly5.1 background.

All mice were housed at the central animal facility of the University of Konstanz in individually ventilated cages. Access to food and water was not restrained and mice were accustomed to a standard 12-hour light/ 12-hour dark cycle. Animal experiments complied with the German animal experimentation regulations approved by the Ethics Review Board of the Regierungspräsidium Freiburg. G*Power software[176] was used to predetermine sample size of all animal experiments.

7.2.2 Cell culture

Human leukemia T cell lines (MOLT-4, CEM) were cultured in RPMI-1640 medium supplemented with 10% FBS, 2 mM l-glutamine and 20 µg/ml gentamycin. Jurkat lT cells were cultured in complete RPMI-1640 medium with reduced amounts of FBS

(5%). HepG2 and Caco2 cell lines as well as murine EL-4 cells were maintained in DMEM, supplemented with 10% FBS, 2 mM l-glutamine and 20 µg/ml gentamycin.

Cells were cultured at 37°C with 5% CO_2 under humidified conditions and routinely sub-cultured to maintain logarithmic growth. For long-term storage, early passages were resuspended in freezing medium (complete medium with 10% DMSO) and subsequently preserved in the vapor phase of liquid nitrogen. All cell lines were tested negative for mycoplasma contamination (Venor GeM Kit; Minerva biolabs).

Mouse primary T cells were maintained in RPMI 1640 medium, supplemented with 10% FBS, 2 mM l-glutamine, 20 µg/ml gentamycin and 50 µM β-mercaptoethanol unless otherwise stated. For the analysis of metabolic defects, l-glutamine was substituted by 2 mM α-ketoglutarate. Primary cells were cultured at 37°C with 5% CO_2 under humidified conditions.

7.2.3 Transient transfection

All plasmids used were described earlier. For plasmid propagation, appropriate bacterial clones were grown in Luria-Bertani Broth (LB) medium before plasmids were isolated using the PureYield™ Plasmid Midiprep System (Promega) according to the manufacturer's instructions. Plasmid quality and quantity were assessed on a NanoDrop 2000 spectrophotometer (Thermo Fisher Scientific) and plasmid integrity was verified by restriction digestion (Technical Supplementary.Figure 49).

Jurkat lT cells were seeded at a density of 3×10^5 cells/ml one day prior to electro-poration using an Amaxa Nuclefection device (Lonza). For transient transfection, 10^6 cells were washed with PBS, resuspended in 100 µl SA-buffer B (150 mM Na2HPO4, 20 mM HEPES, 15 mM MgCl2, 5 mM KCl, 50 mM mannitol; pH 7.2) together with 2 µg plasmid DNA and transferred into a Gene Pulser® Cuvette (Biorad) where they were exposed to program X-005. Co-transfection with 0.2 µg β-galactosidase plasmid was performed for subsequent normalization of transfection efficiency. Electroporated cells were then pooled in pre-warmed antibiotic-free complete medium before they were seeded and incubated overnight for further treatment.

7.2.4 Luciferase reporter Assay

For the verification of endogenous LRH-1 activity, transfection was performed using a construct that contains 5 repeats of the LRH-1 response element cloned from the SHP promoter. To investigate the influence of cell proliferation on LRH-1 expression, cells were transfected with a 1.5 human LRH-1 promoter construct or the control plasmid MCS3 before they were treated with 50 ng/ml PMA and 1.1 µg/ml ionomycin or challenged by serum withdrawal for 24h.

Cells were then pelleted and incubated with 100 µl lysis buffer (100 mM K_2HPO_4, 0.2% TritonX-100; pH 7.8) on ice for 15 min. After removal of remaining particles, 30 µl of the cell lysate was transferred into a white flat-bottom 96-well plate. Further injection of 50 µl ATP solution (10mM ATP dissolved in 20mM $MgCl_2$, 35 mM glycyl-glycine containing assay buffer) and 50 µl luciferin (270 µm coenzyme-A lithium salt, 470 µM luciferin kalium salt in assay buffer) per well was automatically performed before chemiluminescence was assessed as relative light units (RLU) by an Infinite 200 PRO microplate reader (Tecan).

To normalize deviating transfection efficiencies, hydrolysis of the chromogen o-nitrophenyl-β-D-galactopyranosid (ONPG) by β-galactosidase was assessed. Therefore, 30 µl of cell lysate were incubated with 100 µl Z-buffer (60 mM Na_2HPO_4, 40 mM NaH_2PO_4, 50 mM β-mercaptoethanol) and 0.2 mg/ml ONPG in a transparent 96-well flat bottom plate. The plate was subsequently sealed and incubated at 37°C in the dark for approximately 120 min, before absorption at 405 nm was measured using an Infinite 200 PRO microplate reader (Tecan).

7.2.5 Isolation of primary T cells

Immature T cells were teased from the thymus by gently pulling the capsule apart with tweezers. Thymocytes were then separated from the fibrous capsule tissue by filtering over a 70 µm nylon membrane. Centrifugation steps were avoided.

For the isolation of mature T cells, appropriate organs were isolated from CO_2 euthanized mice and dissociated by grinding between the frosted ends of object slides,

which were frequently covered with PBS, until only the connective tissue remained. Erythrocyte removal was performed for secondary lymphatic tissues by the administration of ACK lysis buffer (0.15 M NH_4Cl, 10 mM $KHCO_3$, 0.1 mM Na_2EDTA in H_2O; pH 7.4). Cells were centrifuged and washed twice with PBS before they were resuspended in complete medium, separated through a 70 µm cell strainer to obtain single cell suspensions and counted on a hemocytometer. Trypan blue was used for discrimination between live and dead cells.

Human PBMCs were isolated by Ficoll density centrifugation. Therefore, heparin anticoagulated blood was diluted in PBS and underlaid with Ficoll-Hypaque (density: 1.077 g/ml) before it was centrifuged at 400 g for 30 min at room temperature. The interphase was transferred to a fresh tube, washed twice with PBS and cells were counted on a hemocytometer.

7.2.6 Flow Cytometry and Cell Sorting

Single-cell suspensions of freshly isolated T cells were stained with the appropriate fluorophore labeled antibody, diluted in PBS or FACS buffer (2 mM EDTA, 2 mM NaN_3, 2% FBS in PBS) in the dark for 15 min at 4°C. Cells were then washed twice with PBS and either fixed in 1% PFA/PBS or directly measured on a LSRFortessa™ (BD Biosciences). Data were analyzed using FlowJo software (TreeStar). Whenever feasible, staining and washing steps were performed in 96-well V or U-bottom plates (Greiner).

For intracellular cytokine staining, cells were restimulated with 1 µg/ml GP33 peptide (KAVYNFATC; ProImmune) or the control peptide Adn5 (SGPSNTPPEI; ProImmune) and incubated with the Golgi-inhibitor Brefeldin A (10 µg/ml; LKT-Lab) for 5 h. Staining of cell surface markers was performed as described above, before cells were fixed with 4% PFA for 5 min and permeabilized using 0.1% saponin/PBS. For the analysis of regulatory T cells (T_{reg}), splenocytes were stained for intracellular FoxP3 expression using the FoxP3 Fix/Perm Kit (BioLegend) according to the manufacturer's instructions subsequent to surface marker staining.

For cell sorting, splenocytes were stained with the appropriate antibody in PBS as described above. To ensure single cell suspension and remove any agglutinating cells, lymphocytes were passed through a 70 µm cell strainer prior to the measurement. An AriaIII™ (BD Biosciences) was used for cell sorting and the subsequent analysis. For sorting, a 70 µm nozzle was applied and the 4-way purity mask was chosen. Polypropylene collection tubes were pretreated with 500 µl sterile filtered FBS to prevent excessive cell death after sorting and continuously chilled to 4°C during the whole sort process. After sorting, cell fractions were analyzed to verify and quantify purity of the population. Cells were then centrifuged, resuspended in the appropriate amount of pre-warmed medium and seeded for further experiments. In case of RNA isolation, cells were directly resuspended in BL-TG buffer (ReliaPrep; Promega).

7.2.7 T cell activation

All experiments were performed in technical triplicates using 96-well round bottom plates (Greiner) with 200.000 cells/well in complete medium, unless otherwise stated. For activation with plate bound antibody, cell culture plates were coated with the appropriate concentration of anti-CD3 antibody in 50 mM Tris pH 9.0 at 4°C overnight and washed three times with PBS before use. Soluble, azide-free anti-CD28 antibody was added at a concentration of 1 µM whenever stated.

In *Nr5a2* mRNA quantitation experiments, splenocytes were stimulated with 5 µm concanavalin A (ConA) or 5 ng/ml PMA plus 200 ng/ml ionomycin. After harvesting, cells were immediately frozen in the appropriate buffer. Freshly isolated human PBMCs were treated with 5 µg/ml phytohemagglutinin A (PHA-P) for 3 h prior to RNA isolation.

Generation of T cell blasts was induced in unprimed mouse splenocytes by concanavalin (ConA)-mediated TCR cross-linking. Therefore, 3 x 10^6 spleen cells were incubated with 1 µg/ml ConA for 48 h before cells were washed and medium was supplemented with 100 units/ml recombinant IL-2. Cells were cultured for further 72 h to generate T cell blasts. Viable T cells were then purified by centrifugation over a

Histopaque (1.084 g/ml) gradient as described for the isolation of human PBMCs in the section above.

7.2.8 Proliferation assays

The ability of lymphocytes to undergo proliferation after *in vitro* stimulation was assessed by the incorporation of ^{3}H-thymidine. This method is based on incorporation of the radioactively labeled nucleosides into new strands of chromosomal DNA during mitotic cell division.

After the appropriate treatment, cells were cultured for 72 h before 0.5 µCi ^{3}H-thymidine (Hartmann Analytic) in a volume of 20 µl per well were added. Following overnight incubation, cells were transferred to a glass fiber membrane using a semi-automated cell harvester (Packard). In order to determine the mitogen-induced cell proliferation, glass fiber membranes were covered with 50 µl scintillation liquid (Microscint™ 40; Perkin Elmer) per well, incubated for 30 min and measured on a scintillation β-counter. The incorporated radioactivity is proportional to the number of proliferating cells and was determined as counts per minute on detector A (cpm-A).

CFSE staining was performed according to a protocol described before[177]. In short, 2 µl CFSE (5 mM) were diluted in 1 ml PBS and immediately applied to the cell suspension. After an incubation period of 5 min at room temperature in the dark, cells were washed three times with 5% FBS/PBS before cells were seeded for further experiments. When LRH-1 inhibitors were applied, cells were pre-incubated with the appropriate LRH-1 antagonist 30 min before stimulatory treatments.

For cell cycle profile analysis, wt splenocytes were cultured for indicated time points and nuclear DNA content was analyzed. Therefore, cells were subjected to 300 µl hypotonic propidium iodide solution (50 µg/ml propidium iodide, 0.1% Triton-X100, 0.5 x PBS) for 5 min on ice before they were directly analyzed on an LSRFortessa™ (BD Biosciences).

7.2.9 RNA isolation and quantitative real-time PCR

Tissues or cell culture pellets were transferred into 1 ml peqGold TriFast™ and homogenized using a TissueLyser II (Qiagen). RNA isolation was performed according to the manufacturer's instructions. For sorted cells, ReliaPrep™ RNA Mini Kit (Promega) was used as described in the manual. Purity, integrity and quantity of the isolated RNA were determined using a NanoDrop 2000 spectrophotometer (Thermo Fisher Scientific). 1 µg RNA was then transcribed using the High-Capacity cDNA Reverse Transcription Kit (Applied Biosystems) according to the manufacturer's instructions.

Quantitative PCR was performed on a StepOnePlus™ instrument using SYBR® Green PCR Master Mix (both Applied Biosystems). In real-time quantitative PCR experiments, intercalation of SYBR green with amplified, double stranded PCR products and subsequent fluorescence emission is detected and allows conclusions about the expression level of the corresponding gene. However, this method does not provide information about the corresponding protein levels.

All primers were designed to span exon-exon junctions and specificity of PCR products were verified by melting curve analysis (Technical Supplementary Figure 48). Further confirmation was performed for *Nr5a2*, by sequencing of the PCR product (Technical Supplementary Figure 48). Gene expression was normalized to *Actb* or *GAPDH* housekeeping genes, respectively. C_T values were determined using the StepOne software. mRNA levels were related to the transcription of the appropriate housekeeping gene or induction was calculated using the $2^{-\Delta\Delta CT}$ method[178,179].

7.2.10 Cell death assays

Freshly isolated immature and mature T cells were cultured in the presence or absence of increasing doses dexamethasone (Sigma Aldrich), etoposide (Enzo Life Sciences), staurosporine (Sigma Aldrich), plate bound anti-CD3 antibody or solvent control (DMSO/ethanol) for 8 h. Cells were subsequently stained as described above, in Annexin V binding buffer (10 mM HEPES, 150 mM NaCl, 50 mM KCl, 1 mM $MgCl_2$,

1.8 mM $CaCl_2$). Annexin V (1:1000 dilution) was directly added to the antibody mix. Cell death was determined by flow cytometry based on the capacity of Annexin V to bind phosphatidylserine, which is only exposed in apoptotic cells.

7.2.11 Ovalbumin immunization and *in vitro* restimulation

Mice were s.c. injected with 100 µg ovalbumin emulsified in incomplete Freund's Adjuvant (Invivogen). Homogenization was performed using the TissueLyser (Qiagen). After 14 days, spleens were isolated for the analysis of antigen specific T cells by *in vitro* restimulation. Therefore, splenocytes were incubated with increasing doses of ovalbumin protein in complete RMPI-1640 medium under reduced FCS conditions (5% only) for 72 h. Proliferation was assessed by subsequent determination of ^{3}H-thymidine incorporation. Serum samples were used for anti-ovalbumin antibody determination by ELISA.

7.2.12 Analysis of cytokine expression and serum immunoglobulin titers

Secretion of murine IL-2 and IFNγ was quantified by ELISA using matched antibody pairs. All reagents were purchased from BioLegend unless otherwise stated and applied according to the manufacturer's instructions.

Anti-ovalbumin specific IgG antibodies were determined in freshly isolated mouse serum. Therefore, blood was agglutinated for 30 min and then centrifuged twice for 15 min at 1.000 rpm. 96-well polystyrene microtiter plates (Nunc) were pre-treated with ovalbumin (100 µg/ml ovalbumin in 0.1 M $NaHCO_3$, 0.1 M Na_2CO_3; pH 9.5) overnight at 4°C, washed (0.05% Tween-20 in PBS) and serum was diluted (in 1.5% bovine serum albumin/PBS) as indicated. After incubation for 2 h at room temperature, plates were washed again and horse-radish peroxidase labeled goat anti-mouse IgG (1:10.000) was added for 1 hour. After excessive washing, 100 µl TMB substrate (prepared according to the manufacturer's instructions) were added per well and incubated for 10 - 30 min, before the reaction was stopped by the addition of 100 µl 1 M H_2SO_4 per well.

For the determination of cytokine secretion in sorted T cells, polystyrene microtiter plates were pre-treated with 1 µg/ml anti-IL-2 or 2 µg/ml anti-IFNγ antibody, respectively. Cell culture supernatant was diluted in 1% bovine serum albumin and incubated on the ELISA plate overnight at 4°C as well as a serial dilution of recombinant IL-2 or IFNγ as standard. For detection, the appropriate matched antibody was added in a 1:1.000 dilution. In an additional step, peroxidase-coupled streptavidin (Calbiochem) was added before addition of TMB substrate. Between all steps described here, plate was extensively washed with 0.05% Tween-20/PBS as stated above. After the addition of 1 M H_2SO_4, all samples were analyzed within 15 min using the Sunstar™ spectrophotometer (Tecan).

7.2.13 Adoptive transfer studies

L2/L2 or cKO splenocytes were sorted according to their CD4 and CD8α expression with a purity of minimum 98%. CD4 and CD8α positive cells were mixed in a 1:1 ratio with cells derived from Ly5.1 animals and a total of 2 x 10^6 cells were i.p. injected into Rag $1^{-/-}$ recipient mice. After 21 days, mice were sacrificed and secondary lymphatic organs were analyzed for the expression of CD45.1 or CD45.2 using a LSRFortessa™ (BD Biosciences) to assess repopulation ability.

7.2.14 Histology and Immunohistochemistry

To enable histological examination, organs have to be preserved and hardened first. Therefore, tissues were either fixed in 10% neutral formalin solution for 24 h at 4°C or embedded in O.C.T.™ (Tissue-Tek) cryopreservation medium immediately after removal from the euthanized animal.

Formaldehyde fixed tissues were further stored in 1% neutral formalin at 4°C or directly embedded into paraffin using a Microm STP 120 spin tissue processor (Zeiss). Mouse colons and small intestinal segments were swiss-rolled and fixed in 10% formalin prior to paraffin embedding. Supported by Astrid Glöckner, sections with a thickness of 4 µm were generated on a rotary microtome Hyrax C 50 (Zeiss) and mounted onto superfrosted object slides (Marienfeld). Sections were heated to

60°C on the next day and subsequently transferred to xylene for paraffin removal. This and the following steps were repeated three times with an incubation time of 5 min each. For rehydration, sections were subjected to a series of dilutions, starting with 100% ethanol, over 90%, 80% and finally 70% ethanol, before they were carefully rinsed with tap water for 5 min. Staining with hematoxylin and eosin (H/E) was performed by Astrid Glöckner using standard procedures. Sections were subsequently dehydrated with an incubation series, reversed of the one described for rehydration with an incubation time of 20 s for ethanol containing solutions and 5 min treatment with xylene. Limonene was used to finally preserve the sections. In case of anti-F4/80 macrophage staining, sections were covered with proteinase K solution for antigen retrieval directly after rehydration.

For immunohistochemistry, cryopreserved organs were cut in 7 µm section on a cryo microtome (Hyrax) and transferred to Histobond glass slides. Samples were fixed by immersion with fresh acetone for 1 min at room temperature and air dried for 30 min afterwards. To remove excessive cryopreservation medium, sections were washed 2 x 5 min in TBS (25 mM; pH 7.5) before they were subjected to anti-CD16/32 Fc-block cocktail (diluted 1:200 in 5% mouse serum/TBS) in order to prevent unspecific antibody binding. Appropriate primary antibodies were diluted 1:200 in antibody dilution buffer (5% goat serum in TBS) and sections were incubated in a dark, humidified chamber at 4°C overnight. Secondary antibodies were applied after 3 x 5 min washing steps with TBS for 2 h at room temperature to further enhance fluorescence signals. Control staining was performed to verify antibody specificity by application of secondary antibodies only. Residual antibody was washed away by incubation for 3 x 5 min in TBS and subsequently, sections were rinsed carefully with deionized water. DAPI containing Fluoroshield mounting medium (Sigma Aldrich) was used to protect fluorescence and conservation of the sections.

mTmG derived cryo sections were not further processed but directly washed with TBS to remove the O.C.T.™ medium and quickly rinsed with deionized water. Sections were then directly mounted with Fluoroshield (Sigma Aldrich). All histological sections

were analyzed on an AXIO Observer.Z1 (Zeiss) microscope and Fiji software[180] was used for image processing.

7.2.15 Transfer colitis and protection

Splenocytes were sorted based on their $CD4^+$ $CD45Rb^{hi}$ or $CD4^+$ $CD45Rb^{lo}$ expression with a minimum purity of 98%. For the induction of transfer colitis, 0.5 x 10^6 $CD4^+$ $CD45Rb^{hi}$ lymphocytes from L2/L2 or cKO animals were i.p. injected into Rag $1^{-/-}$ lymphopenic hosts. In experiments where the protective role of $CD4^+$ $CD45Rb^{lo}$ was studies, Rag $1^{-/-}$ mice were i.p. injected with 0.5 x 10^6 $CD4^+$ $CD45Rb^{hi}$ cells from Ly 5.1 donor mice plus 0.25 x 10^6 $CD4^+$ $CD45Rb^{lo}$ T cells from either L2/L2 or cKO animals. In both experiments, body weight was determined on a daily basis to follow disease progression and estimate colitis severity. Once the majority of mice reached a critical weight loss of 20% compared to the initial body weight, mice were CO_2 euthanized. For subsequent analyses, secondary lymphatic organs were isolated, stained for the expression of CD4 and CD45.1 and analyzed by flow cytometry. $CD4^+$ $CD45.1^-$ cells were considered as repopulating donor T cells. Colon samples were further applied to RNA isolation and quantitative PCR and histological examination.

7.2.16 LCMV infection and plaque assay

Mice were i.v. injected with 2.5 x 10^5 pfu lymphocytic choriomeningitis virus strain WE (LCMV-WE) in PBS and health status was controlled on a regular basis. At day 6, 8 or 10 post infection (dpi), mice were sacrificed and T cells derived from secondary lymphatic organs were directly stained for flow cytometric analysis or *in vitro* restimulated with viral or control peptides before intracellular IFNγ staining was performed. Furthermore, samples were collected for qPCR and plaque assay. Plaque assay was performed by Juan Huang as described previously[181]. To examine virus-specific cytotoxicity of effector T cells, EL4 cells were incubated with 10 µCi/ml ^{3}H-thymidine overnight and coated with GP33 or Adn5 peptide. Effector cells were added to 2 x 10^4 target cells at the indicated E.T (effector:target) ratio in technical triplicates After an incubation of 16 h, ^{3}H-thymidin content was determined by scintillation counting andDNA fragmentation was determined as previously described[169].

8 Technical Supplementary

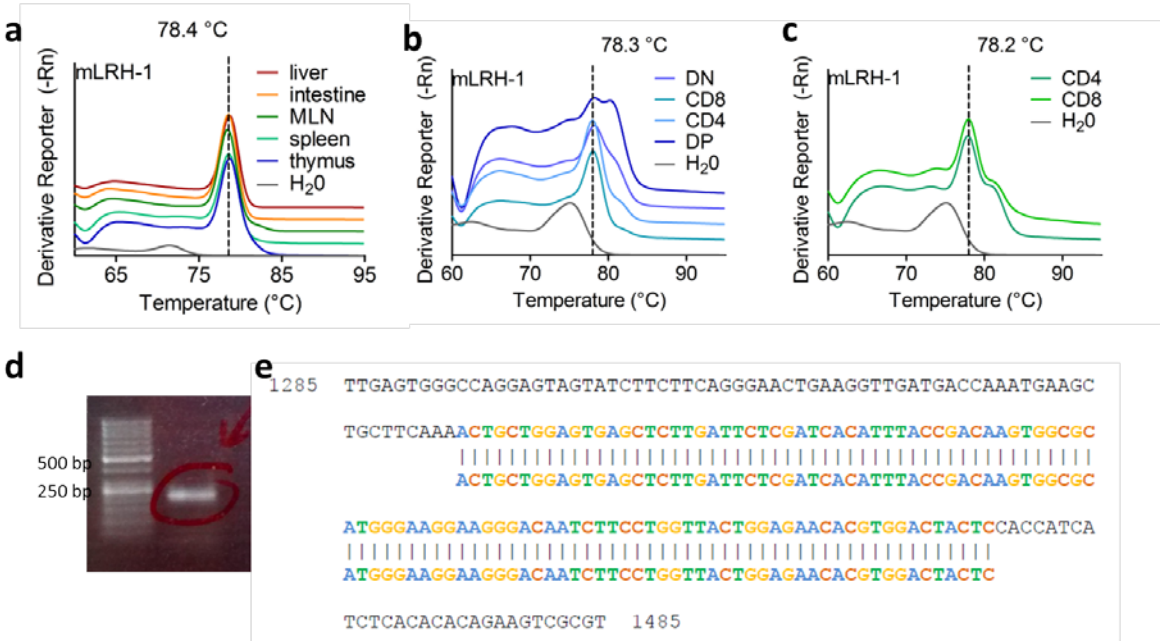

Figure 48: Verification of Nr5a2 specific qPCR products.

(**a-c**) SYBR green melting curves were analyzed for murine (a) organs, (b) thymocyte subsets and (c) purified splenocytes. Specific melting temperatures are indicated. (**d-e**) qPCR products were analyzed by (d) agarose gel electrophoresis and (e) sequencing to further confirm specificity

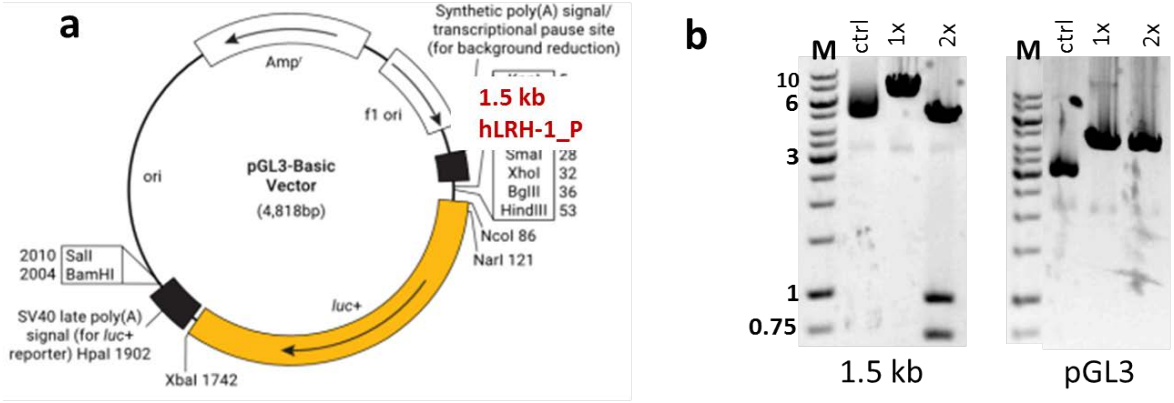

Figure 49: Verification of 1.5 kb human LRH-1 promoter luciferase construct.

(**a**) Illustration of the luciferase construct based on the pGl3 basic vector including the location of the cloned 1.5 kb human LRH-1 promoter. (**b**) Restriction digestion of the 1.5 kb human LRH-1 promoter construct (1.5 kb) as well as the pGl3 basic (pGl3) control plasmid. ctrl: undigested plasmid; 1x: single digestion (BamHI); 2x: double digestion (HindIII, SacI); M: marker; 1 kb GeneRuler (Thermo Scientific); The LRH-1 promoter contains an internal restriction site for HindIII; sequence is attached below.

Sequence of the 1.5 kb human LRH-1 promoter:

indicated in yellow: internal HindIII restriction site

```
1       CTCTAAATAAATTAATAGACCATAAATTCTGTAATGTGAATCTTTAGACAAAGACTGCTA
61      AATCTATCATCTGATATATGAAGTTTTATTACAACAAATGTTTATATATTGAGTTAAAAA
121     TTATCTGTACCCATACACACAACCTGCATTTACTTAATTTAAAAGGAGTGTCAATATTAA
181     AATTGAGGATTTTGGCCAGGTGCGGTGGCTCACGCCTATAATTCCAGCACTTTGGGAGGC
241     CGGGTAGATCATTTGAGGTCACAAGTTTGAGACCAGCCTGGCCAACACGGTGAAACCCCG
301     TCTTGACTAAAAATGCAAAAATTAGCCGGGCATGGTGGTGTGCCCCTGTAATCCCAGCTA
361     CTGGGGAGGCTGAGGCGGGAGAATTGCTTGAACCCGGGAGACAGAAGCTGCAGTGAGCCG
421     AGATCGTGCCACTGCACTCCAGCCTGGGCAACAGAGCGAGAACCCATCTCAAAAAAAAAA
481     AATTGTTATTTTGTTGTTATTGTTGTTTTTGAAGACAGAGTCTCACTCTGTTGCCCAGGC
541     TGGAGTGCGGTGGCATGATCTTGGATTGTGTTCTTCCAGGGTTGCAGAGAGAAGTGCAAC
601     AGCGTCTCATTGCAACCTCTGCCTCCCAGGTTCAAGCAATTCTCCCGCCTCAGCCTCCCA
661     AGTAGCTGGGATTACAGGAGTGCACCATCACACCCAGCTAATTTTTGCATTTTTAGTAGA
721     GATGGAGGTTTCACCATGTTGGCCAGGCTGGTCTCGAACTCCTGACCTCAGGTGATCCGC
781     CTGCCTTGGCTTCCCAAAGTGCTGGGATTACAGGTGTGAGCCACCATGCCCAGCCTAAGA
841     ATAATAACTTTATAACTATGAAAAATGTGTTACATATTCACCATTTTGCCAGCATTAATC
901     TCAAAGCATAAGTTTTACCTTTTGGGGATAAAGAGATAGATTGTGTTTTAGCCATATGAC
961     CAATGTAGAAACAAGCTAAGGTTAACTCCTCATCTAATGAATAGGCCCGATAAAAAAGTT
1021    GGTTGACCACAACATGAATAAATAAATAACCATAAGCTTGGAAATGCTACCTGTAGTATT
1081    TCAGAGTGTCGATCACATTTGTAGTCATCACTTAAAGAATTAATGTCTGCCAATGTTATC
1141    ATCTAAAATGTATTTACAGAGGTCAGAAGAGCTATGTCTGTCCTCCTCTATGCAAAGAGG
1201    TGATGACATCAAGGGGTATGTCACAAGCCAAAGTTTAGTTAGCCTAAGTTAGTTAGCTGG
1261    TTTGCAGTTTTTATCCACTAAGTCTGATCTTCTGACCCCTCAGTTTTACAACTTTCCACT
1321    CTCTGTGCTGCATAGCACCTCTCCACTTCTGAGTTAATCATTTCTTTGCCATTATCTGGC
1381    AAGAATTCTTATCTCTTTTGCTGTCACTTTATAACAGGGTCCTCTTATCAACCTGCATAG
1441    AGTCATGTGATGAGTCAAAGCCTATCAAAAGTTTCCATTCTTCTGATTAGAAACCATCAT
```

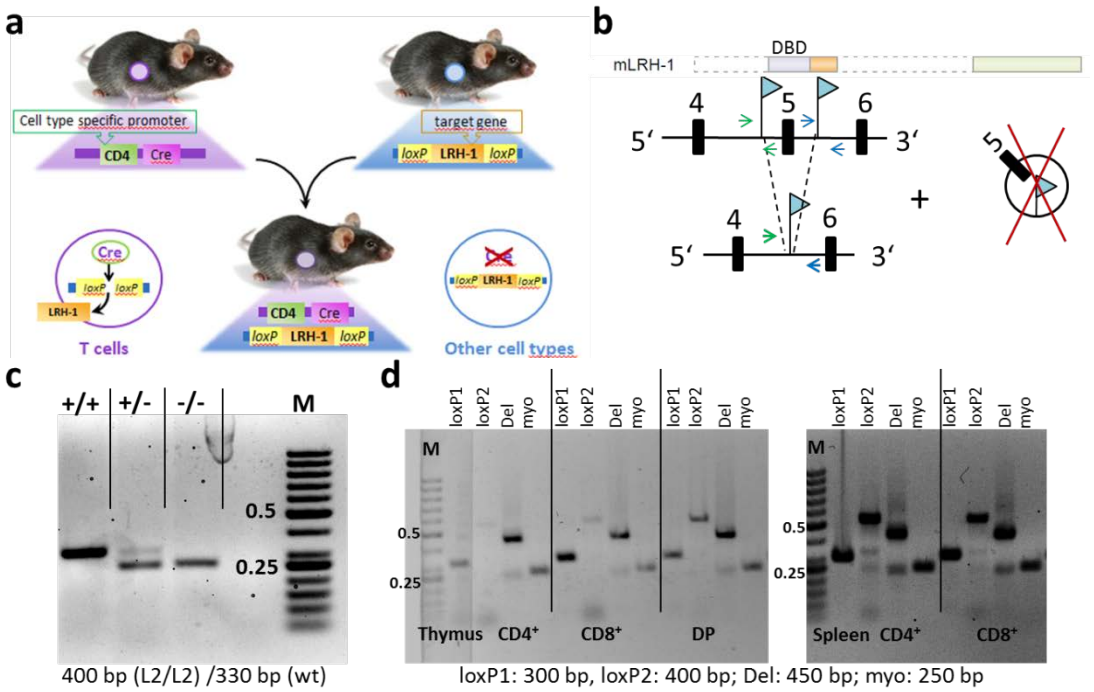

Figure 50: Breeding and genotyping of the *Nr5a2*$^{L2/L2}$ CD4-Cre line. (a) Schematic representation illustrating the process of Cre/lox based conditional deletion. loxP sites are recombined and gene sequence between the loxP sites are excised by Cre recombinase. Expression of Cre recombinase is controlled by the CD4 promoter and hence tissue specific. (b) Detailed illustration of the recombination constructs. Exons of the *Nr5a2* gene are represented by black boxes. *Nr5a2* DBD is flanked by loxP sites (blue flag); for genotyping of the loxP1 site, green primers (arrows) were used; blue primers were used to confirm loxP2. Successful recombination leads to a deletion product using a combination of green and blue primers. (c) Exemplary genotyping for loxP2 shows mice with floxed LRH-1 on both alleles (homozygous; +/+), animals with only one floxed LRH-1 allele (heterozygous; +/-) or wild type (wt) mice without introduction of loxP sites (homozygous; -/-). (d) Verification of genetic deletion in Thymocytes (left) and splenocytes (right). Sorted T cell subsets were analyzed for the presence of loxP1, loxP2, the deletion/recombination product and myogenin (myo) as control). Expected fragment sizes are indicated below the plots. M: 50 bp marker (Fermentas); Sequencing results: attached below; loxP core sequence is marked in yellow.

LoxP1 (primer: ACE225 and ACE228; 266 nt):

ccgcATCTCGGagGTGTTtATACTTTGcAACGCTTCTCCTTATTGAAGCTTGTGAAGTTCATTACAAACAAAGCTCTAGTCTCGAGGTCGACAT
CGATATAACTTCGTATAATGTATGCTATACGAAGTTATGGATCCGTCGAGACTAGAACTCTGCTAAACCCTCCTGTTTCTTTTCCTTGCTTG
TTTCTGCCCCGCTTCCGGGTGTCCTCTCCTCTTCCTTGTTTTTATTTTCACAGGGCATTTTCAAACGTGAGGAGATGaaa

LoxP2 (primer: ACE229 and complementary ACE231; 491 nt):

TAACTCTCCcnAGAATGAGTTCTGCACAGCAGAAAACCTCCAAATAAAAAAGTAGCTTGCATTTCCTTGATCACTCGACTTCGATGGCCCCCC
CTCGAATAACTTCGTATAATGTATGCTATACGAAGTTATTCGAGGTCGATCGACGAAGTTCCTATACTTTCTAGAGAATAGGAACTTCGGCC
GCCACCGCCTCGAGGAGCTCCTGCAGATAACTTCGTATAGCATACATTATACGAAGTTATTCTAGAAGATCTGCGATCTAAGTAAGCTTCCG
CGGTGATCAAATGAAGTGCACTCTAGCAAGGTGCTGGGTACCCCACCATATTGCGTTATTTGCAGTCTGTTTAATCTGTGGAAGGCCAGCAG
GTCAGAGGCTGGAAAATAGCAGCACACCATAACAGTCATGAAGTACAAATTATTTACAGCAGTCACATATTAACTTCACTGGCTGCCAAGCT
GAACCCCGCAGCATTCTTCGncAGTTGaGa

Deletion (primer: ACE225 and complementary ACE231; 373 nt):

AACTCTCCcnaGAAtgAGTTCTGCACaGCAGAAAACCTCCAAATAAAAAAGTAGCTTGCATTTCCTTGATCACTCGACTTCGATGGCCCCCCCT
CGAATAACTTCGTATAATGTATGCTATACGAAGTTATTCGAGGTCGATCGACGAAGTTCCTATACTTTCTAgAGAATAgGAACTTCGGCCGC
CACCGCCTCGAGGAGCTCCTGCagATAACTTCGTATAGCATACATTATACGAAGTTATATCGATGTCGACCTCGAGACTAGAGCTTTGTTTG
TAATGAACTTCACAAGCTTCAATAAGGAGAAGCGTTGCAAAGTATAAACACCTCCGAGATTGCGGGAGGAACAAAAATCAGACCATGGTAT
CCTg

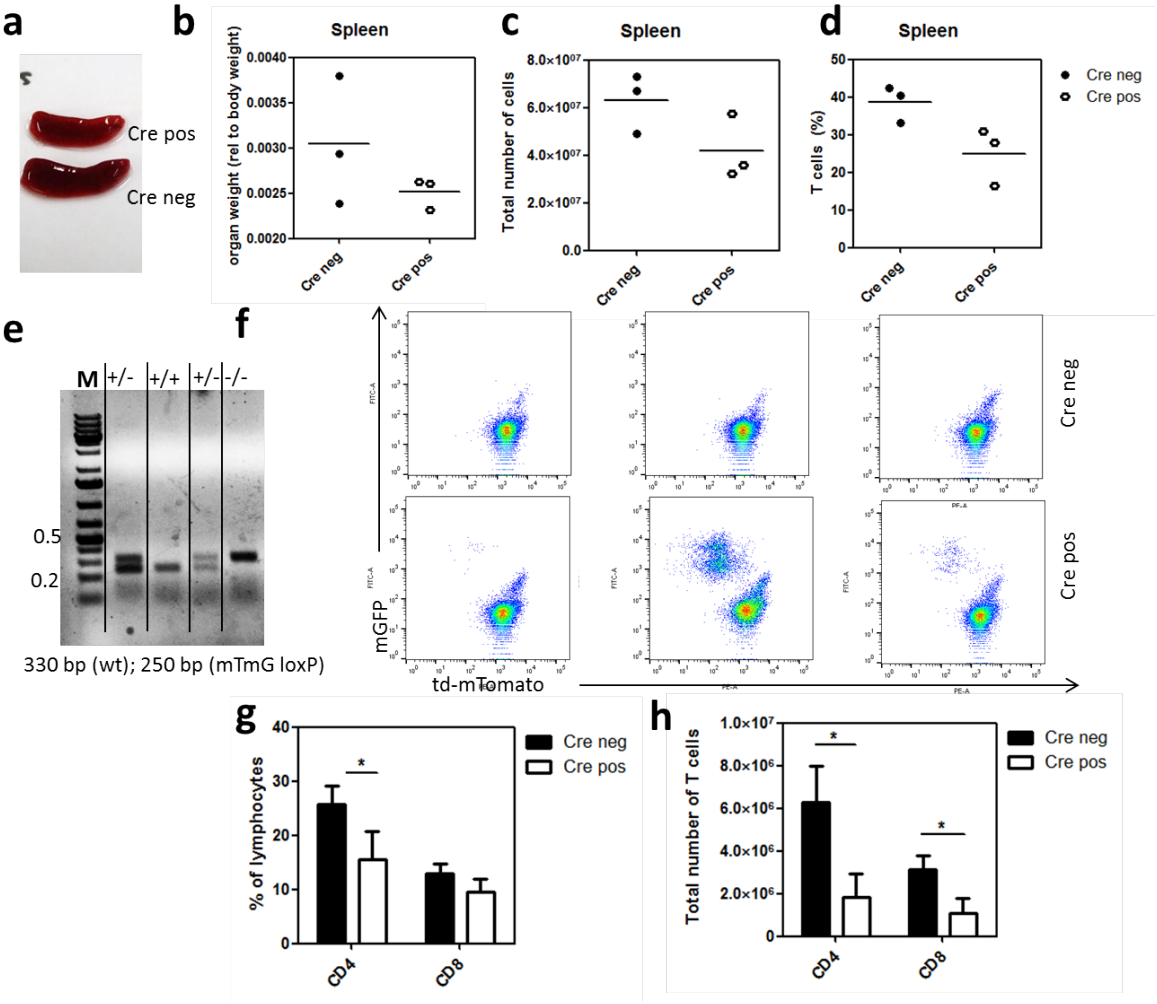

Figure 51: Analysis of *Nr5a2*$^{L2/L2}$ mTmG lck-Cre spleens.

(**a**) Organ size was slightly reduced in *Nr5a2*$^{L2/L2}$ mTmG lck-Cre (Cre pos) mice compared to *Nr5a2*$^{L2/L2}$ mTmG (Cre neg) control animals. (**b**) Spleen weight relative to body weight was reduced in Cre pos mice, accompanied by (**c**) reduced total cell numbers and (**d**) low amounts of CD3^{+} lymphocytes. (**e**) Representative mTmG genotyping blot. M: Marker (1kb plus GeneRuler; Thermo Scientific); +/-: heterozygous (one allele carries the mTmG sequence); +/+: homozygous (both alleles contain mTmG); -/-: wild type (without mTmG). (**f**) Density plots showing the deletion efficiency in *Nr5a2*$^{L2/L2}$ mTmG lck-Cre or control animals. Fluorescence conversion to mGFP indicates successful deletion. (**g**) Relative abundance of CD3^{+}CD4^{+} lymphocytes was significantly reduced after lck-driven deletion of LRH-1; Relative amounts of CD3^{+}CD8^{+} T cells were slightly reduced. (**h**) Total numbers of mature CD3^{+}CD4^{+} and CD3^{+}CD8^{+} were significantly reduced in Cre pos animals.

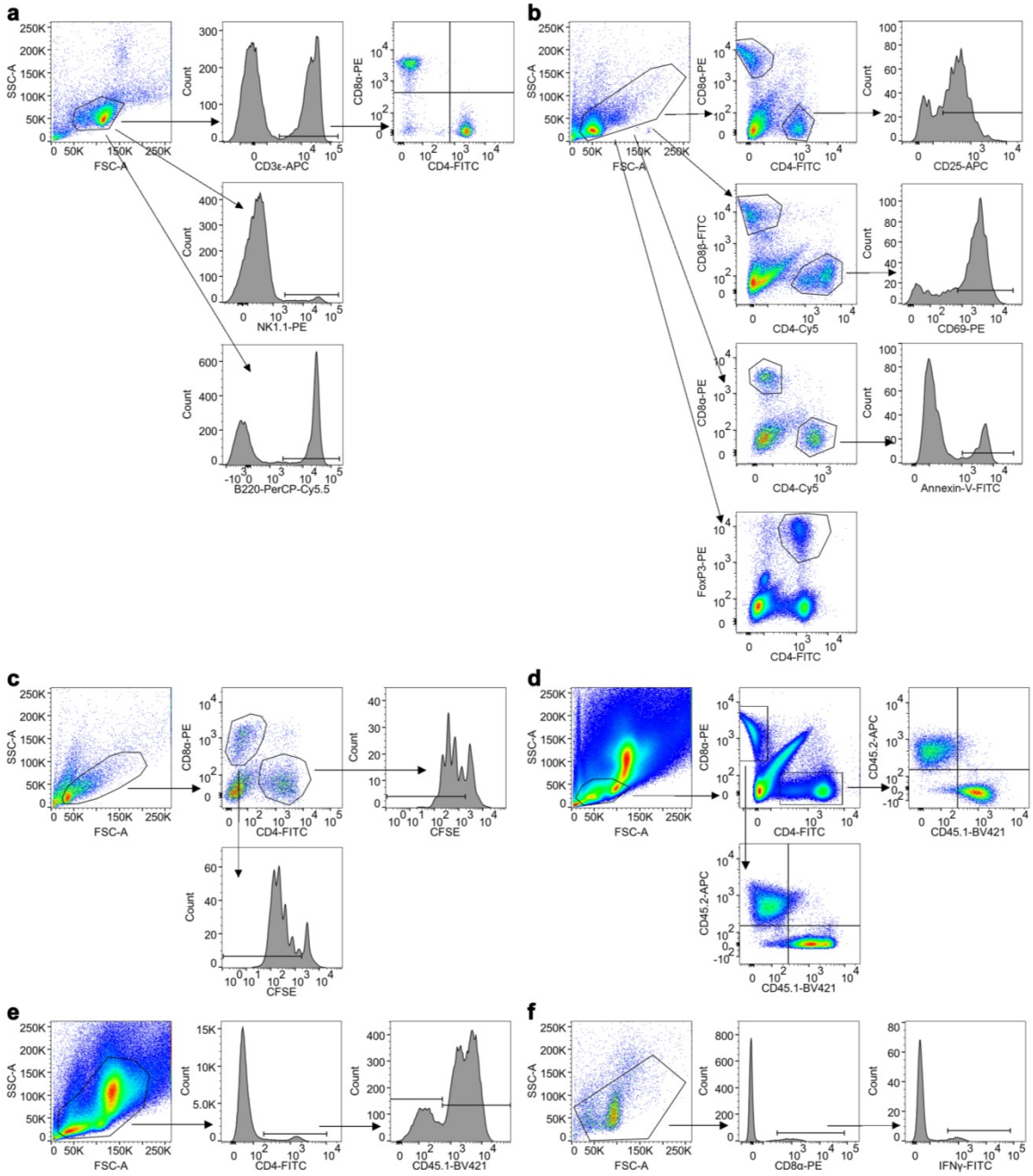

Figure 52: Gating strategies.

(**a**) Histograms were used to gate for CD3⁺, NK1.1⁺ and B220⁺ populations. CD4⁺ and CD8⁺ cells were always gated from CD3⁺ positive lymphocytes. Indicated percentages refer to the lymphocyte population (frequency of grandparents). (**b**) Early activation markers CD25 and CD69 as well as Annexin-V positivity were based on the corresponding CD4⁺ or CD8⁺ lymphocyte populations. CD4⁺FoxP3⁺ cells were gated from a general lymphocyte gate. (**c**) CFSE dilution was analyzed in viable CD4⁺ and CD8⁺ cells. (**d**) Cell surface markers CD45.1 and CD45.2 were differentiated by quadrant gates upon CD4/CD8 determination. (**e**) In experimental colitis/protection experiments, T cell populations were determined based on histograms on viable cells or CD4⁺ viable cells. (**f**) Determination of intracellular IFNγ staining in CD8β⁺ lymphocytes. Same gates were used for L2/L2 and cKO samples during all data analysis.

Abbreviations

(c/m)TEC	(cortical/medullary) thymic epithelial cell
AF1/AF2	activation function 1 (or 2)
AFP	α1-fetoprotein
AICD	activation induced cell death
APC	antigen presenting cell
axLN	axial lymph node
Bcl2	B cell lymphoma 2
CFSE	carboxyfluorescein succinimidyl ester
cKO	conditional knockout
cpm	counts per minute
Cyp7A1	cytochrome P450 family 7A1/cholesterol 7 α-hydroxylase
DAG	diacylglycerol
Dax-1	dosage-sensitive sex reversal, adrenal hypoplasia critical region, on chromosome X, gene 1
DBD	DNA binding domain
D-box	distal box
DC	dendric cell
Dexa	dexamethasone
DN	double negative $CD4^-CD8^-$
DNA	desoxyribonucleic acid
DP	double positive ($CD4^+CD8^+$)
dpi	day(s) post infection
E	embryonic day
ELISA	Enzyme-linked Immunosorbent Assay
ER	endoplasmic reticulum
Etop	etoposide
FasL	Fas (CD95) ligand
FBS	fetal bovine serum
FoxP3	forkhead box protein 3
Ftz-F1	Fushi tarazu factor-1
GC	glucocorticoid

GCK	glucokinase
Gls2	glutaminase 2
GPCR	G protein-coupled receptor
GR	glucocorticoid receptor
IFA	incomplete Freund's adjuvans
IFNγ	interferon gamma
IL-2	interleukin-2
IL-2Rα	interleukin-2 receptor alpha
IP3	inositol 1,4,5-trisphosphate
ITAM	immunoreceptor tyrosine-based activation motif
L2/L2	LRH-1 floxed (flanked by lox P sites)
LAT	linker of activated T cells
LBD	ligand binding domain
LBP	ligand binding pocket
lck	lymphocyte-specific protein tyrosine kinase
L-Glut	l-glutamine
LRH-1	liver receptor homolog-1
LXR	liver X receptor
MAPK	mitogen-activated protein kinase
MHC	major histocompatibility complex
mLN	mesenteric lymph node
mTmG	membrane targeted tandem dye Tomato membrane GFP
n.s.	not significant
NR	nuclear receptor
ONPG	o-nitrophenyl-β-D-galactopyranosid
PALS	periarteriolar lymphoid sheaths
P-box	proximal box
PCR	polymerase chain reaction
PDX-1	pancreatic and duodenal homeobox-1
pfu	plaque forming units
PIP2	phosphatidyl inositol bisphosphate
PKA	cAMP-dependent protein kinase
PKC	phosphokinase C

PLCγ1	phospholipase Cγ1
pMHC	peptide/MHC complex
PPAR	peroxisome-proliferator-activated receptor
RAG	recombination-activation gene
RXR	retinoid X receptors
S.D.	standard deviation
SF-1	steroidogenic factor-1
SH2	Src-homology domain
SHP	small heterodimer partner
SLP76	SH2 domain containing lymphocyte protein of 76 kDa
SP	single positive
SRC1	steroid receptor co-activator 1
Stauro	staurosporine
SUMO	small ubiquitin-like modifier
Suppl	supplementation
TCR	T cell receptor
TLR	Toll-like receptor
TMB	3,3′,5,5′-Tetramethylbenzidin
w/o	without
wt	wild type
ZAP70	ζ-chain associated protein kinase 70
α-Keto	α-ketoglutarate

Publications

Seitz, C., Huang, J., Geiselhöringer, A. Galbani-Bianchi, P., Reinhold, C., Corazza, N., Schnalzger, T., Schoonjans, K., Brunner, T. Nuclear receptor Liver Receptor Homolog-1 (Nr5a2) is critical for the regulation of T cell expansion and associated effector functions. Submitted

Grabinger, T., Bode, K.J., Demgenski, J., **Seitz, C**., Delgado, M.E., Kostadinova, F., Reinhold, C., Etemadi, N., Wilhelm, S., Schweinlin, M., Hanggi, K., Knop, J., Hauck, C., Walles, H., Silke, J., Wajant, H., Nachbur, U., Wei-Lynn, W., Brunner, T. Inhibitor of Apoptosis Protein-1 Regulates Tumor Necrosis Factor-Mediated Destruction of Intestinal Epithelial Cells. Gastroenterology 152, 867-879 (2017).

Hoffmann, E., Streichert, K., Nischan, N., **Seitz, C.**, Brunner, T., Schwagerus, S., Hackenberger, C.P., Rubini, M. Stabilization of bacterially expressed erythropoietin by single site-specific introduction of short branched PEG chains at naturally occurring glycosylation sites. Molecular bioSystems 12, 1750-1755 (2016).

List of Figures

List of Tables

References

1. Evans, R.M. & Mangelsdorf, D.J. Nuclear Receptors, RXR, and the Big Bang. *Cell* 157, 255-266 (2014).

2. Perissi, V. & Rosenfeld, M.G. Controlling nuclear receptors: the circular logic of cofactor cycles. *Nat Rev Mol Cell Biol* 6, 542-554 (2005).

3. Robinson-Rechavi, M., Carpentier, A.S., Duffraisse, M. & Laudet, V. How many nuclear hormone receptors are there in the human genome? *Trends in genetics : TIG* 17, 554-556 (2001).

4. Huang, P., Chandra, V. & Rastinejad, F. Structural overview of the nuclear receptor superfamily: insights into physiology and therapeutics. *Annual review of physiology* 72, 247-272 (2010).

5. Sever, R. & Glass, C.K. Signaling by nuclear receptors. *Cold Spring Harbor perspectives in biology* 5, a016709 (2013).

6. Helsen, C. *et al.* Structural basis for nuclear hormone receptor DNA binding. *Molecular and cellular endocrinology* 348, 411-417 (2012).

7. Pawlak, M., Lefebvre, P. & Staels, B. General molecular biology and architecture of nuclear receptors. *Current topics in medicinal chemistry* 12, 486-504 (2012).

8. Glass, C.K. & Ogawa, S. Combinatorial roles of nuclear receptors in inflammation and immunity. *Nature reviews. Immunology* 6, 44-55 (2006).

9. Giguere, V., Hollenberg, S.M., Rosenfeld, M.G. & Evans, R.M. Functional domains of the human glucocorticoid receptor. *Cell* 46, 645-652 (1986).

10. Miesfeld, R. *et al.* Genetic complementation of a glucocorticoid receptor deficiency by expression of cloned receptor cDNA. *Cell* 46, 389-399 (1986).

11. Freedman, L.P. *et al.* The function and structure of the metal coordination sites within the glucocorticoid receptor DNA binding domain. *Nature* 334, 543-546 (1988).

12. Danielsen, M., Hinck, L. & Ringold, G.M. Two amino acids within the knuckle of the first zinc finger specify DNA response element activation by the glucocorticoid receptor. *Cell* 57, 1131-1138 (1989).

13. Le Jossic, C. & Michel, D. Striking evolutionary conservation of a cis-element related to nuclear receptor target sites and present in TR2 orphan receptor genes. *Biochemical and biophysical research communications* 245, 64-69 (1998).

14. Tzameli, I. & Moore, D.D. Role reversal: new insights from new ligands for the xenobiotic receptor CAR. *Trends in endocrinology and metabolism: TEM* 12, 7-10 (2001).

15. Weatherman, R.V., Fletterick, R.J. & Scanlan, T.S. Nuclear-receptor ligands and ligand-binding domains. *Annual review of biochemistry* 68, 559-581 (1999).

16. Olefsky, J.M. Nuclear receptor minireview series. *The Journal of biological chemistry* 276, 36863-36864 (2001).

17. Echeverria, P.C. & Picard, D. Molecular chaperones, essential partners of steroid hormone receptors for activity and mobility. *Biochimica et biophysica acta* 1803, 641-649 (2010).

18. Bulynko, Y.A. & O'Malley, B.W. Nuclear receptor coactivators: structural and functional biochemistry. *Biochemistry* 50, 313-328 (2011).

19. Glass, C.K. & Rosenfeld, M.G. The coregulator exchange in transcriptional functions of nuclear receptors. *Genes & development* 14, 121-141 (2000).

20. Amoutzias, G.D. *et al.* A protein interaction atlas for the nuclear receptors: properties and quality of a hub-based dimerisation network. *BMC systems biology* 1, 34 (2007).

21. Westin, S., Rosenfeld, M.G. & Glass, C.K. Nuclear receptor coactivators. *Advances in pharmacology* 47, 89-112 (2000).

22. Mangelsdorf, D.J. *et al.* The nuclear receptor superfamily: the second decade. *Cell* 83, 835-839 (1995).

23. Nuclear Receptors Nomenclature, C. A unified nomenclature system for the nuclear receptor superfamily. *Cell* 97, 161-163 (1999).

24. Xie, W. & Evans, R.M. Orphan nuclear receptors: the exotics of xenobiotics. *The Journal of biological chemistry* 276, 37739-37742 (2001).

25. Novac, N. & Heinzel, T. Nuclear receptors: overview and classification. *Current drug targets. Inflammation and allergy* 3, 335-346 (2004).

26. Lindsley, C.W. 2014 prescription medications in the United States: tremendous growth, specialty/orphan drug expansion, and dispensed prescriptions continue to increase. *ACS chemical neuroscience* 6, 811-812 (2015).

27. Barnes, P.J. Anti-inflammatory actions of glucocorticoids: molecular mechanisms. *Clinical science* 94, 557-572 (1998).

28. Ashwell, J.D., Lu, F.W. & Vacchio, M.S. Glucocorticoids in T cell development and function*. *Annual review of immunology* 18, 309-345 (2000).

29. Purton, J.F., Boyd, R.L., Cole, T.J. & Godfrey, D.I. Intrathymic T cell development and selection proceeds normally in the absence of glucocorticoid receptor signaling. *Immunity* 13, 179-186 (2000).

30. Zhang, Y. *et al.* Orphan receptor small heterodimer partner suppresses tumorigenesis by modulating cyclin D1 expression and cellular proliferation. *Hepatology* 48, 289-298 (2008).

31. Yuk, J.M. *et al.* The orphan nuclear receptor SHP acts as a negative regulator in inflammatory signaling triggered by Toll-like receptors. *Nature immunology* 12, 742-751 (2011).

32. Hazel, T.G., Nathans, D. & Lau, L.F. A gene inducible by serum growth factors encodes a member of the steroid and thyroid hormone receptor superfamily. *Proceedings of the National Academy of Sciences of the United States of America* 85, 8444-8448 (1988).

33. Calnan, B.J., Szychowski, S., Chan, F.K., Cado, D. & Winoto, A. A role for the orphan steroid receptor Nur77 in apoptosis accompanying antigen-induced negative selection. *Immunity* 3, 273-282 (1995).

34. Masuyama, N. *et al.* Akt inhibits the orphan nuclear receptor Nur77 and T-cell apoptosis. *The Journal of biological chemistry* 276, 32799-32805 (2001).

35. Cao, X. *et al.* Retinoid X receptor regulates Nur77/TR3-dependent apoptosis [corrected] by modulating its nuclear export and mitochondrial targeting. *Molecular and cellular biology* 24, 9705-9725 (2004).

36. Li, H. *et al.* Cytochrome c release and apoptosis induced by mitochondrial targeting of nuclear orphan receptor TR3. *Science* 289, 1159-1164 (2000).

37. Galarneau, L. *et al.* The alpha1-fetoprotein locus is activated by a nuclear receptor of the Drosophila FTZ-F1 family. *Molecular and cellular biology* 16, 3853-3865 (1996).

38. Fayard, E., Auwerx, J. & Schoonjans, K. LRH-1: an orphan nuclear receptor involved in development, metabolism and steroidogenesis. *Trends in cell biology* 14, 250-260 (2004).

39. Galarneau, L., Drouin, R. & Belanger, L. Assignment of the fetoprotein transcription factor gene (FTF) to human chromosome band 1q32.11 by in situ hybridization. *Cytogenetics and cell genetics* 82, 269-270 (1998).

40. Li, M. *et al.* Cloning and characterization of a novel human hepatocyte transcription factor, hB1F, which binds and activates enhancer II of hepatitis B virus. *The Journal of biological chemistry* 273, 29022-29031 (1998).

41. Nitta, M., Ku, S., Brown, C., Okamoto, A.Y. & Shan, B. CPF: an orphan nuclear receptor that regulates liver-specific expression of the human cholesterol 7alpha-hydroxylase gene. *Proceedings of the National Academy of Sciences of the United States of America* 96, 6660-6665 (1999).

42. Zhang, C.K. *et al.* Characterization of the genomic structure and tissue-specific promoter of the human nuclear receptor NR5A2 (hB1F) gene. *Gene* 273, 239-249 (2001).

43. Desclozeaux, M., Krylova, I.N., Horn, F., Fletterick, R.J. & Ingraham, H.A. Phosphorylation and intramolecular stabilization of the ligand binding domain in the nuclear receptor steroidogenic factor 1. *Molecular and cellular biology* 22, 7193-7203 (2002).

44. Miao, J. *et al.* Ligand-dependent regulation of the activity of the orphan nuclear receptor, small heterodimer partner (SHP), in the repression of bile acid biosynthetic CYP7A1 and CYP8B1 genes. *Molecular endocrinology* 25, 1159-1169 (2011).

45. Fernandez-Marcos, P.J., Auwerx, J. & Schoonjans, K. Emerging actions of the nuclear receptor LRH-1 in the gut. *Biochimica et biophysica acta* 1812, 947-955 (2011).

46. Ellinger-Ziegelbauer, H., Glaser, B. & Dreyer, C. A naturally occurring short variant of the FTZ-F1-related nuclear orphan receptor xFF1rA and interactions between domains of xFF1rA. *Molecular endocrinology* 9, 872-886 (1995).

47. Pare, J.F., Roy, S., Galarneau, L. & Belanger, L. The mouse fetoprotein transcription factor (FTF) gene promoter is regulated by three GATA elements with tandem E box and Nkx motifs, and FTF in turn activates the Hnf3beta, Hnf4alpha, and Hnf1alpha gene promoters. *The Journal of biological chemistry* 276, 13136-13144 (2001).

48. Sablin, E.P., Krylova, I.N., Fletterick, R.J. & Ingraham, H.A. Structural basis for ligand-independent activation of the orphan nuclear receptor LRH-1. *Molecular cell* 11, 1575-1585 (2003).

49. Ortlund, E.A. *et al.* Modulation of human nuclear receptor LRH-1 activity by phospholipids and SHP. *Nature structural & molecular biology* 12, 357-363 (2005).

50. Steffensen, K.R. *et al.* Functional conservation of interactions between a homeodomain cofactor and a mammalian FTZ-F1 homologue. *EMBO reports* 5, 613-619 (2004).

51. Lazarus, K.A., Wijayakumara, D., Chand, A.L., Simpson, E.R. & Clyne, C.D. Therapeutic potential of Liver Receptor Homolog-1 modulators. *The Journal of Steroid Biochemistry and Molecular Biology* 130, 138-146 (2012).

52. Bohan, A., Chen, W.S., Denson, L.A., Held, M.A. & Boyer, J.L. Tumor necrosis factor alpha-dependent up-regulation of Lrh-1 and Mrp3(Abcc3) reduces liver injury in obstructive cholestasis. *The Journal of biological chemistry* 278, 36688-36698 (2003).

53. Fernandez-Marcos, P.J., Auwerx, J. & Schoonjans, K. Emerging actions of the nuclear receptor LRH-1 in the gut. *Biochim Biophys Acta* 1812, 947-955 (2011).

54. Lee, J.M. *et al.* A nuclear-receptor-dependent phosphatidylcholine pathway with antidiabetic effects. *Nature* 474, 506-510 (2011).

55. Lee, J.M. *et al.* A nuclear-receptor-dependent phosphatidylcholine pathway with antidiabetic effects. *Nature* 474, 506-510 (2011).

56. Benod, C. *et al.* Structure-based discovery of antagonists of nuclear receptor LRH-1. *The Journal of biological chemistry* 288, 19830-19844 (2013).

57. Corzo, C.A. *et al.* Antiproliferation activity of a small molecule repressor of liver receptor homolog 1. *Molecular pharmacology* 87, 296-304 (2015).

58. Yang, F.M. *et al.* Liver receptor homolog-1 localization in the nuclear body is regulated by sumoylation and cAMP signaling in rat granulosa cells. *The FEBS journal* 276, 425-436 (2009).

59. Lazarus, K.A., Wijayakumara, D., Chand, A.L., Simpson, E.R. & Clyne, C.D. Therapeutic potential of Liver Receptor Homolog-1 modulators. *The Journal of steroid biochemistry and molecular biology* 130, 138-146 (2012).

60. Stein, S. & Schoonjans, K. Molecular basis for the regulation of the nuclear receptor LRH-1. *Current opinion in cell biology* 33, 26-34 (2015).

61. Wagner, R.T., Xu, X., Yi, F., Merrill, B.J. & Cooney, A.J. Canonical Wnt/beta-catenin regulation of liver receptor homolog-1 mediates pluripotency gene expression. *Stem cells* 28, 1794-1804 (2010).

62. Pare, J.F. *et al.* The fetoprotein transcription factor (FTF) gene is essential to embryogenesis and cholesterol homeostasis and is regulated by a DR4 element. *The Journal of biological chemistry* 279, 21206-21216 (2004).

63. Heng, J.C. *et al.* The nuclear receptor Nr5a2 can replace Oct4 in the reprogramming of murine somatic cells to pluripotent cells. *Cell stem cell* 6, 167-174 (2010).

64. Gu, P. *et al.* Orphan nuclear receptor LRH-1 is required to maintain Oct4 expression at the epiblast stage of embryonic development. *Molecular and cellular biology* 25, 3492-3505 (2005).

65. Rausa, F.M., Galarneau, L., Belanger, L. & Costa, R.H. The nuclear receptor fetoprotein transcription factor is coexpressed with its target gene HNF-3beta in the developing murine liver, intestine and pancreas. *Mechanisms of development* 89, 185-188 (1999).

66. Annicotte, J.S. *et al.* Pancreatic-duodenal homeobox 1 regulates expression of liver receptor homolog 1 during pancreas development. *Molecular and cellular biology* 23, 6713-6724 (2003).

67. Lee, Y.K. *et al.* Liver receptor homolog-1 regulates bile acid homeostasis but is not essential for feedback regulation of bile acid synthesis. *Molecular endocrinology* 22, 1345-1356 (2008).

68. Freeman, L.A. *et al.* The orphan nuclear receptor LRH-1 activates the ABCG5/ABCG8 intergenic promoter. *Journal of lipid research* 45, 1197-1206 (2004).

69. Delerive, P., Galardi, C.M., Bisi, J.E., Nicodeme, E. & Goodwin, B. Identification of liver receptor homolog-1 as a novel regulator of apolipoprotein AI gene transcription. *Molecular endocrinology* 18, 2378-2387 (2004).

70. Venteclef, N., Haroniti, A., Tousaint, J.J., Talianidis, I. & Delerive, P. Regulation of anti-atherogenic apolipoprotein M gene expression by the orphan nuclear receptor LRH-1. *The Journal of biological chemistry* 283, 3694-3701 (2008).

71. Oosterveer, M.H. *et al.* LRH-1-dependent glucose sensing determines intermediary metabolism in liver. *The Journal of clinical investigation* 122, 2817-2826 (2012).

72. Xu, P. *et al.* LRH-1-dependent programming of mitochondrial glutamine processing drives liver cancer. *Genes & development* 30, 1255-1260 (2016).

73. Vacchio, M.S., King, L.B. & Ashwell, J.D. Regulation of thymocyte development by glucocorticoids. *Behring Institute Mitteilungen*, 24-31 (1996).

74. Davies, E. & MacKenzie, S.M. Extra-adrenal production of corticosteroids. *Clinical and experimental pharmacology & physiology* 30, 437-445 (2003).

75. Cima, I. *et al.* Intestinal epithelial cells synthesize glucocorticoids and regulate T cell activation. *The Journal of experimental medicine* 200, 1635-1646 (2004).

76. Sadovsky, Y. *et al.* Mice deficient in the orphan receptor steroidogenic factor 1 lack adrenal glands and gonads but express P450 side-chain-cleavage enzyme in the placenta and have normal embryonic serum levels of corticosteroids. *Proceedings of the National Academy of Sciences of the United States of America* 92, 10939-10943 (1995).

77. Sherr, C.J. Cancer cell cycles. *Science* 274, 1672-1677 (1996).

78. Botrugno, O.A. *et al.* Synergy between LRH-1 and beta-catenin induces G1 cyclin-mediated cell proliferation. *Molecular cell* 15, 499-509 (2004).

79. Bianco, S., Jangal, M., Garneau, D. & Gevry, N. LRH-1 controls proliferation in breast tumor cells by regulating CDKN1A gene expression. *Oncogene* 34, 4509-4518 (2015).

80. Chand, A.L., Herridge, K.A., Thompson, E.W. & Clyne, C.D. The orphan nuclear receptor LRH-1 promotes breast cancer motility and invasion. *Endocrine-related cancer* 17, 965-975 (2010).

81. Zhou, J. *et al.* Interactions between prostaglandin E(2), liver receptor homologue-1, and aromatase in breast cancer. *Cancer research* 65, 657-663 (2005).

82. Thiruchelvam, P.T. *et al.* The liver receptor homolog-1 regulates estrogen receptor expression in breast cancer cells. *Breast cancer research and treatment* 127, 385-396 (2011).

83. Kramer, H.B. *et al.* LRH-1 drives colon cancer cell growth by repressing the expression of the CDKN1A gene in a p53-dependent manner. *Nucleic acids research* 44, 582-594 (2016).

84. Wang, S.L. *et al.* Increased expression of hLRH-1 in human gastric cancer and its implication in tumorigenesis. *Molecular and cellular biochemistry* 308, 93-100 (2008).

85. Schoonjans, K. *et al.* Liver receptor homolog 1 contributes to intestinal tumor formation through effects on cell cycle and inflammation. *Proceedings of the National Academy of Sciences of the United States of America* 102, 2058-2062 (2005).

86. Benod, C. *et al.* Nuclear receptor liver receptor homologue 1 (LRH-1) regulates pancreatic cancer cell growth and proliferation. *Proceedings of the National Academy of Sciences of the United States of America* 108, 16927-16931 (2011).

87. Petersen, G.M. *et al.* A genome-wide association study identifies pancreatic cancer susceptibility loci on chromosomes 13q22.1, 1q32.1 and 5p15.33. *Nature genetics* 42, 224-228 (2010).

88. Lin, Q. *et al.* LRH1 as a driving factor in pancreatic cancer growth. *Cancer letters* 345, 85-90 (2014).

89. Lefevre, L. *et al.* LRH-1 mediates anti-inflammatory and antifungal phenotype of IL-13-activated macrophages through the PPARgamma ligand synthesis. *Nature communications* 6, 6801 (2015).

90. Schwaderer, J., Gaiser, A.K., Phan, T.S., Delgado, M.E. & Brunner, T. Liver receptor homolog-1 (NR5a2) regulates CD95/Fas ligand transcription and associated T-cell effector functions. *Cell death & disease* 8, e2745 (2017).

91. Schwaderer, J. LRH-1/NR5a2 in regulation of the immune system. PhD thesis, University of Konstanz, Konstanz, 2017.

92. Zinkernagel, R.M. & Doherty, P.C. Immunological surveillance against altered self components by sensitised T lymphocytes in lymphocytic choriomeningitis. *Nature* 251, 547-548 (1974).

93. Babbitt, B.P., Allen, P.M., Matsueda, G., Haber, E. & Unanue, E.R. Binding of immunogenic peptides to Ia histocompatibility molecules. *Nature* 317, 359-361 (1985).

94. Miller, J.F. The discovery of thymus function and of thymus-derived lymphocytes. *Immunological reviews* 185, 7-14 (2002).

95. Godfrey, D.I., Kennedy, J., Suda, T. & Zlotnik, A. A developmental pathway involving four phenotypically and functionally distinct subsets of CD3-CD4-CD8- triple-negative adult mouse thymocytes defined by CD44 and CD25 expression. *Journal of immunology* 150, 4244-4252 (1993).

96. Germain, R.N. T-cell development and the CD4-CD8 lineage decision. *Nature reviews. Immunology* 2, 309-322 (2002).

97. Davis, M.M. & Bjorkman, P.J. T-cell antigen receptor genes and T-cell recognition. *Nature* 334, 395-402 (1988).

98. von Boehmer, H. & Fehling, H.J. Structure and function of the pre-T cell receptor. *Annual review of immunology* 15, 433-452 (1997).

99. Mombaerts, P. *et al.* RAG-1-deficient mice have no mature B and T lymphocytes. *Cell* 68, 869-877 (1992).

100. von Boehmer, H., Teh, H.S. & Kisielow, P. The thymus selects the useful, neglects the useless and destroys the harmful. *Immunology today* 10, 57-61 (1989).

101. Singer, A. & Bosselut, R. CD4/CD8 coreceptors in thymocyte development, selection, and lineage commitment: analysis of the CD4/CD8 lineage decision. *Advances in immunology* 83, 91-131 (2004).

102. Zuniga-Pflucker, J.C. T-cell development made simple. *Nature reviews. Immunology* 4, 67-72 (2004).

103. Kurobe, H. *et al.* CCR7-dependent cortex-to-medulla migration of positively selected thymocytes is essential for establishing central tolerance. *Immunity* 24, 165-177 (2006).

104. Klein, L., Hinterberger, M., Wirnsberger, G. & Kyewski, B. Antigen presentation in the thymus for positive selection and central tolerance induction. *Nature reviews. Immunology* 9, 833-844 (2009).

105. Van Parijs, L. & Abbas, A.K. Homeostasis and self-tolerance in the immune system: turning lymphocytes off. *Science* 280, 243-248 (1998).

106. Surh, C.D. & Sprent, J. Homeostatic T cell proliferation: how far can T cells be activated to self-ligands? *The Journal of experimental medicine* 192, F9-F14 (2000).

107. Bell, E.B., Sparshott, S.M., Drayson, M.T. & Ford, W.L. The stable and permanent expansion of functional T lymphocytes in athymic nude rats after a single injection of mature T cells. *Journal of immunology* 139, 1379-1384 (1987).

108. Rocha, B., Dautigny, N. & Pereira, P. Peripheral T lymphocytes: expansion potential and homeostatic regulation of pool sizes and CD4/CD8 ratios in vivo. *European journal of immunology* 19, 905-911 (1989).

109. Baumann, S. *et al.* Glucocorticoids inhibit activation-induced cell death (AICD) via direct DNA-dependent repression of the CD95 ligand gene by a glucocorticoid receptor dimer. *Blood* 106, 617-625 (2005).

110. Krammer, P.H., Arnold, R. & Lavrik, I.N. Life and death in peripheral T cells. *Nature reviews. Immunology* 7, 532-542 (2007).

111. Lenardo, M.J. Interleukin-2 programs mouse alpha beta T lymphocytes for apoptosis. *Nature* 353, 858-861 (1991).

112. Benczik, M. & Gaffen, S.L. The interleukin (IL)-2 family cytokines: survival and proliferation signaling pathways in T lymphocytes. *Immunological investigations* 33, 109-142 (2004).

113. Kieper, W.C. & Jameson, S.C. Homeostatic expansion and phenotypic conversion of naive T cells in response to self peptide/MHC ligands. *Proceedings of the National Academy of Sciences of the United States of America* 96, 13306-13311 (1999).

114. Cho, B.K., Rao, V.P., Ge, Q., Eisen, H.N. & Chen, J. Homeostasis-stimulated proliferation drives naive T cells to differentiate directly into memory T cells. *The Journal of experimental medicine* 192, 549-556 (2000).

115. Goldrath, A.W., Bogatzki, L.Y. & Bevan, M.J. Naive T cells transiently acquire a memory-like phenotype during homeostasis-driven proliferation. *The Journal of experimental medicine* 192, 557-564 (2000).

116. Murali-Krishna, K. & Ahmed, R. Cutting edge: naive T cells masquerading as memory cells. *Journal of immunology* 165, 1733-1737 (2000).

117. Cesta, M.F. Normal structure, function, and histology of the spleen. *Toxicologic pathology* 34, 455-465 (2006).

118. Nolte, M.A., Hamann, A., Kraal, G. & Mebius, R.E. The strict regulation of lymphocyte migration to splenic white pulp does not involve common homing receptors. *Immunology* 106, 299-307 (2002).

119. Balogh, P., Horvath, G. & Szakal, A.K. Immunoarchitecture of distinct reticular fibroblastic domains in the white pulp of mouse spleen. *The journal of histochemistry and cytochemistry : official journal of the Histochemistry Society* 52, 1287-1298 (2004).

120. Saito, H. *et al.* Reticular meshwork of the spleen in rats studied by electron microscopy. *The American journal of anatomy* 181, 235-252 (1988).

121. Nolte, M.A., Hoen, E.N., van Stijn, A., Kraal, G. & Mebius, R.E. Isolation of the intact white pulp. Quantitative and qualitative analysis of the cellular composition of the splenic compartments. *European journal of immunology* 30, 626-634 (2000).

122. Kraal, G. Cells in the marginal zone of the spleen. *International review of cytology* 132, 31-74 (1992).

123. Steiniger, B. & Barth, P. Microanatomy and function of the spleen. *Advances in anatomy, embryology, and cell biology* 151, III-IX, 1-101 (2000).

124. Garside, P. *et al.* Visualization of specific B and T lymphocyte interactions in the lymph node. *Science* 281, 96-99 (1998).

125. Mitchell, J. Lymphocyte circulation in the spleen. Marginal zone bridging channels and their possible role in cell traffic. *Immunology* 24, 93-107 (1973).

126. Wang, X. & Cyster, J. Spleen. 2017 [cited 04/10/2017]Available from: http://www.cell.com/immunity/image-resource-spleen

127. Willard-Mack, C.L. Normal structure, function, and histology of lymph nodes. *Toxicologic pathology* 34, 409-424 (2006).

128. Germain, R.N. Immunology. The ins and outs of antigen processing and presentation. *Nature* 322, 687-689 (1986).

129. Pamer, E. & Cresswell, P. Mechanisms of MHC class I--restricted antigen processing. *Annual review of immunology* 16, 323-358 (1998).

130. Townsend, A.R., Gotch, F.M. & Davey, J. Cytotoxic T cells recognize fragments of the influenza nucleoprotein. *Cell* 42, 457-467 (1985).

131. Townsend, A. *et al.* Association of class I major histocompatibility heavy and light chains induced by viral peptides. *Nature* 340, 443-448 (1989).

132. Harding, C.V. Pathways of antigen processing. *Current opinion in immunology* 3, 3-9 (1991).

133. Gatfield, J. & Pieters, J. Essential role for cholesterol in entry of mycobacteria into macrophages. *Science* 288, 1647-1650 (2000).

134. Crotty, S. A brief history of T cell help to B cells. *Nature reviews. Immunology* 15, 185-189 (2015).

135. Nakae, S., Iwakura, Y., Suto, H. & Galli, S.J. Phenotypic differences between Th1 and Th17 cells and negative regulation of Th1 cell differentiation by IL-17. *Journal of leukocyte biology* 81, 1258-1268 (2007).

136. Yang, Y., Xu, J., Niu, Y., Bromberg, J.S. & Ding, Y. T-bet and eomesodermin play critical roles in directing T cell differentiation to Th1 versus Th17. *Journal of immunology* 181, 8700-8710 (2008).

137. Abbas, A.K. *et al.* Regulatory T cells: recommendations to simplify the nomenclature. *Nature immunology* 14, 307-308 (2013).

138. Kung, J.T. Recent developments in CD8+ T-lymphocyte memory research. *Journal of the Formosan Medical Association = Taiwan yi zhi* 98, 736-739 (1999).

139. Huse, M., Quann, E.J. & Davis, M.M. Shouts, whispers and the kiss of death: directional secretion in T cells. *Nature immunology* 9, 1105-1111 (2008).

140. Komura, J. & Watanabe, S. Desmosome-like structures in the cytoplasm of normal human keratinocyte. *Archives for dermatological research = Archiv fur dermatologische Forschung* 253, 145-149 (1975).

141. Basta, S. & Alatery, A. The cross-priming pathway: a portrait of an intricate immune system. *Scandinavian journal of immunology* 65, 311-319 (2007).

142. Cantrell, D.A. T-cell antigen receptor signal transduction. *Immunology* 105, 369-374 (2002).

143. Myung, P.S., Boerthe, N.J. & Koretzky, G.A. Adapter proteins in lymphocyte antigen-receptor signaling. *Current opinion in immunology* 12, 256-266 (2000).

144. Morris, G.P. & Allen, P.M. How the TCR balances sensitivity and specificity for the recognition of self and pathogens. *Nature immunology* 13, 121-128 (2012).

145. Parekh, D.B., Ziegler, W. & Parker, P.J. Multiple pathways control protein kinase C phosphorylation. *The EMBO journal* 19, 496-503 (2000).

146. Powrie, F. T cells in inflammatory bowel disease: protective and pathogenic roles. *Immunity* 3, 171-174 (1995).

147. Powrie, F. *et al.* Inhibition of Th1 responses prevents inflammatory bowel disease in scid mice reconstituted with CD45RBhi CD4+ T cells. *Immunity* 1, 553-562 (1994).

148. Ostanin, D.V. *et al.* T cell transfer model of chronic colitis: concepts, considerations, and tricks of the trade. *American journal of physiology. Gastrointestinal and liver physiology* 296, G135-146 (2009).

149. Powrie, F., Leach, M.W., Mauze, S., Caddle, L.B. & Coffman, R.L. Phenotypically distinct subsets of CD4+ T cells induce or protect from chronic intestinal inflammation in C. B-17 scid mice. *International immunology* 5, 1461-1471 (1993).

150. Izcue, A., Coombes, J.L. & Powrie, F. Regulatory T cells suppress systemic and mucosal immune activation to control intestinal inflammation. *Immunological reviews* 212, 256-271 (2006).

151. Powrie, F. Immune regulation in the intestine: a balancing act between effector and regulatory T cell responses. *Annals of the New York Academy of Sciences* 1029, 132-141 (2004).

152. Rowe, W.P. *et al.* Arenoviruses: proposed name for a newly defined virus group. *Journal of virology* 5, 651-652 (1970).

153. Lehmann-Grube, F. Portraits of viruses: arenaviruses. *Intervirology* 22, 121-145 (1984).

154. Butz, E.A. & Bevan, M.J. Massive expansion of antigen-specific CD8+ T cells during an acute virus infection. *Immunity* 8, 167-175 (1998).

155. Murali-Krishna, K. *et al.* Counting antigen-specific CD8 T cells: a reevaluation of bystander activation during viral infection. *Immunity* 8, 177-187 (1998).

156. Moskophidis, D., Assmann-Wischer, U., Simon, M.M. & Lehmann-Grube, F. The immune response of the mouse to lymphocytic choriomeningitis virus. V. High numbers of cytolytic T lymphocytes are generated in the spleen during acute infection. *European journal of immunology* 17, 937-942 (1987).

157. McIntyre, K.W., Bukowski, J.F. & Welsh, R.M. Exquisite specificity of adoptive immunization in arenavirus-infected mice. *Antiviral research* 5, 299-305 (1985).

158. Schulz, M. *et al.* Major histocompatibility complex--dependent T cell epitopes of lymphocytic choriomeningitis virus nucleoprotein and their protective capacity against viral disease. *European journal of immunology* 19, 1657-1667 (1989).

159. Trautmann, T. *et al.* CD4+ T-cell help is required for effective CD8+ T cell-mediated resolution of acute viral hepatitis in mice. *PloS one* 9, e86348 (2014).

160. Karrer, U. *et al.* On the key role of secondary lymphoid organs in antiviral immune responses studied in alymphoplastic (aly/aly) and spleenless (Hox11(-)/-) mutant mice. *The Journal of experimental medicine* 185, 2157-2170 (1997).

161. Odermatt, B., Eppler, M., Leist, T.P., Hengartner, H. & Zinkernagel, R.M. Virus-triggered acquired immunodeficiency by cytotoxic T-cell-dependent destruction of antigen-presenting cells and lymph follicle structure. *Proceedings of the National Academy of Sciences of the United States of America* 88, 8252-8256 (1991).

162. Sevilla, N. *et al.* Immunosuppression and resultant viral persistence by specific viral targeting of dendritic cells. *The Journal of experimental medicine* 192, 1249-1260 (2000).

163. Althage, A. *et al.* Immunosuppression by lymphocytic choriomeningitis virus infection: competent effector T and B cells but impaired antigen presentation. *European journal of immunology* 22, 1803-1812 (1992).

164. Seiler, P. *et al.* Crucial role of marginal zone macrophages and marginal zone metallophils in the clearance of lymphocytic choriomeningitis virus infection. *European journal of immunology* 27, 2626-2633 (1997).

165. Higashiyama, H., Kinoshita, M. & Asano, S. Expression profiling of liver receptor homologue 1 (LRH-1) in mouse tissues using tissue microarray. *Journal of molecular histology* 38, 45-52 (2007).

166. Muzumdar, M.D., Tasic, B., Miyamichi, K., Li, L. & Luo, L. A global double-fluorescent Cre reporter mouse. *Genesis* 45, 593-605 (2007).

167. Van Parijs, L. *et al.* Uncoupling IL-2 signals that regulate T cell proliferation, survival, and Fas-mediated activation-induced cell death. *Immunity* 11, 281-288 (1999).

168. Corazza, N., Eichenberger, S., Eugster, H.P. & Mueller, C. Nonlymphocyte-derived tumor necrosis factor is required for induction of colitis in recombination activating gene (RAG)2(-/-) mice upon transfer of CD4(+)CD45RB(hi) T cells. *The Journal of experimental medicine* 190, 1479-1492 (1999).

169. Schwaderer, J., Gaiser, A.K., Phan, T.S., Delgado, M. & Brunner, T. Liver receptor homolog-1 (NR5a2) regulates CD95/Fas ligand transcription and associated T-cell effector functions. *Cell death & disease* 8, e2745 (2017).

170. Miyazaki, M. *et al.* Thymocyte proliferation induced by pre-T cell receptor signaling is maintained through polycomb gene product Bmi-1-mediated Cdkn2a repression. *Immunity* 28, 231-245 (2008).

171. van der Valk, J. *et al.* Fetal Bovine Serum (FBS): Past - Present - Future. *Altex* (2017).

172. Chan, M.L. *et al.* Limited CD4+ T cell proliferation leads to preservation of CD4+ T cell counts in SIV-infected sooty mangabeys. *Proceedings. Biological sciences* 277, 3773-3781 (2010).

173. Atanasov, A.G. *et al.* Cell cycle-dependent regulation of extra-adrenal glucocorticoid synthesis in murine intestinal epithelial cells. *FASEB journal : official publication of the Federation of American Societies for Experimental Biology* 22, 4117-4125 (2008).

174. Coste, A. *et al.* LRH-1-mediated glucocorticoid synthesis in enterocytes protects against inflammatory bowel disease. *Proceedings of the National Academy of Sciences of the United States of America* 104, 13098-13103 (2007).

175. Wolfer, A. *et al.* Inactivation of Notch 1 in immature thymocytes does not perturb CD4 or CD8T cell development. *Nature immunology* 2, 235-241 (2001).

176. Faul, F., Erdfelder, E., Lang, A.G. & Buchner, A. G*Power 3: a flexible statistical power analysis program for the social, behavioral, and biomedical sciences. *Behavior research methods* 39, 175-191 (2007).

177. Quah, B.J., Warren, H.S. & Parish, C.R. Monitoring lymphocyte proliferation in vitro and in vivo with the intracellular fluorescent dye carboxyfluorescein diacetate succinimidyl ester. *Nature protocols* 2, 2049-2056 (2007).

178. Livak, K.J. & Schmittgen, T.D. Analysis of relative gene expression data using real-time quantitative PCR and the 2(-Delta Delta C(T)) Method. *Methods* 25, 402-408 (2001).

179. Pfaffl, M.W., Horgan, G.W. & Dempfle, L. Relative expression software tool (REST) for group-wise comparison and statistical analysis of relative expression results in real-time PCR. *Nucleic acids research* 30, e36 (2002).

180. Schindelin, J. *et al.* Fiji: an open-source platform for biological-image analysis. *Nature methods* 9, 676-682 (2012).

181. Wasem, C. *et al.* Sensitizing antigen-specific CD8+ T cells for accelerated suicide causes immune incompetence. *The Journal of clinical investigation* 111, 1191-1199 (2003).